Novel *in vivo* imaging approaches to study embryonic and adult neurogenesis in the mouse

Dissertation for the attainment of the academic degree of *Doctor rerum naturalium*
Given by the Fakultät *Mathematik und Naturwissenschaften* of the Technical University of Dresden

Alessio Attardo

Born on the 12th of October 1978 in Palermo (Italy)

Reviewers:

Prof. Dr. Huttner W. B.

Max Planck Institute of Molecular Cell Biology and Genetics, Dresden (Germany)

Prof. Dr. Götz M.

GSF – National Research Centre for Environment and Health, Institute for Stem Cell Research, Munich (Germany)

Dr. Tanaka E.

Max Planck Institute of Molecular Cell Biology and Genetics, Dresden (Germany)

Ai miei cari genitori

Acknowledgments

Many people without whom this work would not have been possible deserve my thanks, I apologize in advance for those who deserve acknowledgment and are not present here.

My sincere thanks go to **Wieland (Prof. Dr. Huttner W.B.)** for the precious guide and advise, the endless scientific freedom and the great resources that he has granted me along these years. I also thank him for the friendly atmosphere and for being a mentor more than a "boss".

Many thanks deserves **Federico (Calegari F.)** for the long discussions and the patient guide that he has given me during these years, but also for the pleasant dinners in which science has been successfully mixed with fondue or roasted pork!

Klaus (Dr. Fabel K.) has been (and I hope will be) a precious collaborator and hard worker, without whom the adult neurogenesis field would not benefit of Tis21-GFP! I thank him for the long and fruitful discussions in front of the many perfused mice…

I must thank **Magdalena (Prof. Dr. Götz M.)** and **Gerd (Dr. Kempermann G.)** for their open, enthusiastic collaboration and interesting discussions that have contributed not only to this work but also to my personal scientific growth.

Veronique and Jennifer (Dr. Dubreuil V. and **"frau Fisch")** deserve many thanks because they have always been available for interesting discussion and giving a sharp advice.

Karen (Dr. Echeverri K.) and **Eugenio (Dr.Fava E.)** deserve a special thank for the advices given to me during the preparation of this work.

I thank **Silvia (Dr. Cappello S.)** for being a great collaborator and a good friend, with whom I enjoyed long telephonic scientific discussions and long genotyping nights.

I thank very much **Katja and Christiane (Langenfeld K. and Haffner C.)** for turning a blind eye over my continuous "thefts" of their reagents.

Jan and **Kurt (Dr. Peychl J and Dr. Anderson K.)** and the whole light microscopy facility deserve my thanks for their patience and essential guide through the shiny universe of imaging.

Ronald (Dipl. Ing. Naumann R.) is the "father" of the *Tubb3*-GFP line, all my thanks go to him for his precision and efficiency in generating, and advise in maintaining a transgenic colony.

I thank **Jussi, Anke** and the whole staff of the biomedical services facility for making our life easier with their impeccable mouse management and friendly personal relationships.

Last but not least, I have to thank the whole group for the friendly and open working atmosphere, the endless scientific discussions and the many dinners and beers enjoyed together!

Thank you very much, to all of you.

Summary

Neurogenesis is the process of generation of neurons during embryonic development and adulthood. The focus of this doctoral work is the study of the cell biological aspects of neurogenesis and the mechanisms regulating the switch of neural stem cells from proliferation to differentiation.

During embryonic development neurogenic divisions occur at the apical or basal side of the pseudostratified epithelium that forms the wall of the neural tube, the neuroepithelium. Apical asymmetric neurogenic divisions (AP) give rise to a neuron and a progenitor cell, while basal symmetric neurogenic divisions (BP) give rise to two neurons. The first part of this thesis is focused on the study of some cell biological aspects of BPs. We first validated the use of the *Tis21*-GFP knock in mouse line, previously generated in our laboratory. We found that the totality of neurogenic progenitors is marked by the expression of a nuclear GFP. We calculated the abundance of BPs overtime since the onset of neurogenesis showing that BPs overcome APs over development. Using confocal microscopy and two-photon time-lapse imaging of acute brain organotypic slice culture, we studied the loss of apical contact of the basal dividing cells. We found that both neurogenic and non-neurogenic basally dividing progenitors miss the apical contact; apical contact and most probably the apical domain of the plasma membrane are lost prior mitosis. We generated and characterized a second mouse line, the *Tubb3*-GFP line; this line expresses a plasma membrane-localized GFP in neurons. These two lines were crossed to obtain a new line (TisTubb-GFP) allowing detection of neurogenic divisions and tracking daughter cells using two-photon time-lapse imaging of acute brain organotypic slice culture. Using this model: (i) we imaged symmetric neurogenic divisions of BPs, identifying daughter cells as neurons, during imaging; (ii) we compared the kinetics of βIIItubulin-GFP appearance after apical or basal mitosis, showing that daughters of BPs express βIIItubulin-GFP faster than daughters coming from apical divisions; (iii) we imaged neuronal migration and localization of the Golgi apparatus.

Neurogenesis in the adult is confined to two specific regions in the telencephalon: the sub ependymal zone, lining the ventricle, and dentate gyrus of the hippocampus. In both regions stem cells with astrocytic characteristics are thought to give rise to a transit amplifying cell population that generates neurons. The second part of this thesis focuses on the adult neurogenic progenitors lineage. Tis21-GFP expression was found and characterized in the two adult neurogenic regions from early postnatal to adulthood. Using a panel of markers for the adult neurogenic cell lineage and confocal imaging, we characterized Tis21-GFP expression, in the dentate gyrus. Tis21-GFP is first expressed in the neurogenic subpopulation of doublecortin positive cells. Tis21-GFP is inherited by the neurons and eventually degraded. Moreover, our data suggest that mitotic Tis21-GFP cells are an indicator of the levels of neurogenesis more accurate than doublecortin positive cells, in the early postnatal mouse.

The TisTubb-GFP mouse line allows identification of BPs by following the daughter fate. TisTubb-GFP mice could be used to study the effect of candidate gene mutations on the generation of BPs. In combination with FACS, the TisTubb-GFP line could allow quantifying the number of progenitor cells as well as neurons. This would offer a quick and precise read out for changes during embryonic neurogenesis. The *Tis21*-GFP mouse line allows identification of neurogenic cells in the adult brain in vivo. This could be used for studying cell biological characteristics of the neurogenic cells in the adult.

I Introduction

The birth of neurons

Neurons are a class of cells, very different from each other in morphology and cell membrane potential, specialized in propagating and modulating electric currents. They form complex networks able to acquire inputs, compute information and eventually give an output; these networks acquire the highest complexity in mammals [1]. In rodents, neurons start being generated early during development but their generation continues throughout life [2, 3]. During development neurons are massively generated in extended areas of the embryo and they are able to migrate away form their birthplace (i.e. GABAergic interneurons, generated in the basal telencephalon, or Cajal Retzius neurons, generated in the cortical hem, migrate to the dorsal telencephalon), before establishing their functional connections [4]. Postnatally neurons are generated in specific areas of the nervous system and they still migrate from their birthplace to different sites where they finally establish their functional connections (this migration can span several millimetres, like, the migration of olfactory neuron progenitors) [3]. Neurons are post-mitotic cells, they do not divide anymore, and therefore, their final number is regulated by three factors.

(i) Expansion of the progenitor pool that will give rise to the neurons [5].

(ii) Amount of neurons that will be generated by each progenitor [1, 5, 6].

(iii) Death of differentiated cells.

Understanding in detail the regulation of these processes would explain how the number of neurons is determined as well as why the generation of neurons is limited during adulthood.

The process by which progenitor cells generate neurons, called neurogenesis, is tightly regulated in time and space, in the developing and adult organism. Regulation of this process during embryonic development is crucial for achieving the correct number of neurons in the adult brain [5, 6], and it is becoming more and more clear that this process is a target of evolution in the primate lineage [1, 7]. However, it is still unclear what the significance of neurogenesis could be during adulthood, it seems that generation of new neurons is implicated to some extent in maintaining the plasticity of the adult brain [3].

The focus of this doctoral work is the study of neurogenesis and, specifically, the study of the neurogenic progenitors during embryonic development and adulthood in the mouse telencephalon. The mouse is the most suitable mammal model organism because of the possibility of genetic manipulation and the highly developed imaging tools. We focused on the cortex because it is the region whose size has especially increased during evolution, and it is the only region where neurogenesis is known to continue during adulthood. This introduction will describe: (1) the mechanisms of central nervous system patterning with a focus on cortical telencephalon, (2) the mechanisms regulating neurogenesis in the embryo and how control of neurogenesis is a key event in evolution. The mechanisms regulating neurogenesis in the adult and the biological significance of adult neurogenesis will be discussed thereafter (3), together with our approach to the study of neurogenesis in the embryo and the adult (4).

I – 1. The specification and patterning of the mouse cortex

In the mouse, all neurons and glia are generated by a single sheet of epithelial cells called the neuroepithelium, which forms the walls of the neural tube (Fig. 1, A and B). Induction of the neuroepithelium takes place very early in development, when, during gastrulation, the invaginating underlying sheet of mesoderm contacts the ectoderm specifying the neuroectoderm [8, 9]. The neuroectoderm is composed by neuroepithelial (NE) cells (Fig. 1, C) that, through proliferation and morphogenetic movements form the neural tube, which will become the central nervous system of the adult animal (Gilbert, S. F. (1994) *Developmental biology 4th edition*, (Sinauer Associates Inc.)). The neural tube is specified, along the antero-posterior axis of the developing animal, to form specific structures such as, from caudal to rostral, the spinal cord, the hindbrain, the midbrain and the forebrain (Fig. 1, D). Starting at embryonic day 7 (E7) in the mouse, the Anterior Visceral Endoderm, an extra embryonic tissue located at the anterior side of the embryo, produces molecules such as Cerberus and Dickkopf that interact with molecules like Wnts, BMPs, Activin and Nodal, produced in the posterior part by the Node. The interplay between these molecules (and others like Chordin Noggin and Follistatin) generates the first regionalization of the tube, into spinal cord, hindbrain, midbrain and forebrain (Fig. 1, A, B and D) [10].

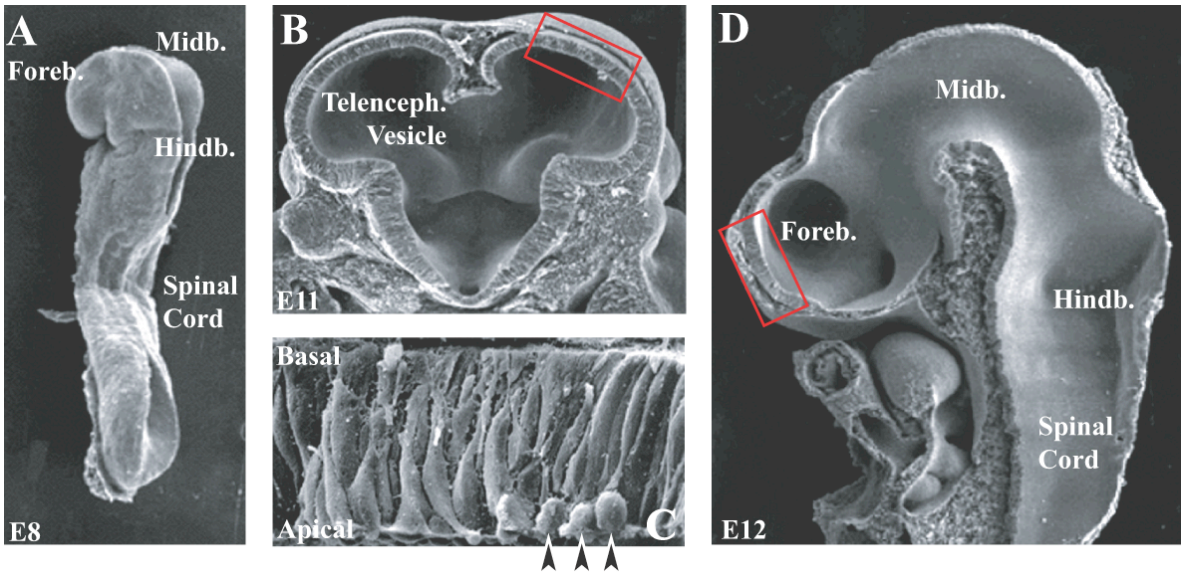


Figure 1 (Previous page) –Scanning electron microscopy pictures illustrating the development of the neural tube and the organization of the neuroepithelium in the mouse. (**A**) Posterior-lateral view of the E8 unclosed neural tube; the future forebrain, midbrain, hindbrain and spinal cord are indicated. (**B**) Transverse section through the E11 forebrain, note the developing two telencephalic vesicles. (**C**) Transverse section of the neuroepithelium with the apical side down and the basal side up (this orientation will be kept during this whole doctoral work); note the mitotic apical rounded cells (arrowheads). (**D**) Sagittal section through the E12 neural tube; the future forebrain, midbrain, hindbrain and spinal cord are indicated. The red rectangle indicate areas of the neuroepithelium represented in C. Pictures taken from the website www.med.unc.edu.

I - 1.1.
From forebrain to telencephalon

After antero-posterior induction and closing of the neural tube, factors expressed in different regions of the developing forebrain, provide the dorso-ventral and further antero-posterior patterning, giving rise to the telencephalon. The anterior most subset of cells (Anterior Neural Ridge) (Fig. 2, A, ANR) is necessary for the specification of the telencephalon, *via* production of Wnts antagonists like Tlc (a Frizzled soluble analog) [11], and growth factors such as Fgf8 [12]. The ventral domain in the developing telencephalon is specified by Sonic hedgehog (Shh) expression (Fig. 2, A, orange); Shh controls the formation of the ganglionic eminences and the expression of ventral specific transcription factors in the telencephalon such as Mash1, Dlx2 and Gli1/2 [10]. The action of Shh is antagonized, in the presumptive cortical region, by the Gli3 gene (Fig.2, C), which is a target of Shh but acts as repressor [13]. Furthermore, BMPs and Wnt3a, produced in the dorsal midline (roof plate first and cortical hem later) (Fig.2, A, green), give positional information as well as stimulating cell proliferation that contribute to the expansion of the dorsal cortical domain [14].

The positional information generated by the signalling centres is transformed in locally graded expression of transcription factors; the spatio-temporal interaction of homeodomain and basic Helix-Loop-Helix (bHLH) transcription factors generate the first genetically encoded map of the future telencephalon [15]. In the cortical domain, for instance, the transcription factors Pax6 and Emx2 have a complementary and overlapping expression pattern. Emx2 is expressed more posteriorly and medially while Pax6 is more anteriorly and laterally expressed (Fig. 2, B, upper panels). Deletion of Emx2 leads to expansion of the anterior domains (like the motor areas), conversely mutation of Pax6 leads to an expansion of the posterior domains (like the visual areas) (Fig. 2, B, lower panels) [16]. The same effect is found along the dorso-ventral axis:

deletion (complete or partial) of both genes leads to a ventralization of the developing telencephalon with failure of cortical development [17]. The developing ventral telencephalon is subdivided in lateral and medial ganglionic eminences (Fig. 2, D, LGE and MGE), which later will give rise to the striatal and pallial component of the basal ganglia respectively. This subdivision is generated by a specific expression of transcription factors: Gsh2 and Gli1/2 (more dorsally), Nkx1.2 (more ventrally), Mash1 and Dlx1/2 (spanning the whole developing basal telencephalon) (Fig. 2, C). The overlap and segregation of the above (and other) transcription factors, induces a subpopulation of progenitors to generate specific subsets of neurons: glutamatergic dorsally, GABAergic and Cholinergic basally (Fig. 2, D). These neurons migrate, in an inside-out manner, to the appropriate place where they establish their final connections and build the multilayered adult cortex (Fig, 2, E) [18].

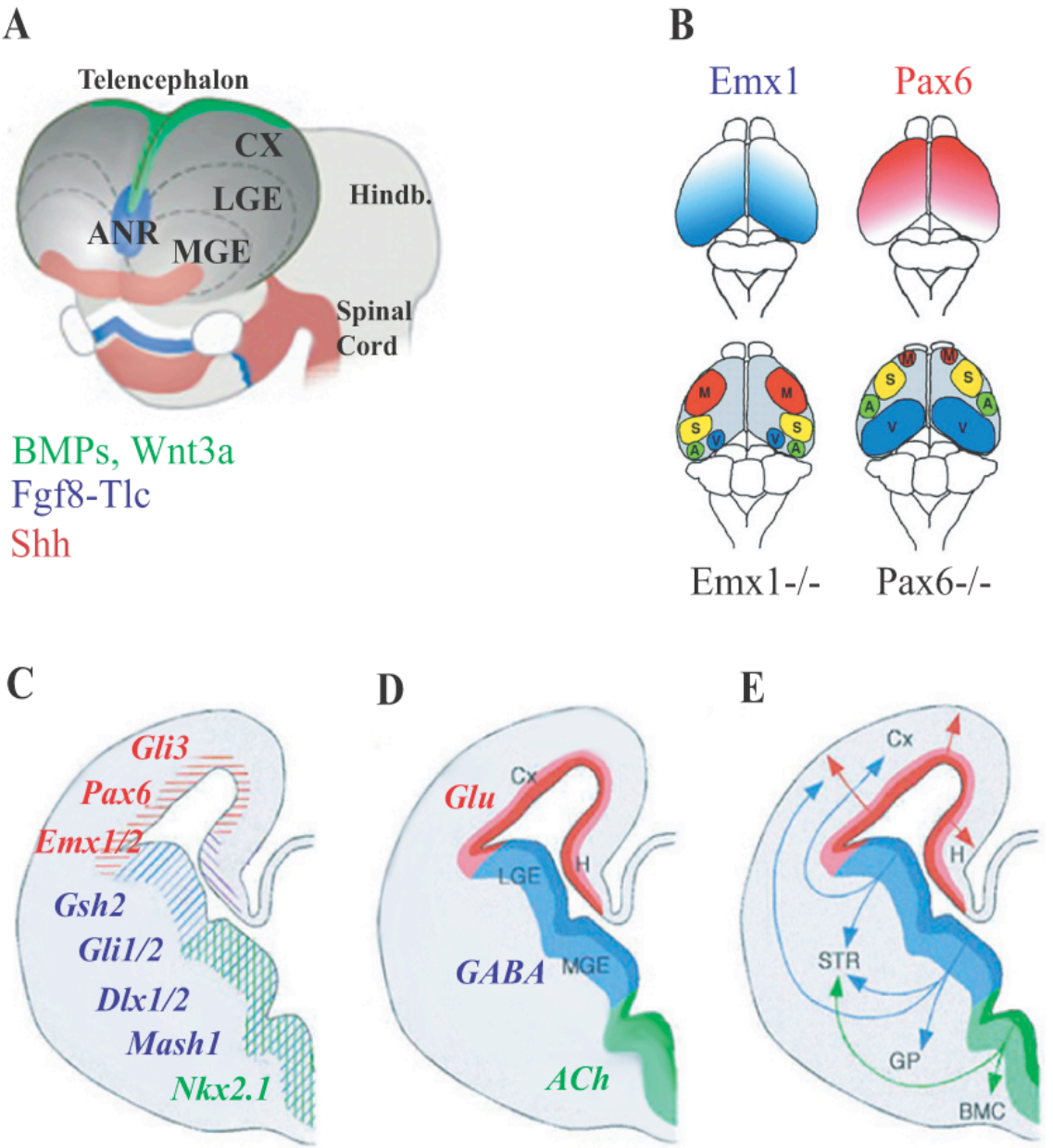


Figure 2 – Schematic drawings illustrating the distribution of determinants and gene expression during telencephalic patterning and the migration of the specific neuronal subclasses. (**A**) Frontal-side view of the developing telencephalon indicating the location of the organizers. Green regions are positive for BMPs and Wnt3a, blue regions are positive for Fgf8 (and the ANR for Tlc), orange regions are positive for Shh. ANR = Anterior Neural Ridge; CX = Cortex; LGE = Lateral Ganglionic Eminence; MGE = Medial Ganglionic Eminence. (**B**) Dorsal view of the developing telencephalon indicating the expression of Emx1 (blue) and Pax6 (red). The lower panels indicate the expansion of motor or visual areas in case of one the two genes being mutated. M = Motor; V = Visual. (**C-E**) Transverse view of the developing telencephalon indicating the expression domains of various transcription factors (**C**), the kind of neurons generated in specific regions (**D**) and the routes of migration that these neurons follow to their final destination (**E**). **A**, modified from [19]; **B**, modified from [16]; **C-E** modified from [18].

I – 2. Mechanisms regulating neurogenesis in the embryo

The focus of this doctoral work is the cortical neurogenesis and the term neuroepithelium, when not further specified, indicates the cortical neuroepithelium. Many changes happen at the cellular and tissue level of the neuroepithelium from the beginning to the end of neurogenesis. A simple cuboidal proliferative epithelium transforms in a pseudo stratified, first, and truly stratified epithelium, later. The proliferative divisions decrease in number merging with the increasing differentiative divisions, while neurons accumulate on the basal side of the germinal layers.

I - 2.1.
The neuroepithelium changes with neurogenesis

Before neurogenesis. The neuroepithelium is constituted by proliferating cuboidal highly polarized cells, positive for the neural stem cell marker Nestin [20], defining the germinal Ventricular zone (VZ) (Fig. 3, A, E8). The polarization of these cells is reflected by the organization of their plasma membrane: proteins like Prominin1 [21] and Megalin [22] are specifically localized on the apical domain of the plasma membrane (Fig. 3, A, E8, blue solid line). Tight and adherens junctions are present at the apical most end of the basolateral plasma membrane (Fig. 3, A, pink and green boxes respectively) [23-25], and receptors for basal lamina constituents are concentrated in the basal plasma membrane, that is in contact with the basal lamina (Fig. 3, A, brown stripe) [26]. These NE cells show a characteristic Interkinetic Nuclear Migration (INM) from the apical (ventricular) to the basal (pial) side of the neuroepithelium during the G1 phase of the cell cycle and *vice versa* during G2, with the S phase on the basal side and mitosis at the apical, ventricular surface (Fig. 3, A, E8, arrows) [27]. The speed of nuclear movement varies during the cell cycle, being faster when apically directed and slower, and more discontinuous, when basally directed [28].

Onset of neurogenesis**.** An increasing number of NE cells stop proliferative symmetric divisions and start dividing asymmetrically, generating a progenitor and a neuron, or symmetrically, generating two neurons [28]. Moreover, they gradually differentiate into Radial Glial cells (Fig. 3, A, E10, yellow cells), down regulating some of their epithelial

features, acquiring specific glial characteristics and changing the pattern of INM [29]. The major cell biological changes are listed below.

(i) NE cells lose tight junctions, but not adherens junctions, and the apical-versus-basal delivery of specific viral protein changes [23, 30, 31].

(ii) Immunoreactivity for the stem cell marker Prominin1 is gradually lost [32].

(iii) The structure of the apical domain of the NE cells plasma membrane changes. Microvilli are lost and large pleiomorphic protuberances appear [32].

(iv) NE cells acquire ultra structural glial characteristics, like the presence of granules of glycogen [33].

(v) NE cells express various molecules characteristic of astrocytic differentiation: the astrocyte-specific glutamate transporter (GLAST) [34], the calcium binding protein S100□ [35], RC2 [36] and brain-lipid-binding protein (BLBP) [37].

(vi) Human RG cells express the glial acidic fibrillary protein (GFAP) [38]; interestingly mouse RG cells are negative for this marker but they are able to express a reporter gene when driven by the human GFAP promoter [39].

(vii) RG cells show INM but, differently from NE cells, the nuclei of the RG cells do not reach the most basal end of the cell, instead they stop at the edge of the developing neuronal layer (NL) [29].

In addition, a subset of NE cells and RG cells do not reach the ventricular side but rather lose apical contact and divide on the basal side, close to the developing NL, generating two neurons [28, 40, 41] (this doctoral work). These cells are considered as a different intermediate progenitor cell population (see later for details) and referred to as Basal Progenitors (BPs); in contrast the apically-dividing neurogenic cells, here are referred to as APs (Fig. 3, A, E10).

During neurogenesis**.** All NE cells transform into RG cells; the number of BPs increases forming another germinal zone between the VZ and the growing NL: the subventricular zone (SVZ) (Fig. 3, A and B) [42]. SVZ cells lack radial organization [42] and apical contact [41] (this doctoral work). The majority of the SVZ cells (previously believed to generate exclusively glia) generate neurons via symmetric division, from the onset to the end of neurogenesis (Fig. 3, A) [28, 40, 41].

End of embryonic neurogenesis. The progenitors of the VZ undergo symmetric neurogenic divisions and are consumed (Fig. 3, A, E15) [40], the whole VZ becomes thinner and disappears (Fig. 3, B). The SVZ progenitors switch to generation of glial cells, until birth and postnatally [43]. However, generation of neurons is not interrupted in the adult brain and, even if restricted to only two specific sites, adult neurogenesis is

responsible for the production of a considerably high amount of neurons that functionally integrate in the olfactory and hippocampal circuitry [3].

I - 2.2.
Cell divisions in the neuroepithelium are symmetric and asymmetric as defined by daughter cells fate

All the cells of the neuroepithelium, NE, RG and BP, divide symmetrically or asymmetrically. The definition of symmetry and asymmetry, used in this work, is based on the fate of daughter cells originated by the division; a symmetric division generates identical daughters while an asymmetric division generates different daughters. Since neurogenic division can be asymmetric or symmetric, there are three possible kinds of divisions coexisting within the germinal zones of the neuroepithelium.

(i) Symmetric proliferative. These are division of neural stem cells (capable of self renewal and generation of neurons and glia) generating two stem cells that continue dividing.

(ii) Symmetric neurogenic. These are divisions of progenitor cells generating two post mitotic neurons.

(iii) Asymmetric neurogenic. These are divisions of progenitor cells generating two cells with different fates, a progenitor cycling cell and a post mitotic neuron.

The relative proportion of these different kinds of divisions changes during development.

Prior to neurogenesis**.** All the neural stem cells undergo only proliferative symmetric divisions (at the ventricular surface, fig. 3, A) so that their number increases exponentially (Fig. 3, C pink curve) making up the VZ (Fig. 3, B, yellow area).

Onset of neurogenesis**.** An increasing subpopulation of progenitors switches from symmetric proliferative to asymmetric and symmetric neurogenic divisions (Fig. 3, C). The result of this switch is the progressive slowing down of the growth of the VZ, which is now formed by two coexisting cell populations: proliferating and differentiating. Moreover, the VZ generate cells that do not migrate towards the apical side but divide basally (the BPs), this leads to its further shrinking. BPs, segregated to the basal side (Fig. 3, A), build the SVZ (Fig. 3, B, green area), and, interestingly, they outnumber APs (Fig. 3, C) [28].

End of neurogenesis. Symmetric neurogenic divisions consume all the neurogenic progenitors (Fig. 3, A, E15). This leads to a further reduction of the VZ (Fig. 3, B, yellow area).

It was calculated that progenitors, in the mouse, undergo only 11 cell cycles during neurogenesis [44], so that, if one considers the neurogenic potential of the progenitors to be constant, the number of progenitors at the moment of the switch to neurogenesis is the limiting factor determining the final amount of neurons generated. An early onset of neurogenesis (Fig., 3, D, "early") will result in the generation of a certain number of neurons (represented by the slope of the red arrow corresponding to the "early point). However, if the onset of neurogenesis is delayed (3 cell cycles in the example, "late"), the pool of precursors will be greater (Fig., 3, D, pink dashed curve); this will result in the generation of a greater amount of neurons (represented by the slope of the red arrow corresponding to the "late" point). This means that the balance between symmetric proliferative and asymmetric-symmetric neurogenic divisions is of crucial importance for the regulation of neurogenesis.

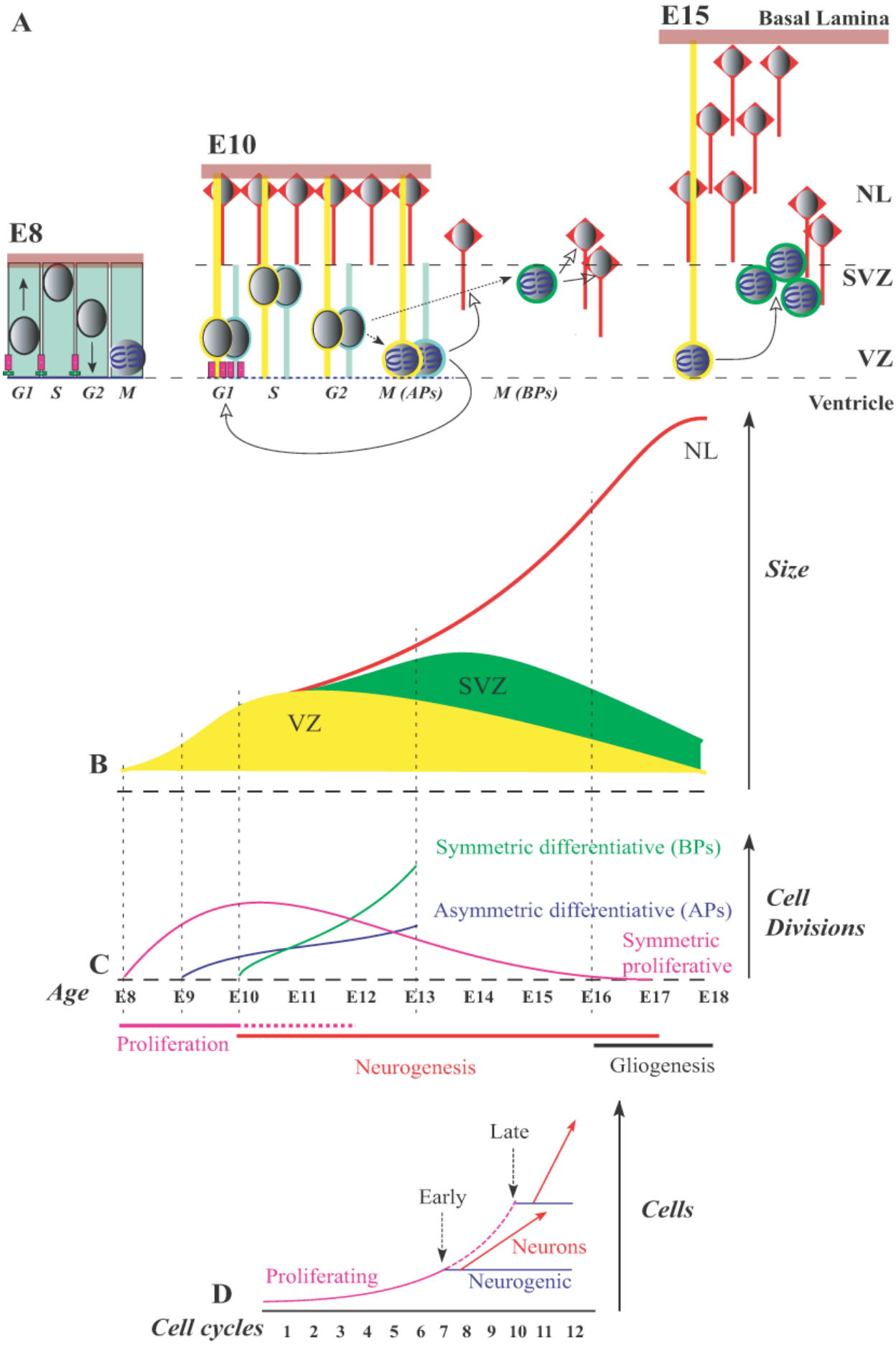

A
E15
Basal Lamina
E10
E8
NL
SVZ
VZ
G1 S G2 M
G1 S G2 M (APs)
M (BPs)
Ventricle
NL
SVZ
VZ
Size
B
Symmetric differentiative (BPs)
Asymmetric differentiative (APs)
Symmetric proliferative
Cell Divisions
C
Age
E8 E9 E10 E11 E12 E13 E14 E15 E16 E17 E18
Proliferation
Neurogenesis
Gliogenesis
Late
Early
Neurons
Proliferating
Neurogenic
Cells
D
Cell cycles
1 2 3 4 5 6 7 8 9 10 11 12

Figure 3 (Previous page) – Schematic representation of the changes occurring the in the neuroepithelium with neurogenesis. (**A**) Cartoon illustrating some of the cell biological features of the neuroepithelium described in the text, prior (**E8**), at the onset (**E10**) and at the end (**E15**) of neurogenesis. Cuboidal (E8) or short blue cells (E10) represent NE cells; yellow elongated cells (E10-E15) represent RG cells; red cells (E10-E15) represent neurons. Pink rectangles (E8-E10) represent tight junctions; green rectangles (E8) represent adherens junctions; brown thick stripes (E8-E15) represent the basal lamina. Solid rows at E8 represent the direction of INM; dashed arrows in E10 represent the possibility of a cell to divide apically (APs) or basally (BPs); empty arrows in E10 and E15 represent the cell fate of the daughters. G1, S, G2, M = phases of the cell cycle. (**B**) Changes in cell abundance in the germinal zones (VZ yellow and SVZ green) and in the neuronal layer (NL red) prior, during and at the end of neurogenesis. (**C**) Variation during development of the different kind of mitoses taking palace in the neuroepithelium. Note that, while the high of the green and blue curve are reflecting data coming from measurements [28], the height of the pink curve is arbitrary so that the three curves cannot be directly compared. (**D**) Relationship between the length of the proliferative phase and the increase in the number of neurons (represented by the slope of the two red arrows). Note that all the curves do not reflect quantitative calculations but indicate qualitative trends. **B**, **C** and **D** modified respectively from [45, 28] and Huttner W.B. (unpublished).

I - 2.2.1.
Asymmetric cell division correlates with asymmetric distribution of cell fate determinants

In the fruit fly *Drosophila melanogaster*, neuroblasts and ganglion mother cells are generated by an asymmetric cell division in which specific sets of determinants are asymmetrically distributed among daughters [26, 46]. In the mouse, similarly, asymmetric differentiative divisions may correlate with asymmetric distribution of cell fate determinants [47, 48]. In the developing cortex some of the genes regulating the patterning of the telencephalon were shown to influence the balance between symmetric and asymmetric cell division. Over expression of the transcription factor Emx2, in dissociated progenitor culture, increased the size of single-cell-derived clones, strongly suggesting an increase in the number of symmetric proliferative divisions. Conversely, mice lacking Emx2 show, *in vivo*, a change in the orientation of cleavage planes of apical mitotic cells, which is associated with asymmetric cell fate [49]. The role of the transcritption factor Pax6 seems to be less clear. The number of asymmetric divisions, calculated by measuring the inclination of the mitotic cleavage planes, increases more rapidly in the Pax6 mutant than in the WT developing mouse cortex [50]. However, the neurogenic potential of the progenitors seems to decrease [51].

Many signalling pathways are involved in the balance between symmetric proliferative versus asymmetric neurogenic cell division, and many of them can act in either directions accordingly to the developmental moment and the single cell context the signal is acting in. Interestingly the same signalling pathways have a similar role during

adult neurogenesis. This role will be discussed later, to suggest that embryonic and adult neurogenesis share similar mechanisms. The Shh signalling pathway, implicated in the patterning of the ventral telencephalon, has a role in keeping the cortical progenitors in a proliferative state, *via* activation of Gli genes [52, 53]. The Wnt signalling pathway is involved in the maintenance of the progenitors pool, in the early proliferative stage [54-57], but is as well, later on, involved in neurogenic differentiation, depending on Shh and Fgf2 [58-60]. The Notch signalling pathway, of key importance in maintaining the cells in a progenitor state in Drosophila, has a pivotal role in mouse progenitor division as well [61]. Forced expression of constitutively active Notch was shown to keep the progenitors in the proliferative state [62, 63]. The same result was obtained by forcing the expression of Notch effectors like the bHLH transcription factor HES1 [64]. Similarly, loss of Numb (asymmetrically segregated in Drosophila and suggested to repress Notch [65]) and Numblike (shown to directly bind Notch1 in mouse [66]) increases the progenitor cell number in the developing mouse forebrain [67]. Although asymmetric distribution of Notch1 is controversial in the mouse (mostly because of the low specificity of the available antibodies, see [47, 66]), asymmetric distribution of Numb was shown to correlate with asymmetric neurogenic cell divisions *in vitro* [68].

Although asymmetric distribution of a protein involved in cell signalling (the EGF receptor), during asymmetric division, was recently shown during astrocyte differentiation [69]; there is no report of a similar case in neuronal differentiation. In all the studies afore mentioned, the symmetric or asymmetric nature of a progenitor division was assessed either *a posteriori*, by the daughters fate, or by measurement of the cleavage plane orientation. It was not possible to identify interphase neurogenic cells, a marker to distinguish between symmetric proliferative and asymmetric neurogenic divisions was missing. This marker was identified as the gene *Tis21*, an antiproliferative gene expressed during the G1 phase of all neurogenic cells [70]. A knock-in mouse, in which GFP (localized to the nucleus) marks the whole population of neurogenic progenitors (*Tis21*-GFP) [28], was used to analyze apical mitoses and to correlate symmetric proliferative (GFP negative) and asymmetric neurogenic (GFP positive) divisions with symmetric and asymmetric distribution of determinants (Fig. 4) [71]. This work showed that apical plasma membrane is symmetrically distributed in case of symmetric cell fate and asymmetrically distributed in case of asymmetric cell fate (Fig. 4, blue apical portion), suggesting that the cell keeping the apical plasma membrane is the one that divides again, while the cell loosing it becomes a post mitotic

neuron (Fig. 4, B). This finding opens interesting possibilities. Asymmetric distribution of the apical plasma membrane could imply the asymmetric distribution of junctional proteins (Fig. 4, A and B, pink boxes), among these βcatenin was shown to play a key role in progenitor cells proliferation [55]. Asymmetric distribution of apical plasma membrane could allow only one of the two cells (the progenitor cell that will continue dividing) to keep receiving signals from the ventricle, therefore retaining its mitotic potential (note that Megalin, a protein specifically localized in the apical plasma membrane, was shown to be a receptor for Shh [22]).

Some of the molecules involved in mitosis were recently shown to interfere with the regulation of neurogenesis. The Asp protein was shown to be involved in regulating mitotic spindle function, in Drosophila [72, 73], and to be crucial determinant of cortical size in humans [74, 75]. Aspm was recently suggested to be involved in regulating the precision of splitting/segregating the apical plasma membrane. In the mouse, *in vivo* knockdown of the protein, showed a mislocalization of the centrosomes in the mitotic progenitors and an increase in asymmetric cell divisions, with reduction in the proliferative progenitors pool [76]. Similarly, another centrosomal protein, Nde1, was implicated in maintaining the progenitors in the symmetric proliferative state. Ablation of Nde1 led to the increase of horizontal division planes concomitantly with a reduction in the proliferative progenitor pool, increasing the number of early born neurons (and decreasing the number of the late born neurons since the progenitors get consumed earlier) [77].

I - 2.3.
Segregation versus accumulation, the role of cell cycle length

The sufficient amount of a factor necessary for cell fate determination can be reached either by asymmetric segregation or by regulating the amount of time this factor is allowed to act (or to be accumulated) in a cell. This mechanism, proposed under the name of the "*cell cycle length hypothesis*" [78] (Fig. 4, C), implies that neurogenic cells do not necessarily need to have a greater amount of a certain factor at the moment in which they are born; rather a longer cell cycle could be sufficient to specify the fate of daughter cells, allowing a given factor to act longer or to be accumulated. With the progression of neurogenesis, the cell cycle length varies in the progenitors: the length of

the G1 phase, specifically, increases [44]. Transcription factors such as Pax6 were implicated in cell cycle regulation [50]; however, lengthening of the cell cycle was believed to be a consequence of the differentiation process. Recently this view was challenged by the finding that artificial lengthening of the cell cycle could, *per se*, induce premature neurogenesis [78]. Similar results were obtained with over expression of other cell cycle regulators like p27 [79] and PC3 (the rat homolog of *Tis21*), however it is not clear if cell cycle lengthening is the only activity of these proteins [80, 81]. Furthermore, some growth factors act via regulation of cell cycle length. Neurotrophin3 was shown to lengthen G1, promoting differentiative divisions [82]; conversely, shortening of the G1 phase by bFGF [82] or IGF-1 [83] shifts the symmetric-asymmetric division balance towards the symmetric proliferative state. The "*cell cycle length hypothesis*" seems to be confirmed by a growing amount of evidences. In the monkey it was shown that progenitors of visual area 17 have a shorter cell cycle (calculated by cumulative labelling with BrdU and 3H-thymidine) when compared to the neighbouring area 18; this correlates with the greater amount of neurons present in area 17 at the end of neurogenesis [84]. Moreover, using the *Tis21*-GFP mouse line, a direct correlation between cell cycle length and neurogenic divisions was found. Cortical neurogenic progenitors have a longer cell cycle when compared to the proliferative progenitors, and, most interesting, BPs have a cell cycle even longer than APs (Fig 4, C) [85].

Cell cycle progression is linked to another peculiar feature of the progenitors: the Interkinetic Nuclear Migration (INM). INM regulation, the mechanisms underlying it and its importance in the regulation of neurogenesis are very poorly understood. NE cells differ from RG cells and both differ from BPs in regard to INM. Nuclei of NE cells migrate from the apical to the basal side of the cell, while nuclei of RG cells do not reach the basal most tip of the cell, stopping at the edge of the neuronal layer. BPs do not complete their migration towards the ventricle and instead divide on the basal side of the neuroepithelium. Time-lapse imaging of mouse organotypic slice culture showed that progenitor cells, subjected to RNA interference for Lis1, cannot complete ventricle directed movement nor mitosis [86]. Lis1, whose absence causes severe impairment in neuronal migration, is a protein forming a complex with dynein and dynactin, which regulate microtubule dynamics [87, 88]; RNA interference experiments suggest that apically directed nuclear movement is dependent on microtubules. In addition to microtubules, actin filaments seem being involved in INM; Cytochalasin B, a drug interfering with actin polymerization, blocks this process in chick [89, 90]. Moreover, it

seems that Cytochalasin B treatment could block INM without blocking the cell cycle, leading to an increase of neurogenesis in chick [91]. Despite the fact that cell cycle length has not been quantified, this work suggests a role of INM independent from the cell cycle length in the regulation of neurogenesis.

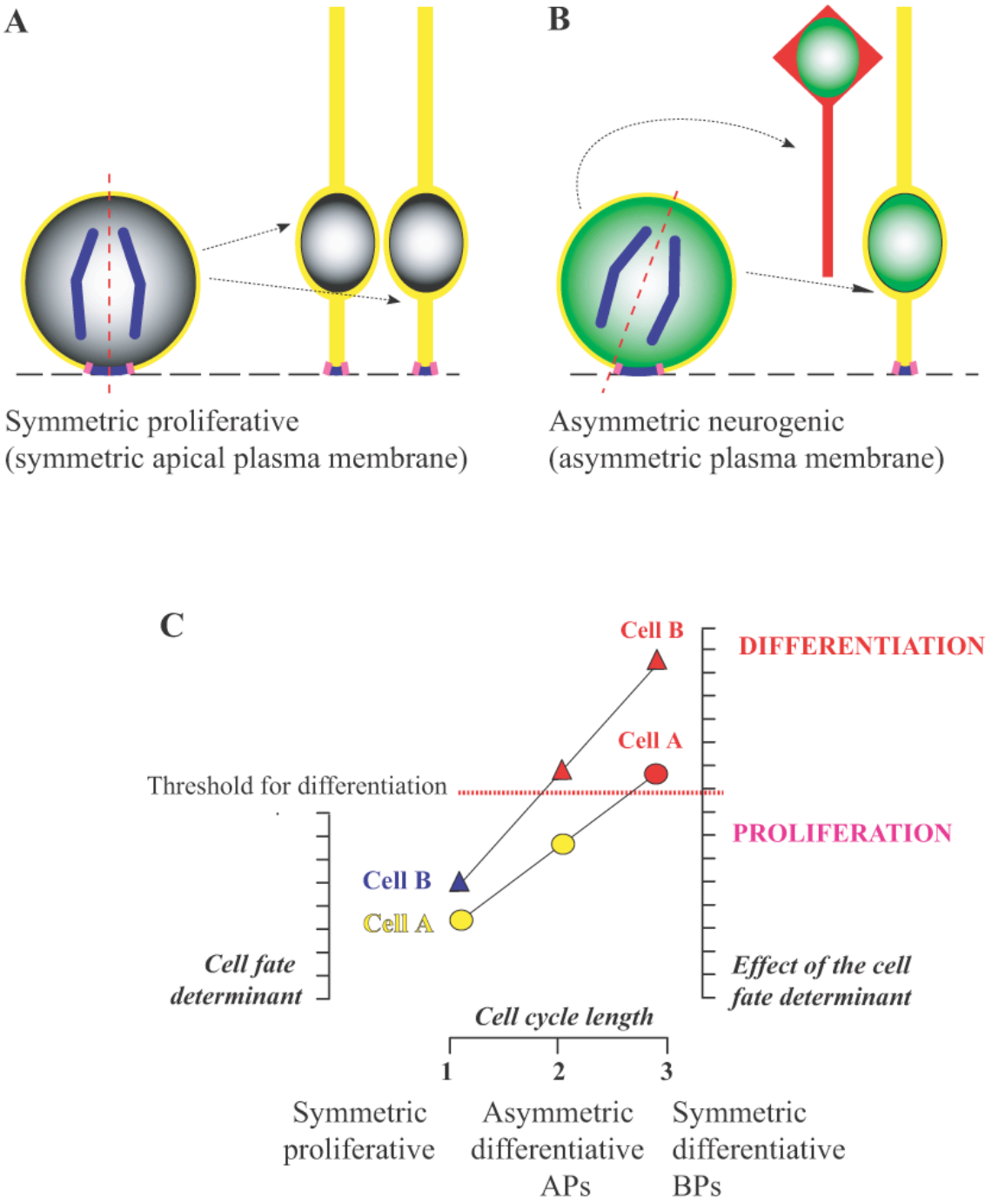


Figure 4 – Schematic representation of some of the cell biological features of progenitor cells. (**A-B**) During a symmetric proliferative division (**A**) the apical plasma membrane (blue line) is precisely split in two and the two daughters inherit both apical plasma membrane (blue line) and junctions (pink boxes). During an asymmetric neurogenic division (**B**) only one of the daughters inherits the apical plasma membrane and junctional proteins. Green represents *Tis21*-GFP. (**C**) The "*cell cycle length hypothesis*" [78]. The circles and triangles represent two different cells; blue and yellow, prior differentiation, red after differentiation. Numbers represent different possible durations of the cell cycle, corresponding to the cell fate outcome correlating with the specific length (arbitrary units). **C** modified from [78].

I - 2.4.
The BP is a different cell intermediate

The "*cell cycle length hypothesis*" implies the existence of a progenitor, which generates two differentiated cells (Fig. 4, C, number 3). This kind of cell was supposed to exist only at the end of neurogenesis, being the last stage of ventricular zone progenitors that get consumed by the generation of two post mitotic differentiated cells [45]. Almost at the same time three different groups found the presence of these symmetric neurogenic cells at the basal side of the mouse and rat developing cortex, and imaged their symmetric neurogenic division [28, 40, 92]. BPs are intermediate neurogenic progenitors; they derive from NE or RG cells, but they differ in several ways.

(i) BPs loose their apical contact prior to mitosis [92].

(ii) BPs divide on the basal side of the neuroepithelium [28, 40, 92].

(iii) BPs divide symmetrically to generate neurons [28, 40, 92].

(iv) BPs have a G2 phase of the cell cycle longer than the other progenitors [85].

Very little is known about BPs, partially because of the absence of a reliable marker, but there is a growing number of genes shown to be specifically expressed in the SVZ like *Manic-Fringe* [93], *SVET1* [94], *Cux1* and *2* [95, 96] and *Tbr2* [97], most of which are transcription factors. However, it is not clear what is the relation between the expression of the afore mentioned genes and BP cell fate. Using the marker for neurogenic progenitors Tis21, it was shown that since the beginning of neurogenesis almost all of the basal mitoses generate neurons. In addition, the number of neurogenic divisions is higher on the basal than the apical side (BPs outnumber APs very early during neurogenesis), and because each BP can generate double the amount of neurons of an AP, it seems clear that the major site of neurogenesis in the cortex is not the ventricular surface but the basal side [28]. This observation is particularly interesting in the evolutionary context, since it has been suggested that, with evolution of the primate lineage, the major neurogenic contribution comes from structures located more basally [42, 98].

I – 2.5.
Neurogenesis and evolution

The degree of encephalization (the ratio between brain weight and body weight) increases in the primate and specifically in the human lineage. Moreover, the human brain is roughly three times bigger than the chimpanzee brain [99], and many times bigger than the mouse one. This increase in size particularly affects the cerebral cortex (Fig. 5, A), the largest brain structure, where higher cognitive functions are performed. The enlarged and more complex cortex reflects at least two developmental features.

The generation of neurons belonging to different classes. Upper cortical layers neurons, generated late in neurogenesis, are over-represented in the primate cortex and, especially in humans, these are generally neurons that connect the cortex with itself but do not project out of the cortex [100].

The generation of more neurons during a longer period of embryonic neurogenesis. The longer period of embryonic neurogenesis includes two different phases. (i) A longer proliferative period, so that each progenitor undergoes more cell cycles before starting differentiative divisions [5]. (ii) A longer differentiative period; it was calculated that cortical progenitors undergo 11 rounds of neurogenic cell division in mice [44], at least 28 in macaque [5] and probably more in humans.

Comparative analysis of embryonic neurogenesis in mouse monkey and humans showed that generation of a greater number of late-born neurons is coupled to the appearance of a new germinal structure called outer sub ventricular zone (OSVZ) [98]. It seems that, during evolution of the primate lineage, the bulk of cortical neurogenesis has shifted more basally [42, 98] (Fig. 5, C); this suggests that BPs could be an evolutionary step towards the "basalization" of neurogenesis (i.e. formation of the OSVZ). However, it is not clear whether the OSVZ is only neurogenic or mixed proliferative and neurogenic, so that it is not possible to equate it with the mouse SVZ (almost exclusively neurogenic but including also a 10% of symmetric dividing non-neurogenic cells). Cell cycle length also plays a key role in this structure. In the monkey, precursors have a shorter cell cycle in cortical areas richer in neurons. A shorter cell cycle implies more rounds of progenitors divisions per time unit before neurogenesis sets in, and this produces a greater number of progenitors that will generate, in turn, more neurons [84]. This observation suggests that the balance between symmetric proliferative and asymmetric differentiative divisions in the neuroepithelium could be one of the key

evolutionary changes in the primate lineage. For instance, ASPM, controlling the cleavage plane orientation precision during mitosis, may be crucial to ensure a correct splitting of the small apical plasma membrane domain, allowing more cycles of proliferative divisions. The precision of the splitting of the apical domain of the plasma membrane might be a crucial issue in the progenitors of the neuroepithelium that become more and more elongated with the increase of cortical thickness along the primate lineage [29, 48, 76]. Coherently, *ASPM* DNA sequence shows specific changes within the evolution of the primate lineage; moreover patients with mutations in the ASPM protein sequence show a decrease in brain size without gross change in the overall structure [101, 102].

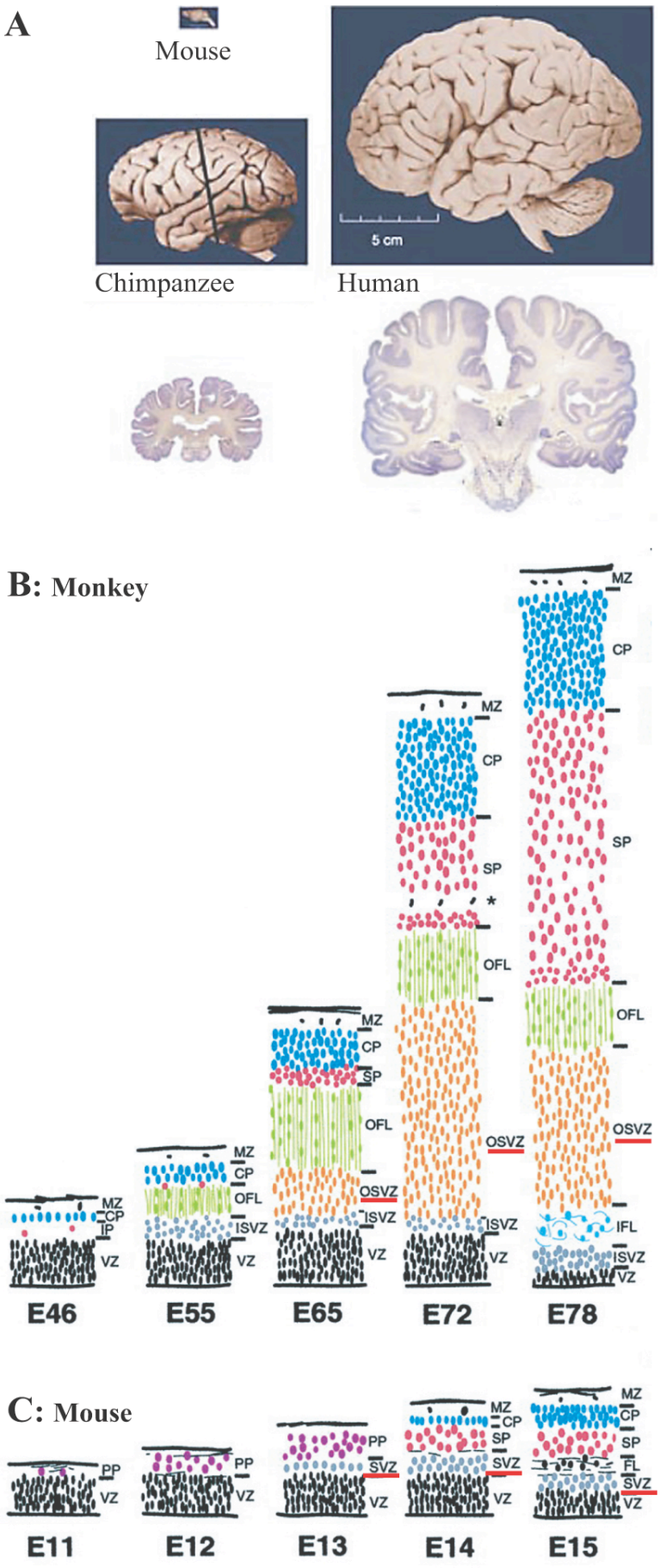


Figure 5 – Comaprison of the anatomical changes of the developing germinal layers in relation with brain size and complexity. (**A**) Comparison of mouse, chimpanzee and human brain sizes and gyrification, note that the pictures different size reflects the real proportion of the brains. (**B** and **C**) Schematic drawing of a section through the developing monkey (**B**) and mouse (**C**) telencephalon highlighting the presence of a different germinal layer in the monkey and the relative difference in size between monkey VZ-OSVZ and mouse VZ-SVZ suggesting a shift in the bulk of neuronal generation toward the basal side of the germinative region. VZ = ventricular Zone; SVZ = Sub ventricular Zone; CP = Cortical Plate; MZ = Marginal Zone; OFL = Outer Fiber Layer; SP = Sub plate; IFL = Inner Fiber Layer; FL = Fiber Layer. A modified from [103]; B and C modified from[98].

I – 3. Neurogenesis during adulthood

For a long time neurogenesis was thought to be only an embryonic feature, new neurons were not believed to be generated during adulthood. With the introduction of [H^3]-thymidine it was possible to detect cell synthesizing DNA and the first reports of neurogenesis in the adult were published from Altman [104-106] (for review see [3]). At present, adult neurogenesis is known in many organisms: invertebrates, vertebrates and mammals [107] including primates [108-110] and humans [111]. In fishes and songbirds, adult neurogenesis is a broad phenomenon related either with the growth of the brain (zebrafish) [112] or with learning, and seasonal cycles (songbirds) [113]. In mice, the generation of neurons during adulthood is more spatially confined, however it accounts for a considerable amount of neurons. The rostral migratory stream (RMS)(see later for details) carries more than 30.000 neuroblasts per day [114] while in the rat about 9.000 new neurons per day are generated in the Dentate Gyrus (DG) of the Hippocampus [115]. The significance of adult neurogenesis in mice is not clear but it seems to correlate with plasticity and learning [116]. In adult mice, new neurons are generated in two specialized sites of the telencephalon: the cell layer lining the ventricle, commonly called adult sub ventricular zone or sub ependymal zone (SEZ), and the Dentate Gyrus of the Hippocampus (DG). SEZ-born neurons migrate towards the olfactory bulb (OB) through the RMS [117] and become granule or periglomerular neurons functionally integrated in the existing circuitry (Fig. 6, A) [118]. DG-born neurons, generated in the sub granule cell layer (SGCL), migrate into the granule cell layer (GCL) to become functional excitatory hippocampal granule cells (Fig. 6, C) [119, 120].

I - 3.1.
Neurogenesis continues from the embryo to the adult

It seems that both SEZ and DG, directly bridge embryonic neurogenesis over birth.

The SEZ is a remnant of the embryonic ventral germinal layers (ganglionic eminences). In the early postnatal mouse, there is evidence suggesting that the embryonic VZ transforms into the ependymal multiciliated cell layer and for RG cells to transform into astrocytes (that still keep ventricular contact and a single primary cilium) with stem cell properties (Fig. 6, E) [121-123].

The DG has a different origin. While the hippocampus is generated by the convolution of the posterior most cortical areas, the DG is formed by the sequential migration of progenitors from the SVZ. In the rat, a first wave of migrating progenitors (first germinative matrix) comes from the dorsal SVZ at embryonic day 21; a second wave of migration comes at postnatal day 3 (second germinative matrix). These progenitors give rise to the outer shell of the DG (GCL) and to the progenitors (third germinative matrix) that reside in the DG of the hippocampus (in the hilus and SGCL) for the rest of the life of the animal. The third germinative matrix, made by progenitors with astrocytic characteristics [124], is the only origin of new neurons and it is the source of all the neurons generated during adulthood (Kempermann, G. (2006) *Adult neurogenesis, stem cells and neuronal development in the adult brain* (Oxford University Press 2006)).

The differences between the SEZ and DG are many.

Embryonic derivation. The SEZ progenitors have a ventral origin, as suggested by the expression of the ventral specific transcription factor Gli1 [125], while DG progenitors have a dorsal origin as suggested by the expression of the dorsal specific transcription factor Pax6[126].

Classes of neurons generated. SEZ progenitors give rise to interneurons [118], while DG progenitors give rise to excitatory neurons (DG) [120].

Three-dimensional organization of the germinal zones and neuronal precursors.

(i) SEZ progenitors keep a contact with the ventricle, while DG progenitors do not.

(ii) SEZ progenitors form chains of long-distance migrating neuronal precursors (Fig. 6, A) [117, 127], while DG progenitors generate precursors that migrate for a short distance (Fig. 6, C) [119, 120]

(iii) The cell-cell contacts between SEZ and DG are differently arranged in the three dimensions (extensively discussed in [3, 128-130]).

In spite of all the above differences, the cell lineage from progenitors to mature neurons seems to be common between the SEZ and DG. A quiescent (or extremely slowly dividing unless mobilized [131]) population of stem cells with astrocytic characteristics (including GFAP expression [132]) gives rise to a fast-dividing population of neuronally committed cells that generates mature neurons (Fig. 6). There are different nomenclatures designating the different cell types of the adult germinal zones ([130, 133, 134]), but for the purpose of this introduction and for coherence with the embryonic

nomenclature used previously, a simplified nomenclature, based on daughter cell fate, will be adopted.

Astrocytes/Stem cells. These cells are slow cycling, self renewing, symmetrically dividing, and able to generate neuronal- and glial-restricted precursors. They have astrocytic characteristics and include Nestin (only in the DG) and GFAP positive cells. They correspond to the B cells of [133], A cells of [130] and type 1 cells of [134] (Fig. 6).

Transit amplifying cells. These cells are fast cycling, dividing (but with a limited self renewal capacity), restricted to the generation of neurons. They include doublecortin (Dcx), and PSA-NCAM positive cells and they are also referred to as neuroblasts, migrating immature neurons or simply neuronal precursors. They correspond to the C and A cells of [133], D cells of [130] and type 2b and 3 of [134] (Fig. 6).

Neurons. These cells are post mitotic and in some cases still migrating. They include non-mitotic Dcx, Calretinin, Prox1, NeuN and Calbindin positive cells (in accordance with the degree of maturation of the cell). They correspond to the post mitotic A cells of [133], G cells of [130] and 5/6 of [134] (Fig. 6).

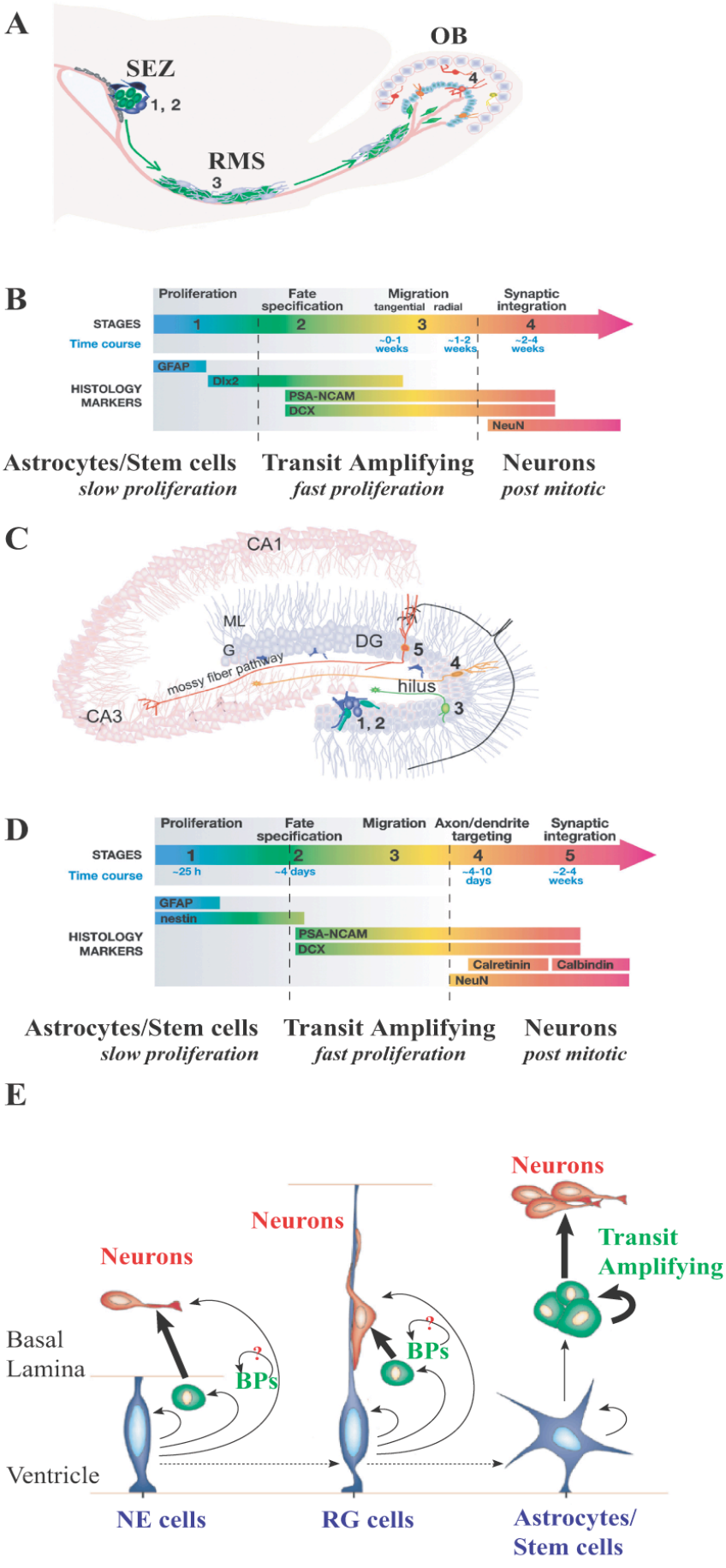


Figure 6 – Schematic representation of the cell lineages during neurogenesis in the adult mouse. (**A**) Sagittal view of the adult mouse telencephalon showing the generation and migration of the olfactory neurons. (**B**) Temporal sequence of histological marker expression in SEZ neurogenesis, indicated together with the terminology used in this work to describe the three main cell populations. (**C**) Transverse view of the adult mouse hippocampus showing the generation and migration of the granule hippocampal neurons. (**D**) Temporal sequence of histological marker expression in DG neurogenesis, indicated together with the terminology used in this work to describe the three main cell populations. (**E**) Cartoon representing the neurogenic lineage during embryonic and adult neurogenesis. Note that the cartoon suggests a continuity (also in some cell biological features, like the presence of a single primary cilium in the stem cells) between embryonic and adult stem cell lineage. SEZ = Sub Ependymal Zone; RMS = Rostral Migratory Stream; OB = Olfactory Bulb; DG = Dentate Gyrus; CA = Cornum Ammonii; BPs = Basal Progenitors; NE = Neuroepithelial; RG = Radial Glia. A-D modified from [3]; E modified from [128].

I - 3.2.
Adult neurogenesis is modulated similarly to embryonic neurogenesis but it is restricted to specific "niches"

Neurogenesis during adulthood shares many features with the embryonic generation of neurons. Some of the genes implicated in the control of neurogenesis during embryonic development seem to have a similar role in adulthood. The *Emx2* gene, which was suggested to play a role in the increase of proliferative divisions during embryonic development [49], seem to have a very similar role in the adult. Over expression of *Emx2* in acutely dissociated SEZ cells led to an increase of proliferative divisions; conversely knock-down of Emx2 increased the number of asymmetric neurogenic divisions [135]. The *Pax6* gene, expressed during hippocampal neurogenesis [126], marks the astrocytes/stem cells GFAP positive population as well as the transit amplifying PSA-NCAM positive cell population [136]. Hypomorphic rat mutants (Sey/+) show a decrease in the number and the proliferation of the astrocytes/stem cells, implicating *Pax6* in the maintenance of the astrocytes/stem cells in the adult cortex. A decrease in the number of newly generated neurons was observed as well but it is not clear if it reflects a decrease in the neurogenic potential (as in the embryo [51]) or more simply a reduction of the number of the neurogenic progenitors [136].

In addition many of the signalling pathways implicated in the control of neurogenesis during embryonic development seem to have a similar role in adulthood. The Shh pathway, which is involved in patterning the ventral neural tube [10] and in sustaining the symmetric proliferative divisions during neurogenesis [52], plays a role as well in the SEZ and DG where it sustains proliferation of both astrocytes/stem cells and transit amplifying progenitors [137-139]. Notch, which is involved in the maintenance of embryonic progenitors (see chapter 2.2.1), and its ligands Delta-like and Jagged are expressed in the SEZ, RMS and DG [140]. Similar to the embryo, *in vivo* forced expression of the activated Notch1 form, in the adult, led to a decrease in neurogenesis and migration of all cell types in the RMS [141].

Neurogenesis is very strongly restricted to precise regions in the adult, defined as stem cell niches (for review see [129, 142-144]). It was shown that progenitors, coming from one of the two neurogenic regions can generate neurons if transplanted into the other region; conversely SEZ or DG progenitors fail to generate neurons when transplanted into

regions that are not physiologically neurogenic, the, so called, “non permissive” regions [144]. Along the same line, progenitors from “non permissive” regions, such as the substantia nigra, generate neurons *in vitro* and if transplanted into the adult hippocampus, a ”permissive” region [145]. Moreover, infusion of growth factors is able to increase the neurogenic potential of regions otherwise “ non permissive”. Infusion of the brain-derived neurotrophic factor, into the lateral ventricle of adult rats, led to the generation of new neurons in “non permissive” regions like the parenchyma of the striatum, septum, thalamus and hypothalamus [146]. Besides playing similar roles during embryonic and adult neurogenesis, some signalling pathways are involved in maintaining a permissive niche for adult neurogenesis. The Wnt signalling pathway, which is involved in patterning of the telencephalon [147], maintenance of the progenitor pool, as well as differentiation [148], has also an important role in the adult hippocampus. Wnt3, which is necessary for hippocampal development [149], when over expressed is sufficient to increase neurogenesis from the astrocyte/stem cell population *in vitro* and *in vivo* [150]. Moreover, Wnt3 is expressed by mature astrocytes in the SGCL of the DG and astrocytes/stem cells express receptors for the Wnt and Wnt/βcatenin signalling pathways. *In vitro* co-culture with mature astrocytes induced neurogenesis in astrocytes/stem cells [151]. Taken together, these data show a double role of Wnt in inducing neurogenic divisions and in maintaining, at the same time, a permissive niche for the generation of neurons. The BMPs antagonist Noggin, implicated in the embryonic specification of the forebrain [152], has as well a role in maintaining a permissive niche for neurogenesis during adulthood. It was shown that ependymal cells of the SEZ secrete Noggin that antagonizes the action of local BMPs. Moreover, ectopic Noggin expression promoted neuronal differentiation of SEZ cells into the striatum [153]. Studies on songbirds have shown a strong correlation between vasculogenesis and neurogenesis [154], suggesting that blood vessels could be important players in the maintenance of the adult neurogenic niche. In the adult mouse many factors stimulating vasculogenesis were shown to stimulate neurogenesis (e.g. VEGF [155, 156], IGF1 [157], bFGF [158]); in addition, endothelial cells were shown to induce both cell proliferation and neurogenesis in culture [159].

I - 3.3.
Modulation and significance of adult neurogenesis

The extent of adult neurogenesis (the term neurogenesis has been used, throughout the present work, to define generation of new neurons rather than survival of the newly generated neurons) is modulated by many factors (extensively reviewed in [160-162]). Some of them are discussed in the following section, in which the possible significance of the generation of neurons in the adult is addressed.

Environmental factors. For the hippocampus the literature about the link between learning-neurogenesis, and the reverse impaired neurogenesis-learning deficits is copious. The classical example is the increase in neurogenesis and survival of newly born neurons caused, respectively, by voluntary running and by housing in an enriched environment [163, 164]. Many other factors that decrease the amount of neurogenesis correlate with poorer performances in learning tasks: stress, aging, but also substances such as alcohol, nicotine and opiates. A genetic correlation was shown s well: the difference in physiologic neurogenesis in different laboratory mice strains correlated in parallel with differences in learning performance (see [160] and references therein). In contrast, neurogenesis in the SVZ has a certain degree of independence from the stimuli coming from the OB (and from the OB itself as shown by [165]). Enriched odour exposure was shown to increase the number of newborn neurons in the OB, without affecting the number of newly generated neurons in the SEZ, suggesting that, while environmental factors can affect hippocampal neurogenesis, in the SEZ-OB axis they might have a specific role in survival rather than generation of new neurons [166].

Brain insults. Models of experimentally induced ischemic lesions show generation of new neurons in the hippocampus and in the infarcted area, but the contribution of progenitors migrating from the SEZ and in situ dividing progenitors in the striatum is not clear [167, 168]. However, in the striatum, about 80% of the newly generated neurons were shown to die between 2 and 5 weeks after stroke, probably because of the local " non permissive" environment; this finding makes it very unlikely for adult neurogenesis to be an effective mechanism of brain repair [167, 169].

Aging. Adult neurogenesis decreases with aging. In mouse SEZ the number of astrocytes/stem cells was greatly reduced in old (24-26 months old) mice in comparison to young mice (2-4 months old), concomitantly with the reduction of the EFGF signalling and the reduction in the capacity of discriminating odour fine differences [170, 171]. The same phenomenon is true for the hippocampus, in which decline of BrdU incorporation

and decrease of PSA-NCAM positive cell population was observed in aging rats [172]; such a decrease seem to be related to an increase in corticosteroids levels [173].

I – 4. Aims of this study

I – 4.1.
Embryonic neurogenesis

It seems clear that increasing the proliferation rate alone is not sufficient to generate a more complex brain in the human lineage. As recently shown by Chenn and coworkers, a robust increase of proliferation leads to a lateral expansion of the cerebral wall (and probably an increase in the number of radial units [174]) but not an increase in the thickness of single radial units [55]. We hypothesize that only the synergistic effect of the increase in progenitor number coupled to the shift of the most of neurogenesis towards the basal side, leads to the formation of thicker and more complex brains. In this context we focused on the BPs to elucidate some of the cell biological characteristics that make a BP different from an AP.

I - 4.1.2.
The use of Tis21 and βIIItubulin as markers for studying neurogenesis

The study of APs and BPs as cell populations is greatly helped by the use of a marker allowing the proliferating and the neurogenic cell to be distinguished. *Tis21* (BTG2, in human; PC3, in rat) is a gene with 2 exons coding for a 158 amino acids long protein. It is involved in P53-dependent control of cell cycle progression (G1 to S phase) via interaction with cyclin D1, as shown in cultured cells [175]; but it seems that Tis21 could have a broader influence on transcription of different classes of genes [176-179]. *Tis21* expression was correlated with neurogenesis [180] and its action was implicated in neuronal differentiation *in vitro* [181] and *in vivo* [80, 182]. It was shown that *Tis21* expression marks single neurogenic NE cells and Tis21 protein is inherited by the neurons (that don't express *Tis21* gene) [70] (Fig. 7, B and E). These findings led to the generation of a knock in mouse line in which the first exon of the Tis21 gene was exchanged with the GFP coding sequence, highlighting the neurogenic progenitors (Fig. 7, C and E). The nuclear localization and the stability of the GFP allowed not only single neurogenic progenitors but also their daughters to be tracked; progeny of the neurogenic progenitors was identified as neurons or progenitors according to their migrational

behavior, nuclear size and GFP re-expression after S phase. Moreover, the combination of endogenous GFP with a marker for mitosis allowed to discover the presence of basal mitotic neurogenic progenitors from the onset of neurogenesis in the telencephalon[28].

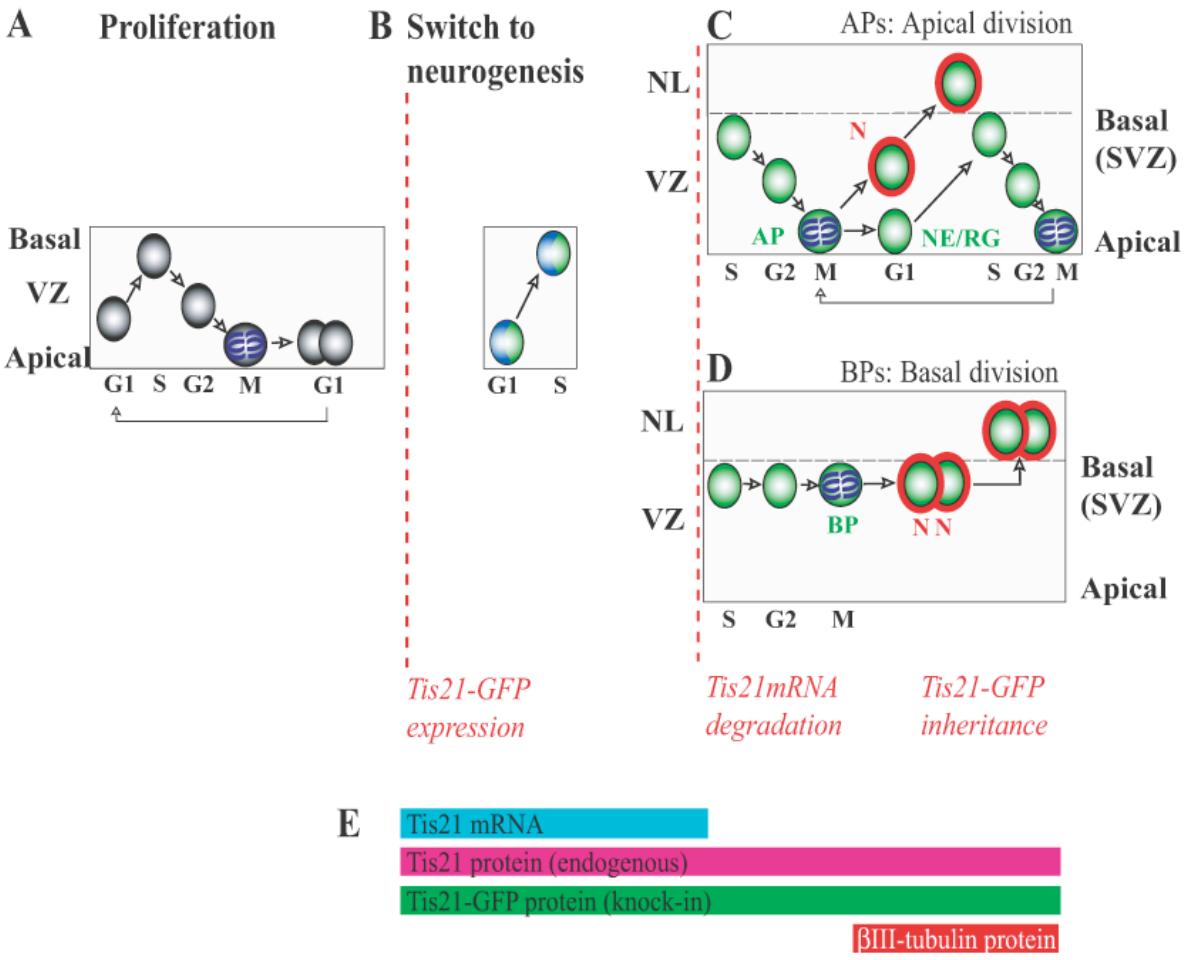


Figure 7 – Schematic drawing describing the expression of the *Tis21* gene correlated with the switch to neurogenesis. (**A**) Nuclei of proliferating cells do not express *Tis21* until some of them switch to neurogenesis. (**B**) When progenitor cells switch to neurogenesis they start expressing *Tis21* (blue half nuclear staining) and transcribing the Tis21 protein. In the *Tis21*-GFP mouse line there is also transcription of Tis21-GFP (green nuclei in **B-D**). Neurogenic cells could divide apically (APs) generating one neuron and a progenitor (**C**) or basally (BPs) generating two neurons and getting consumed (**D**). (**E**) Schematic representation of the time relationship between *Tis21* transcript, Tis21 protein, Tis21-GFP protein and βIIItubulin protein. A-D modified from [28].

In this doctoral work different aspects of the BPs cell biology and the lineage of the daughter cells have been studied (number in brackets refer to the results section).

(II – 1.) *Tis21*-driven GFP expression was validated as a pan neurogenic marker, showing that almost all newborn neurons inherit GFP from the mother.

(II – 1.) The abundance of BPs and APs was monitored in the *Tis21*-GFP mouse, showing that BPs exist since the beginning of neurogenesis and how BPs outnumber APs during development.

(II – 2.) Basal divisions were imaged using two-photon time-lapse in acute brain organotypic slice culture and BPs were identified in fixed tissues, showing that apical contact is lost prior mitosis. A mutant mouse strain was used to study the role of the collapse of the apical contact in the generation of BPs.

To identify newborn cells, arising from Tis21-GFP APs and BPs, as neurons, during the time-lapse, we sought to use a marker expressed immediately after neuronal birth. Neuronal microtubules have unique stability properties achieved through developmental regulation of tubulins and microtubule-associated proteins. One of the most specialized tubulins, specific for neurons, is class III β-tubulin (βIIItubulin or Tubb3). Both up regulation and post-translational processing of βIIItubulin are essential throughout neuronal differentiation. An antibody specifically raised against the non-phosporylated form of βIIItubulin (U-beta6), labeled newly committed neuroblasts expressing neuroepithelial cytoskeletal (Nestin and vimentin) and surface markers (the anti-ganglioside supernatant, A2B5 and the polysialic acid neural adhesion molecule, PSA-NCAM), as well as differentiating neurons in both CNS and PNS. This makes βIIItubulin one of the earliest neuronal lineage markers known so far [183].

(II - 3.1.) A Bacterial Artificial Chromosome (BAC), containing the full-length βIIItubulin gene and 50kb-long up- and downstream regions, was engineered to obtain a new transgenic mouse strain highlighting all the neurons immediately after their birth by expression of GFP targeted to the plasma membrane.

(II - 3.3.) The BAC transgenic mouse line was crossed with the existing *Tis21*-GFP knock-in line.

(II - 3.4. /3.5.) This new transgenic line was used to image, using two–photon time lapse and acute brain organotypic slice culture, mitotic APs and BPs and to track the neurons arising from apical and basal divisions. Young neurons extending processes, seemingly touching the ventricle, and Golgi apparatus moving towards the leading edge of neurons prior to migration were detected, early during neurogenesis.

(II - 3.6.) More interestingly, APs and BPs were shown to be different not only in the daughter's fate but also in the kinetic of acquisition of neuronal characteristics: daughters of BPs express βIIItubulin-driven GFP (βIIItubulin-GFP) significantly faster than daughters coming from apical neurogenic divisions.

I – 4.2.
Adult neurogenesis

The use of base analogs as [H^3]-thymidine, first, and BrdU, later, has changed our view about adult neurogenesis [104-106]: with these base analogs it is possible to detect cycling cells in any given moment of the life of the animal. However, these methods present some disadvantages.

(i) After 3 or 4 cycles of division these base analogs are diluted below detectability level [184], leading either to an underestimation of the number of daughter cells of highly mitotic progenitors or to the necessity to administer high doses (potentially toxic) of the cell tracer.

(ii) Detection of these compounds requires treating fixed tissue, excluding a priori every chance to image neurogenesis in vivo.

(iii) [H^3]-thymidine and BrdU mark every cycling cell including gliogenic progenitors, this makes it necessary to use cellular markers to identify the cell type, especially in cases (like the experimentally induced brain insults) in which dividing glial cells are the major contributors of the proliferating cell population.

Viruses were recently used to track cells in vivo, however some viruses (retroviruses) preferentially infect mitotic cells (precluding in this way the targeting of the slow cycling stem cells), and the low infection efficiency makes it very laborious to study entire cell populations. Moreover, *in vivo* intracranial injection can provoke activation of reactive glia and even death of the animal. In vivo genetic targeting of entire cell populations was recently used for detecting and tracking newly generated neurons. Using the Nestin promoter to drive GFP expression Yamaguchi and co-workers detected and tracked newly generated cells in the SEZ and in the RMS [185], while Kronenberg and co-workers used the same mouse to show adult neurogenesis following brain injury [168]. Transgenically targeted ablation of dividing GFAP-expressing cells in

the SEZ and SGCL showed that GFAP positive progenitors are the source of all new neurons generated during adulthood [132]. It was recently shown that using the doublecortin promoter it is possible to mark the transit amplifying population (Aigner, L. oral communication at ELSO, 2005), and using the proopiomelanocortin promoter to drive GFP expression it was possible to selectively visualize adult newborn neurons but not progenitors [186]. The *in vivo* genetically driven targeting seems to be the most promising approach, allowing *in vivo* labelling of a specific progenitor subpopulation following its fate over time. However, it does not give any information specifically about the neurogenic cells.

I – 4.2.1
The *Tis21*-GFP mouse line is a tool to study adult neurogenesis

In this context a mouse model in which the neurogenic progenitors are selectively labelled with a fluorescent marker could be desirable tool.

(i) It would allow detecting and analyzing neurogenesis focusing specifically on the cells that make neurons *in vivo*.

(ii) It would make possible to elucidate if all transit amplifying cells are neurogenic or if there is a proliferative subpopulation distinct from a neurogenic subpopulation dividing (symmetrically or asymmetrically) to generate neurons, as it happens during development.

(iii) It would allow to study the characteristic of the neurogenic cells in the adult.

(iv) It would help to readily quantify the level of neurogenesis without using cell division tracers.

In this doctoral work the *Tis21*-GFP knock-in mouse was characterized as tool for studying adult neurogenesis.

(II – 4.1.) Tis21-GFP was found in the regions where neurogenesis is known to happen in the adult.

(II – 4.2.) Tis21-GFP was shown to be expressed in a subpopulation of the Dcx positive transit amplifying cell population, suggesting that not all the transit amplifying cells directly generate neurons.

(II – 4.2.) Tis21-GFP was shown to be inherited by the maturing neurons (NeuN, Prox1 positive cells), marking not only the neurogenic progenitors but also the surviving daughter neurons.

(II – 4.3.) Tis21-GFP positive cells proliferation was shown to reflect the known gradients of neurogenesis in the SEZ and DG.

II Results

II – 1. Tis21-GFP as a tool for studying basal progenitors

To validate the use of the *Tis21*-GFP mouse strain to study the totality of neurogenic divisions it was necessary to show that Tis21-GFP positive cells are the only source of neurons during development. It was known that neurons do not express the *Tis21* message but rather inherit the Tis21 protein from the mother [70]. This implies that, if all neurons derive from a Tis21-GFP positive progenitor, all neurons that are close enough to birth and did not degrade yet GFP must display nuclear GFP inherited from the mother NE/RG cell. Therefore neurons were identified as newborn in cryosections and scored for GFP nuclear fluorescence, to ascertain if the entirety of the newborn neurons were GFP positive.

II - 1.1.
Tis21 is a pan neurogenic marker

The neurons were subdivided in two classes: newborn and young neurons, according to their age (time after generation).

Newborn neurons (Fig. 8, arrowheads) were identified accordingly to the following criteria.

(i) βIIItubulin immunoreactivity.

(ii) Nucleus located within the VZ.

(iii) Presence of leading and/or trailing cytoplasmic tail.

(iv) Orientation of the nucleus perpendicular to the ventricular surface.

Young neurons (newborn neurons that have left the VZ) (Fig. 8, arrows) were identified using the same criteria used for the newborn neurons except the positional criterion (ii), that was changed including only neurons of the lower (apical side) border of the NL, and the nuclear orientation criterion (iv) that was changed including only the neurons whose nucleus was parallel to the ventricle. Two different regions of the developing neural tube, Hindbrain (Fig. 8, A) and Telencephalon (Fig. 8, B) at two different developmental stages, E10.5 (Fig. 8, A) and E11.5 (Fig. 8, B), were examined for presence of GFP positive neurons.

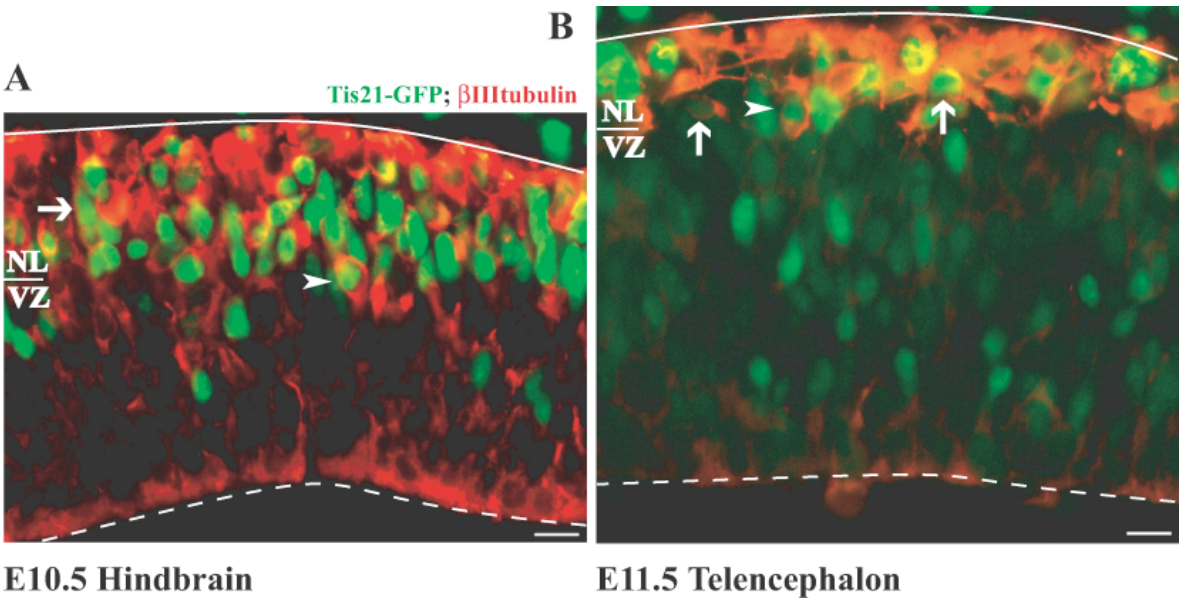


Figure 8 – All newborn neurons display Tis21-GFP fluorescence. Examples of pictures used for assessing GFP presence in newborn and young neurons. Bright field fluorescence photomicrographs of *Tis21*-GFP mouse E10.5 Hindbrain (**A**) and E11.5 Telencephalon (**B**). Cryosections stained with antibody against βIIItubulin. Tis21-GFP was detected by its intrinsic fluorescence = green, βIIItubulin immunofluorescence = red. Arrowheads indicate newborn neurons, arrows indicate young neurons. Dashed line indicates the ventricular surface, solid line indicates the end of the neuronal layer. NL = Neuronal Layer; VZ = Ventricular Zone. Scale bar = 10um.

The results obtained are summarized in the following table (Table 1):

Brain region	**Newborn neurons**			**Young neurons**		
	total	**GFP-positive**	**%**	**total**	**GFP-positive**	**%**
Telencephalon	29	26	90	87	56	64
Hindbrain	27	27	100	138	74	54

Table 1 – All newborn neurons inherit Tis21-GFP. Quantification of GFP-containing newborn and young neurons in the *Tis21*-GFP mouse line, E10.5-E11.5 telencephalon and hindbrain. Tis21-GFP was detected by its intrinsic fluorescence. Data are the sum of 10 fields counted for the telencephalon and 15 fields for the hindbrain, with 0-5 newborn neurons and 1-23 young neurons per field. From [28].

Almost the totality of the newborn neurons was positive for Tis21-GFP, from this we concluded that GFP is inherited by all of neurons after birth. Tis21-GFP is then gradually degraded, as shown by the finding that around 60% of the young neurons are GFP positive, and finally lost by the whole neuronal population (higher layer neurons are GFP negative starting from E15.5, data not shown) [28].

II - 1.2.
The abundance of basal progenitors changes during development

The use of Tis21-GFP as a marker of neurogenic cells allowed to detect basal neurogenic divisions as early as E10.5 in the cortex. We sought, then, to clarify the relationship between BPs and the appearance of the secondary germinal layer known as the Sub ventricular Zone (SVZ), which was believed to exclusively generate glial cells. For this purpose, the abundance of BPs over developmental time was evaluated. Mitotic progenitors were identified by immunostaining with an antibody against the phosporylated form of Histone 3 (PH3). In *Tis21*-GFP embryos, the mitotic progenitors were counted at different developmental stages, from the onset of neurogenesis. Two different regions of the developing CNS were compared: neocortex and hindbrain. Apical (Fig. 9, A, B, arrows) and sub apical (Fig. 9, A, B, asterisks) divisions were grouped in the same class, since both of them were shown to divide asymmetrically to generate neurons [28]; their number was compared to the number of basal mitoses (Fig. 9, arrowheads). Apical/sub apical and basal mitoses were scored for Tis21-GFP expression and plotted as a function of the number of all mitotic cells (GFP negative and positive) found in the VZ and, when present, SVZ mitoses (Fig. 9, A and B).

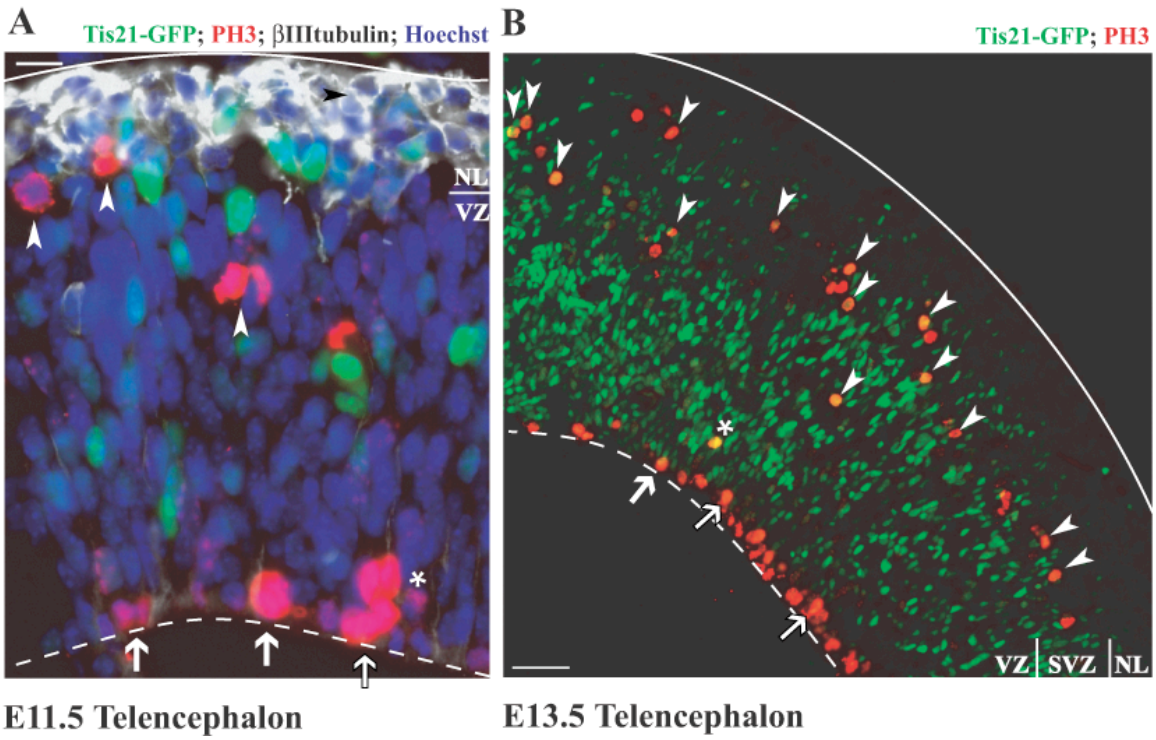


Figure 9 – APs and BPs in the developing neuroepithelium. Pictures showing the coexistence of apically, subapically and basally dividing cells at the onset of neurogenesis. Bright field fluorescence photomicrographs of *Tis21*-GFP mouse E11.5 (**A**) and E13.5 (**B**) Telencephalon. Cryosections stained with an antibody against PH3 (**A** and **B**, red) and with an antibody against βIIItubulin (**A**, white). Green is intrinsic GFP fluorescence, Blue is Hoechst. (**A**) Arrows indicate apically dividing cells, asterisk indicates a subapically dividing cell, arrowheads indicate basally dividing cells. (**B)** Arrows indicate apically dividing neurogenic cells (APs), asterisks indicate subapically dividing cells, arrowheads indicate basally dividing neurogenic cells (BPs). Dashed line indicates the ventricular surface, solid line indicates the end of the neuronal layer. NL = Neuronal Layer; SVZ = Sub ventricular Zone; VZ = Ventricular Zone. Scale bars: 10um in A, 50um in B.

At the onset of neurogenesis (E10.5 telencephalon), GFP positive mitotic cells were observed not only at the apical surface of the neuroepithelium, but also in the basal region of the VZ (Fig. 10, A, blue and yellow curve E10.5). As neurogenesis progressed, the mitotic BPs in the telencephalon (Fig. 10, A, yellow curve) increased in number more rapidly than mitotic APs (Fig. 10, A, blue curve) and outnumbered the latter. The time course of the sum of apical plus basal GFP positive mitotic cells (Fig. 10, A, green curve) was consistent with that of the total (mitotic plus interphase) GFP positive cells in the telencephalic neuroepithelium [28]. In the hindbrain, however, BPs did not show any increase (Fig. 10, B, yellow curve) and their proportion was, at all developmental stages, lower than mitotic APs (Fig. 10, B, blue curve). Along the rostro-

caudal axis of the neural tube, mitotic BPs were most frequently observed in the regions known to form a SVZ at later stages. Indeed, mitotic BPs were found to be abundant in the SVZ of the E13.5 telencephalon (Fig. 9, B). In the telencephalon, almost all (≈90%) of the basal mitotic cells observed at the onset of neurogenesis were found to express GFP (Fig. 10, C), and the same was the case once a SVZ had formed (Fig. 9, B). In contrast in the hindbrain the proportion of GFP positive mitotic cells was never more than 70% of all basal mitotic cells (Fig. 10, C).

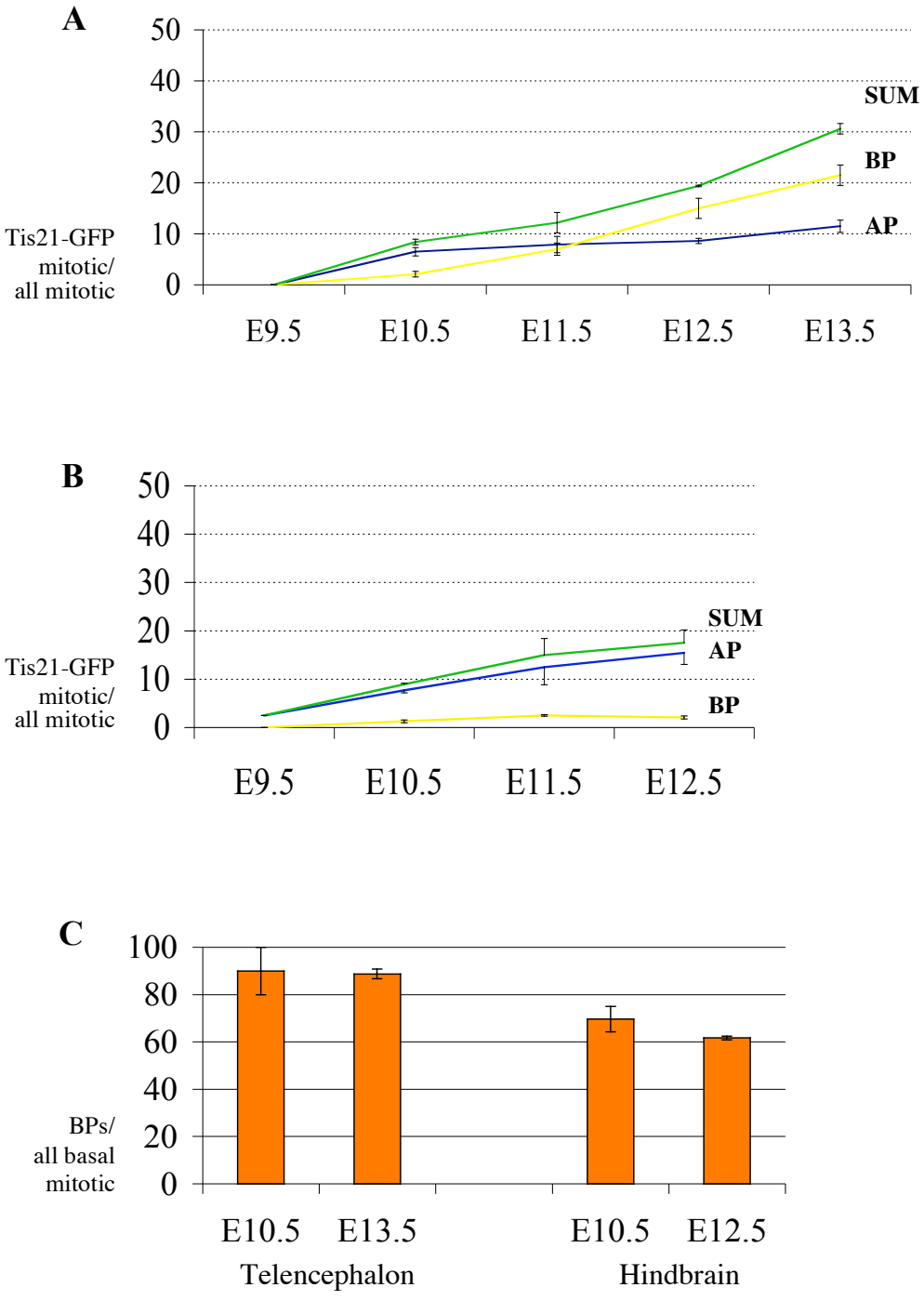


Figure 10 (Previous page) – **Abundance of APs and BPs during development.** (**A-B**) Quantification of mitotic GFP-positive cells at the apical side of the neuroepithelium (blue curve) and in the basal portion of the VZ (plus, when present, the SVZ) (yellow curve), each expressed as percentage of total mitotic cells at the apical side of the neuroepithelium (130-900 cells counted per embryo), as well as the sum of both (green curve), in the telencephalon (**A**) and hindbrain (**B**) at various developmental stages. (**C**) Quantification of mitotic GFP-positive cells in the basal portion of the VZ (plus, when present, the SVZ) of the telencephalon at E10.5 and E13.5 (**A**) and hindbrain at E10.5 and E12.5 (**B**), expressed as percentage of total mitotic cells in the basal portion of the VZ (plus, when present, the SVZ) (4-140 cells counted per embryo). (**A-C**) Data are the mean of two embryos (except for E9.5, which is a single embryo); bars indicate the variation of the individual values from the mean.

From these data we concluded that, from the onset of neurogenesis, neurogenic progenitors dividing at the basal side of the VZ (BPs) coexist with those dividing at the apical side (APs), and eventually outnumber the latter, giving rise to the SVZ, in the mouse embryonic telencephalon. Furthermore, the vast majority (≈90%) of the NE/RG cells dividing on the basal side of the telencephalic neuroepithelium are neurogenic. In contrast in the hindbrain the basal divisions are not only reduced but also percentally less neurogenic (maximum 70% of the basal divisions in the hindbrain are Tis21-GFP positive).

II - 2. Role of the apical contact of basal progenitors

Kosodo and coworkers showed a strong correlation between the inheritance of apical plasma membrane and the fate of daughter cells after apical mitosis [71]. It was also shown that basally dividing cells lose their apical contact prior to mitosis [41]. However, it was still not clear if loss of apical contact happened in both, neurogenic (Tis21-GFP positive) and non-neurogenic (Tis21-GFP negative) symmetrically dividing cell populations on the basal aspect of the neuroepithelium. A difference in fate of the apical contact could contribute explaining the different fate of daughters coming from a basal mitotic Tis21 positive or Tis21 negative cells. Moreover, it was unclear if loss of apical contact implied retraction of the apical domain of the plasma membrane or shedding of it into the lumen. In this doctoral work different imaging approaches have been combined to give an answer to these open questions.

(i) The retraction of the apical plasma membrane prior to mitosis was imaged using time-lapse two-photon microscopy (this approach is here referred to as "dynamic approach").

(ii) The presence of Tis21-GFP was used to distinguish between neurogenic and non-neurogenic basal dividing progenitors.

(iii) The molecule Prominin1 [21] was used as a specific marker of the apical domain of the plasma membrane. (ii and iii are here referred to as "static approach")

II - 2.1.
The dynamic approach: imaging of basal progenitors loosing their apical contact

Single apical and basal mitotic cells were imaged in acute brain organotypic slice culture using two-photon time-lapse microscopy (for more details about the procedure and the experimental set up see the Materials and Methods section). To outline single progenitors, the telencephalic neuroepithelium of E12.5 embryos was targeted *in utero* (see Materials and Methods section for details) with a plasmid coding for GFP localized to the plasma membrane by the targeting signal of the GAP43 protein (GAP43-GFP). After overnight development, the embryos were sliced and living slices of cortical

neuroepithelium were imaged. Five time-lapse two-photon experiments were carried out on acute brain slice culture of E12.5 (+16-20hrs in utero development) electroporated embryos. Each experiment was carried out on a single slice so that each experiment reflects a single embryo; all the experiments are independent from each other. Five movies were suitable for processing and the following data come from these movies.

Mitoses occurring at the apical side of the neuroepithelium were detected in every experiment (Fig. 11, A; Movie 1, supplementary CD). In almost all cases observed apical mitotic kept their basal contact during mitosis (Fig.11, A, arrowheads) in agreement with the data obtained by Miyata and coworkers [92].

Mitoses occurring at the basal side of the neuroepithelium were detected more rarely, in accordance with the relatively low abundance of basal mitoses observed at this developmental stage (E12.5 + 16-20h in utero development) (Fig. 11, B; Movie 2, supplementary CD). In all cases observed basal mitotic cells lack both apical contact and apically oriented plasma membrane (Fig. 11, B, 204'), confirming our previous observations. In two cases it was possible to track the retraction of the plasma membrane prior to mitoses. In one of the cases the retraction started about 140' prior to mitosis (Fig. 11, B, red arrowhead, 60') and terminated immediately before mitosis (Fig. 11, B, red arrowhead, 180').

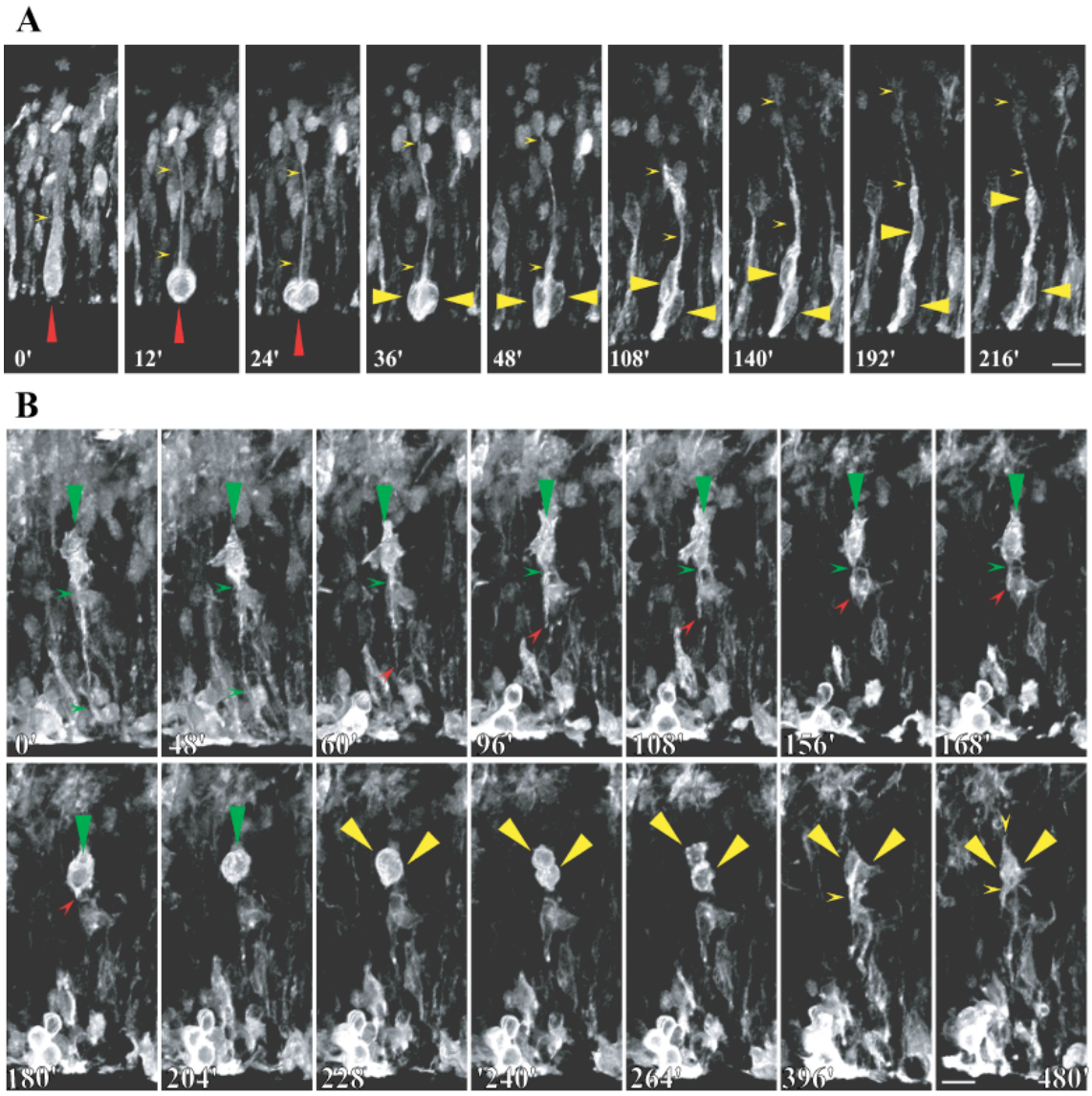


Figure 11 – Cell processes imaged prior to and during apical and basal divisions. Two-photon time-lapse scanning microscopy (acute brain slice cultures *Tis21*-GFP mouse developing cortex) showing an apical (**A**) and a basal (**B**) division of progenitors. Each frame represents a single time point and is the result of the three-dimensional reconstruction of several stacks (2.7um Z stack step, 10' or 12' interval between two frames). Embryos were electroporated *in utero* with a construct coding for GAP43-GFP at E12.5 and allowed to develop for 20h. Brains were dissected and sliced; culture was carried out in controlled environment while imaging was performed. (**A**) An apical cell (red triangle) rounds up and divides (12'-36') the two daughters (yellow triangles) migrate towards the basal side (36'-216'). The yellow arrowheads show the basal process of the cell kept during mitosis. (**B**) A basal cell (green triangle) with its apically directed process (green arrowheads) (0'-48'). Prior to mitosis the cell loses its apical contact (red arrowhead, 60'-180'), however the fate of the apical domain of the plasma membrane is not clear. The cell rounds up (204') and divides (228') giving rise to two daughter cells morphologically similar to newborn neurons (yellow triangles, 240'-480'). Red and green triangles indicate mother cells, yellow triangles indicate daughter cells, white, green and red arrowheads indicate cell processes. Apical side is down, basal side is up. Scale bar = 5um.

We concluded that process retraction happens during the late-S and G2 cell cycle phases, in accordance with the data coming from other laboratories [41]. However, the limited resolution compatible with *in vivo* imaging coupled with the cell-labeling technique used, did not allow us to distinguish whether the apical domain of the plasma membrane was shed or retracted towards the nucleus.

II - 2.2.
The static approach: the apical plasma membrane domain is lost in both neurogenic and non-neurogenic basal dividing cells

The presence or absence of an apically directed process and/or apical plasma membrane was assessed in basal mitotic cells, using confocal microscopy and immunostaining of fixed samples. To assess the presence or absence of an apical contact, the cells dividing on the basal aspect of the *Tis21*-GFP mouse cortical neuroepithelium were outlined using the two different methodologies described below.

(i) Slices of fixed tissue (E11.5 embryos) were stained with an antibody against a cytoplasmic mitosis-specific epitope: MPM2 [187] (Fig. 12, A-D).

(ii) E12.5 embryos were electroporated *in utero* with a construct coding for a cytoplasmic monomeric Red Fluorescent Protein (mRFP) [188] (see materials and methods for details); after 16-20h of *in utero* development, the embryos were collected, fixed and sliced (Fig. 12, E-H). Mitotic cells were identified either by their condensed chromatids (Fig. 12, E) and/or by immunostaining with an antibody anti PH3.

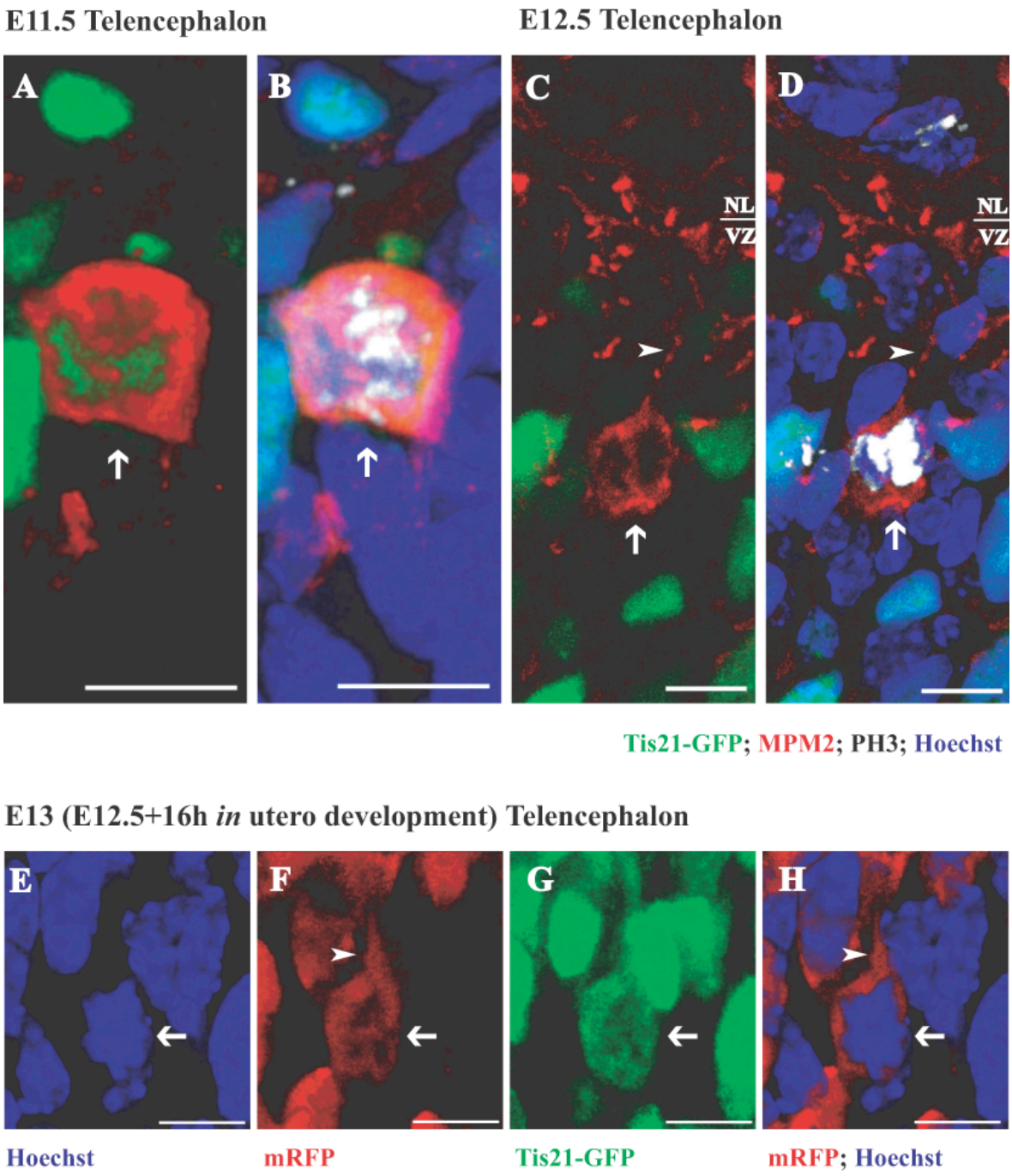


Figure 12 – Both Tis21-GFP positive and Tis21-GFP negative mitotic basal cells lack apical contact. Examples of photomicrographs used for assessing the presence of apical contact or an apically directed process in basal mitotic neurogenic and non-neurogenic progenitors. Three-dimensional reconstruction, obtained from confocal Z stacks (0.5-0.7um step), of mitotic cells of *Tis21*-GFP mouse E11.5 Telencephalon (**A, B**), E12.5 Telencephalon (**C, D**) and E12.5 + 20h *in utero* development (**E-H**). Cryosections stained for the mitotic markers MPM2 (cytoplasm, red) and PH3 (nucleus, white) (**A-D**), or electroporated with mRFP (**E-H**). Green is intrinsic Tis21-GFP fluorescence, Blue is Hoechst. Arrowheads indicate pial directed processes (**C, D** and **E-H**); arrows indicate basal mitotic cells (**A-H**). Apical side is down, basal side is up. NL = Neuronal Layer; VZ = Ventricular Zone. Scale bar = 5um.

The three-dimensional structure of cortical basal mitotic cells was reconstructed from single confocal Z sections and cells were scored for the following criteria.

(i) Presence of nuclear GFP.

(ii) Presence or absence of apical contact.

(iii) Presence or absence of an apically directed cellular process.

Some of the basally dividing cells showed a pial directed process (Fig. 12 C, D, F and H, arrowheads); however, probably due to the little thickness of the slices, it was not possible to track this process all the way to the pial surface. The data are summarized in the table below (Table 2):

	Total	Apical contact	Apical process	No process
TIS21-GFP positive	15	0	2	13
TIS21-GFP negative	8	0	2	6

Table 2 – Both Tis21-GFP positive and Tis21-GFP negative mitotic basal cells lack an apical contact. Quantification of the presence of apical contact or apically directed process (never extending towards the apical side more than one cell diameter) in basal mitotic NE/RG cells in the *Tis21*-GFP mouse E11.5 - E13.0 telencephalon. Tis21-GFP was detected by its intrinsic fluorescence; cell shape was assessed by immunostaining with MPM2 or mRFP electroporation. Data are the sum of 23 fields with 1 dividing cell per field, single confocal Z stacks were collected with a step of 0.5 m, only cells in the middle part of a 14-20um thick slice were scanned. Imaris software was used for three-dimensional reconstruction.

From these data we concluded that basal mitotic cells lack apical contact; however, a small fraction of the basally dividing cells (less than 10%) showed a process directed towards the apical surface, but it never elongated further than one cell diameter. Most probably this process represents an early stage of the collapsing apical membrane.

However, it was sill not clear if the apical plasma membrane domain was retracted or shed in the ventricle during loss of apical contact. To clarify this issue, we used a specific marker for the apical domain of the plasma membrane and the *Tis21*-GFP mouse to detect neurogenic cells. The presence of mitotic cells (apical and basal) was detected in fixed tissue cryosections using the anti MPM2 antibody that highlights the whole cell body; concomitantly the tissue was stained with the apical plasma membrane marker Prominin1 [21] to detect the presence of the apical plasma membrane domain in the mitotic cells. (Fig. 13, A-H). We then scored both Tis21-GFP positive (Fig. 13, A-

D) and Tis21-GFP negative (Fig. 13, E-H) basal mitotic cells for Prominin1 and found that all basal dividing cells, irrespective of the presence or absence of Tis21-GFP, were negative.

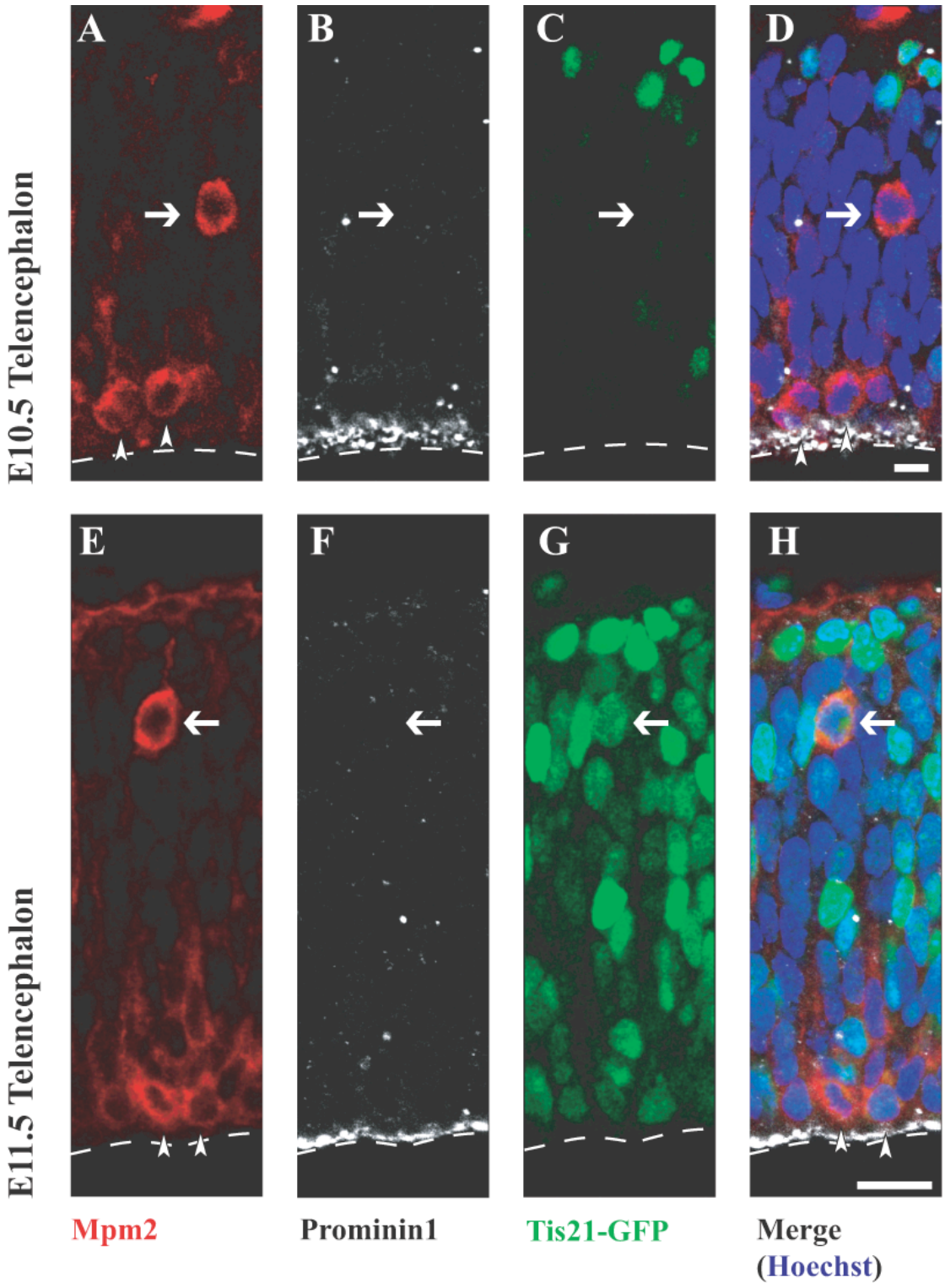


Figure 13 (Previous page) **– Both Tis21-GFP positive and Tis21-GFP negative mitotic basal cells lack the apical domain of the plasma membrane.** (**A**-**H**) Examples of photomicrographs used for assessing the presence of the apical domain of the plasma membrane in basal mitotic neurogenic and non-neurogenic progenitors. Single confocal planes of *Tis21*-GFP mitotic cells. Embryonic telencephalic neuroepithelium, at different time of development: E10.5 (**A**-**D**) and E11.5 (**E**-**H**). Cryosections, 12um thick, stained with anti MPM2 antibody (**A** and **E**, red), anti mouse Prominin1 (**B** and **F**, white) and Hoechst (**D** and **H**, blue); green is Tis21-GFP intrinsic fluorescence. Arrows indicate basal mitotic cells, negative for Prominin1; arrowheads indicate apical mitotic cells positive for Prominin1. Dashed line indicates the ventricular surface. Apical side is down, basal side is up. Scale bar = 10um (**A**-**D**), 15um (**E**-**H**).

These results suggests that the apical domain of the plasma membrane is not maintained during mitosis and are in accordance with the observation that Prominin1 positive particles are found in the lumen of the neural tube [32] and shed by the apical surface of the NE cells (Dubreuil V. unpublished observations). Interestingly, there was no difference between neurogenic (Tis21-GFP positive) and non-neurogenic (Tis21-GFP negative) cells, showing that the absence of apical contact is a common feature of both cell populations.

II - 2.3.
Imaging of the progenitor apical plasma membrane domain in the Tis21-GFP mouse

To corroborate these data we sought to visualize the loss of the apical domain of the plasma membrane using two-photon time-lapse microscopy. For this purpose it was necessary to achieve labeling of single cells, together with specific labeling of the apical domain of these single cells. Moreover, we wanted to do so in the *Tis21*-GFP mouse line, to be able to distinguish BPs from basal non-neurogenic dividing cells. This was obtained by coelectroporating a construct encoding for mRFP, to highlight the cell shape, together with a fusion construct between the mouse Prominin1 and GFP (mProm1-GFP) (kind gift of Dr. Denis Corbeil, Biotechnological Centre (Biotec) of the Technische Universität, Dresden), to specifically target the apical plasma membrane. Using an appropriate concentration of the mProm1-GFP construct (0.5μg/μl) it was possible to achieve an exclusive, reproducible localization on the apical domain of the plasma membrane of the transfected mProm1-GFP (Fig. 14, A and B, arrowheads and Movie 3, Supplementary CD). The simultaneous imaging of the two different channels (red and green) was possible using the two-photon set up available to us; the two different fluorophores (mRFP and GFP) were excited using a single wave length

(890nm) and the two colors were separated by emission filters. Electroporated cells could be detected together with their processes (Fig. 14, C; Movie 4, supplemetary CD) and it was possible to identify them as Tis21-GFP positive or negative. However, the time-lapse was technically difficult. To be able to excite of mRFP at the afore mentioned wavelength, a high amount of energy was required; this was non- compatible with the survival of the slice, causing death of the tissue. Five experiments were carried out, it was not possible to draw a conclusion because of the tissue death or because of it was extremely difficult to detect the mRFP electroporated cells.

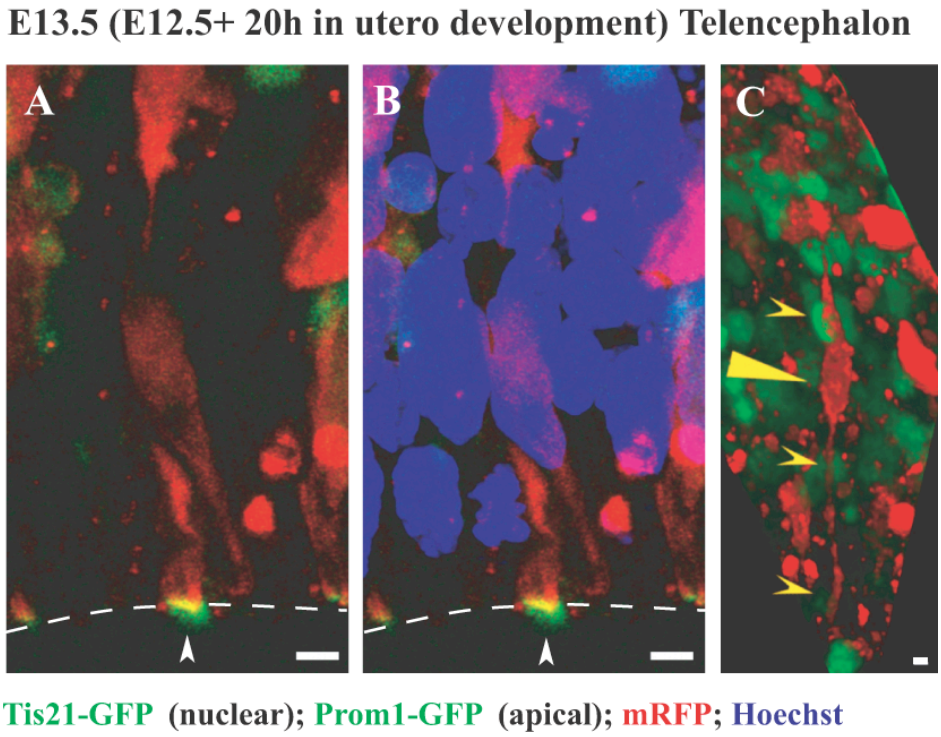


Figure 14 – Specific labeling of the apical domain of the plasma membrane in single cells. (**A-B**) Photomicrographs showing specific apical plasma membrane localization of the electroporated mProm1-GFP. Three-dimensional reconstruction, obtained from single focal planes (0.5-0.7um step), of the apical plasma membrane of cells coelectroporated with mRFP and mProm1-GFP. *Tis21*-GFP embryos were coelectroporated in utero at E12.5 with a construct coding for mPronm1-GFP together with a construct coding for mRFP and allowed to develop for 20h. Brains were dissected, fixed and sliced; imaging was performed on the fixed cryosections stained with Hoechst (Blue). Nuclear green is intrinsic Tis21-GFP fluorescence, apical plasma membrane green is electroporated mProm1-GFP fluorescence, red is electroporated mRFP fluorescence. The white arrowheads indicate the apical domain of the plasma membrane. (**C**) Single time point of a two-photon time-lapse microscopy (Movie 4, supplementary CD), result of the three-dimensional reconstruction obtained from single focal planes (2.7um step) of single NE/RG cells electroporated with mRFP. *Tis21*-GFP embryos were electroporated in utero at E12.5 with a construct coding for mRFP and allowed to develop for 20h. Brains were dissected and sliced; culture was carried out in controlled environment while imaging was performed. The yellow triangle points to the body of a cell, the yellow arrowheads point to the apical and basal processes of this cell. Dashed line indicates the ventricular surface. Apical side is down, basal side is up. Scale bar = 1um.

II - 2.4.
The role of cell polarity in the generation of BPs

NE/RG cells are highly polarized along the apical-basal axis. To elucidate the role of cell polarity in the generation of BPs, we investigated the function of Cdc42 in the developing neuroepithelium. This work was carried out in collaboration with the group of M. Goetz from the GSF, Munich. Cdc24 is a GTPase of the Rho family involved in polarity and intracellular trafficking [189, 190]. Conditional deletion of the *Cdc42* gene, from around E9.5 in the developing cortex, was achieved by crossing a mouse line carrying the exon-2 of the *Cdc42* gene flanked by lox-P sites [191] with a mouse line expressing the Cre recombinase from the Emx1 locus (Emx1::Cre) [192]. Littermates embryos $Cdc42^{\Delta ex2/\Delta ex2}$, $Cdc42^{\Delta ex2/WT}$ and $Cdc42^{WT/WT}$ were electroporated in vivo with GAP43-GFP to label single cortical progenitors; since the plasmid is taken up from the ventricle, it only labels cells with an apical process. The electroporated embryos were cultured *ex* utero for 16 hours [193 194], then the presence or absence of an apical process was assessed by 3D reconstruction of single GAP43-GFP-labeled cells in 60-130 µm thick fixed telencephalic slices using multi-photon microscopy (Fig. 15, A and B). Virtually all the single progenitors GAP43-GFP positive in the $Cdc42^{\Delta ex2/WT}$ cortex showed an apical process that could be followed to the ventricular surface (only 2.7% lacked this process) (Fig. 15, A and C, left column). However, in the $Cdc42^{\Delta ex2/\Delta ex2}$ cortices 13% of the single progenitors GAP43-GFP positive either showed no apically-directed process or showed a process that did not reach the ventricular surface (Fig. 15, B and C, right column).

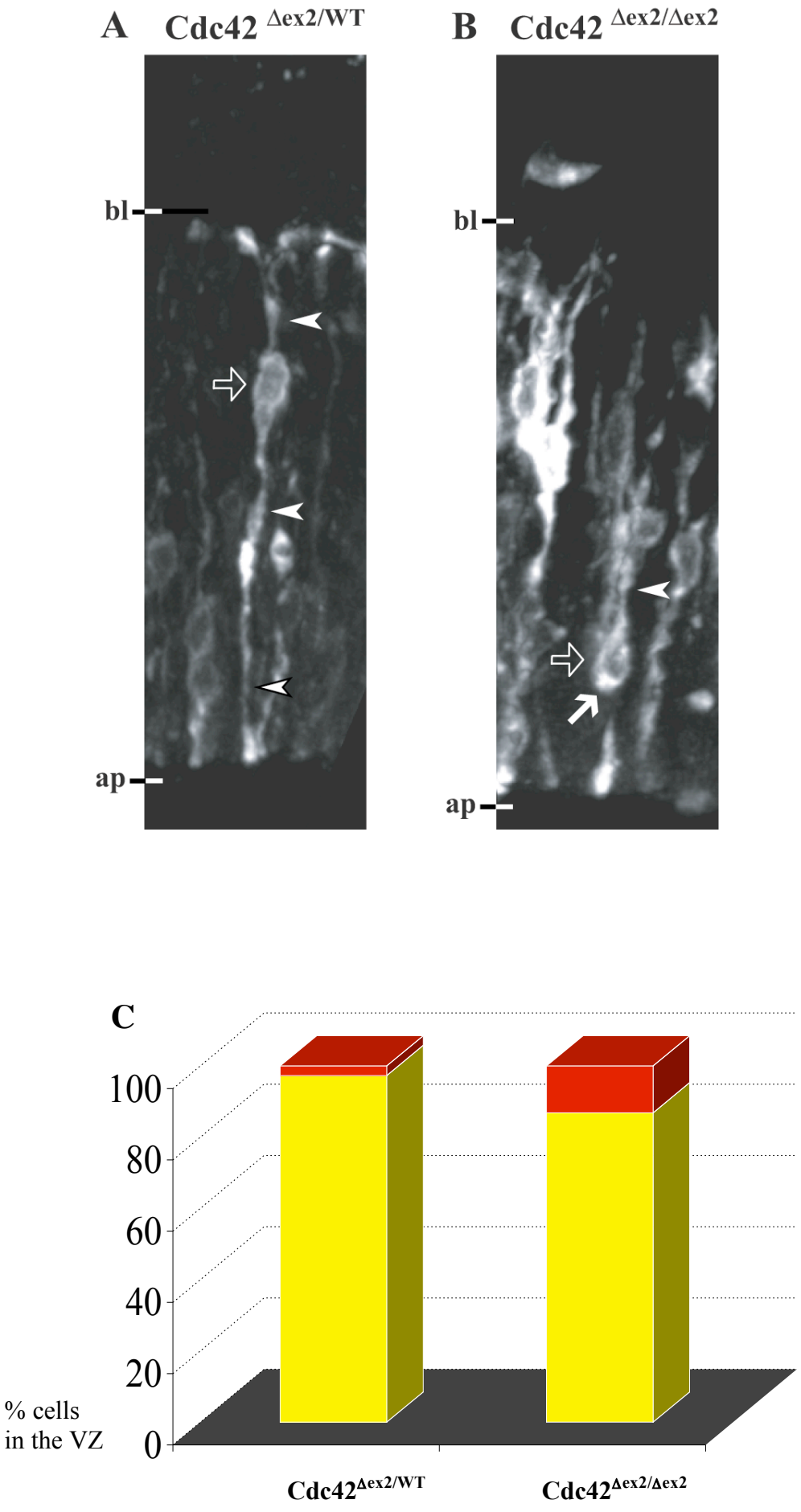


Figure 15 – Cdc42 deficient progenitors lacking apical contact. (**A-B**) Examples of photmicrographs used for assesisng the presence in the heterozygous (**A**) or the absence in the homozygous (**B**) Cdc42 knockout of the apical process of electroporated progenitors. Three-dimensional reconstruction, obtained from single two-photon focal sections (0.5um step, 1024x1024 pixels resolution, maximum intensity projection), of the apical plasma membrane of Cdc42mutant mouse progenitor cells electroporated with GAP43-GFP. Embryos were collected at E10.5, electroporated *ex utero* with a construct coding for GAP43-GFP and allowed to develop for 16h iin colture. Brains were dissected, fixed and sliced; imaging was performed on the fixed slices. Empty arrows indicate the cell bodies; arrowheads indicate apical and basal cell processes; solid arrow indicates the absence of an apically-directed process. (**C**) Quantification of the cells with a process reaching the ventricular surface (yellow) and with a process interrupted before reaching the ventricular surface (red) of $Cdc42^{\Delta ex2/WT}$ (n = 104 cells from 3 animals, 2 litters) and $Cdc42^{\Delta ex2/\Delta ex2}$ (n = 92 cells from 2 animals, 2 litters) embryos. Ap = apical side, Bl = Basal side. Scale bar = 10um. Modified from [195].

These data showed that deletion of *Cdc42* in the telencephalic neuroepithelium leads to an increase of progenitors lacking the apical contact. This correlated with an increase in the number of abventricular mitoses, of Tbr2-positive cells, and of neurons suggesting that deletion of *Cdc42* causes an increase in BP-like cells [195].

II – 3. Study of mitosis of neurogenic NE/RG cells by imaging

A genetic approach to mark the entire neurogenic progenitor population since the onset of neurogenesis was already successfully developed in the lab [28]. We wanted to combine it with the genetic marking of the whole neuronal population, to study neurogenic divisions and track their daughters since the onset of neurogenesis.

II - 3.1.
Generation of the new BAC transgenic line "*Tubb3*-GFP"

The *βIIItubulin* gene (*Tubb3*), which codes for a neuronal specific class of tubulin and is expressed early after differentiation [183, 196], was used to drive GFP expression in order to visualize all the neurons immediately after their birth. A BAC approach was used in order to achieve a reliable neuronal GFP expression, since the *βIIItubulin* minimal promoter was not characterized at the time. A Bacterial Artificial Chromosome (BAC) clone, containing the whole *βIIItubulin* gene and spanning the mouse genome 50kb up- and downstream of the *βIIItubulin* locus was selected. Given the large size of the clone, we were confident it included not only the minimal promoter but also the relevant sequences that control levels, timing and localization of the protein, even if they were located at a great distance from the *βIIItubulin* ORF. The BAC clone modification was achieved by the external company *GENE BRIDGES*, using the recently developed RED-ET based recombination method [197, 198]. By use of a sequence-specific recombinase, a GAP43-GFP (see II – 2.1.) was inserted after the start codon of the *βIIItubulin* ORF (Fig. 16, A and B). The correct modification of the BAC clone was confirmed by digestion with restriction enzymes. The construct, including the modified BAC and the backbone, was purified and linearized by enzymatic digestion. The linearized construct was injected in the male pronucleus of fertilized oocytes, by Ronald Naumann (Dipl. Ing Naumann R., Transgenic Core Facility, MPI-CBG, Dresden). The oocytes were implanted into foster mothers (for details about the procedure and number of injections and embryo transfers see the Materials and Methods section). Two chimeras were positive by Southern blot analysis and PCR. The amount of concatamers integrated in the genome was not checked; the ratio of transgenic versus WT pups generated by each

transgenic mouse showed that integration of the transgene (in this term including either a single copy or a concatamer) occurred in a single locus of an autosomal chromosome. The chromosome where the integration occurred was not identified. Only one male showed germ line transmission: the entirety of the line, here referred to as "*Tubb3*-GFP", was derived from this male by crossing with C57Bl6 mice. The mice showed no obvious phenotype and bred normally giving rise to transgenic pups according to the expected Mendelian ratio. Only heterozygous pups were used for all the experiments. Mice were genotyped by Southern blot hybridization (Fig. 16, C), PCR or genetically by backcrossing.

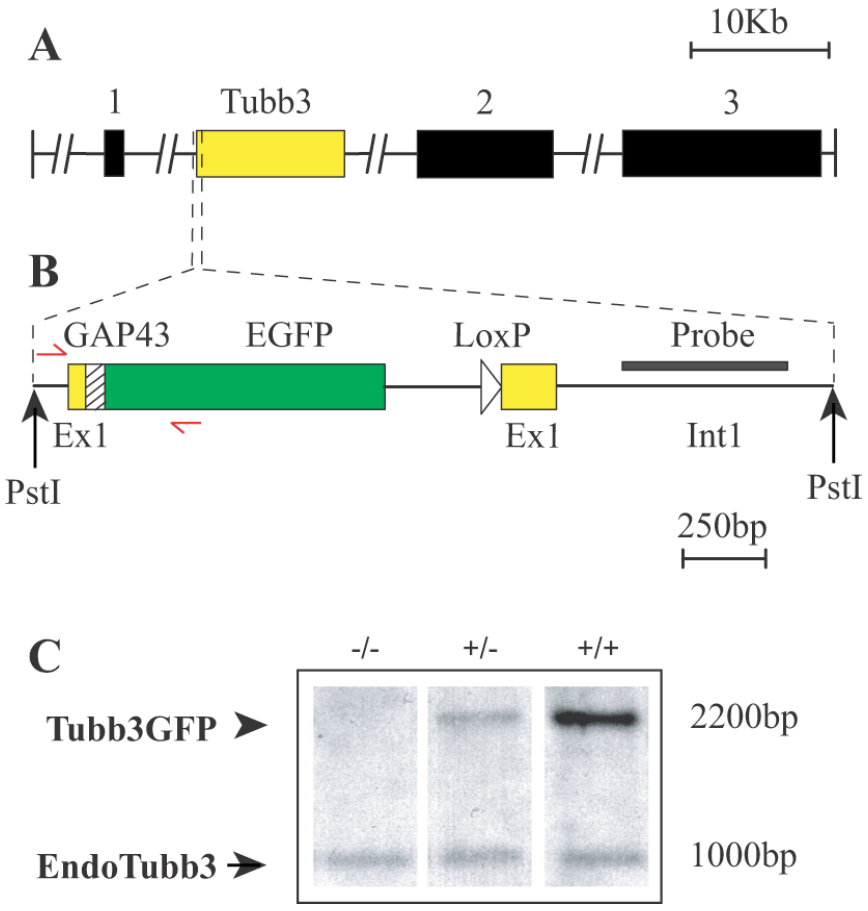


Figure 16 – Generation of the βIIItubulin-GFP construct. (A) Schematic representation of the genomic insert of the BAC clone used for the RED-ET mediated recombination. Solid boxes represent the identified genes present in the clone (Celera ID rp23-214j5). Melanocortin1 receptor (Mc1r) (1), βIIItubulin (Tubb3), RIKEN cDNA2810427I04 gene (2810427I04Rik) (2), growth arrest specific 11 (Gas11) (3). (**B**) Detail of the construct after recombination including: the initial part of exon 1 of the *βIIItubulin* gene (solid left yellow box), the GAP43 localization signal (white-striped box) the myc tag (not shown), the GFP (solid green box), the LoxP site (empty triangle), the second part of the exon 1 of the βIIItubulin gene (solid right yellow box), a portion of the first intron of the *βIIItubulin* gene. Arrows indicate the PstI cut sites used for the southern analysis, the gray bar on exon1 indicates the probe (length

–continues from previous page- in scale) used for the southern hybridization. Half red arrows indicate the oligonucleotides used for genotyping the animals. (**C**) Southern blot analysis of the F2 generation transgenic mice: the lower band (arrow) reflects the endogenous genomic *βIIItubulin* presence (approximately 1000bp), the higher band (arrowhead, approximately 2200bp), including GFP, reflects the presence of the transgenic βIIItubulin-GFP. Note that the intensity of the band is double in the homozygous transgenic animal. -/- = absence of the transgene (WT); +/- = presence of the transgenic allele in one of the parental chromosomes (heterozygous); +/+ = presence of the transgenic allele in both of the parental chromosomes (homozygous).

II - 3.2
βIIItubulin-GFP is restricted to the neuronal plasma membrane and Golgi apparatus

The appearance of green fluorescence in the developing nervous system (CNS and PNS) of *Tubb3*-GFP transgenic mice embryos and early postnatal (E9.5 - P1) correlated precisely with the known temporal and spatial gradients of neurogenesis, and was detectable without antibody enhancement. βIIItubulin-GFP starts being expressed in the trigeminal ganglia at E9.5 (Fig. 17, A and A' arrowheads), then, at E10.5 it is detected throughout the spinal cord (Fig. 17, B, B', E, H,), the hindbrain (Fig. 17, B, B', E, arrowheads) and the ventral portion of the mesencephalon (Fig. 17, B, B' arrow). Later on (E11.5) βIIItubulin -GFP expression starts in the dorsal midbrain (Fig. 17, C, C', I, arrowheads) and ventral telencephalon (Fig. 17, C, C', I, arrows); by E12.5 βIIItubulin -GFP expression starts spreading to the dorsal telencephalon (Fig. 17, D', Q, arrowheads). Note in figure 17 (panels A'-D') the increase of fluorescence levels correlating with the increasing number of neurons being generated. Green fluorescence was maintained in the early postnatal (P1) and adult (P8 weeks) animals nervous system. In old animals (P 60 weeks) the dissected brain was not fluorescent except for the olfactory bulb, where newly generated neurons are known to reside during the entire life of the animal.

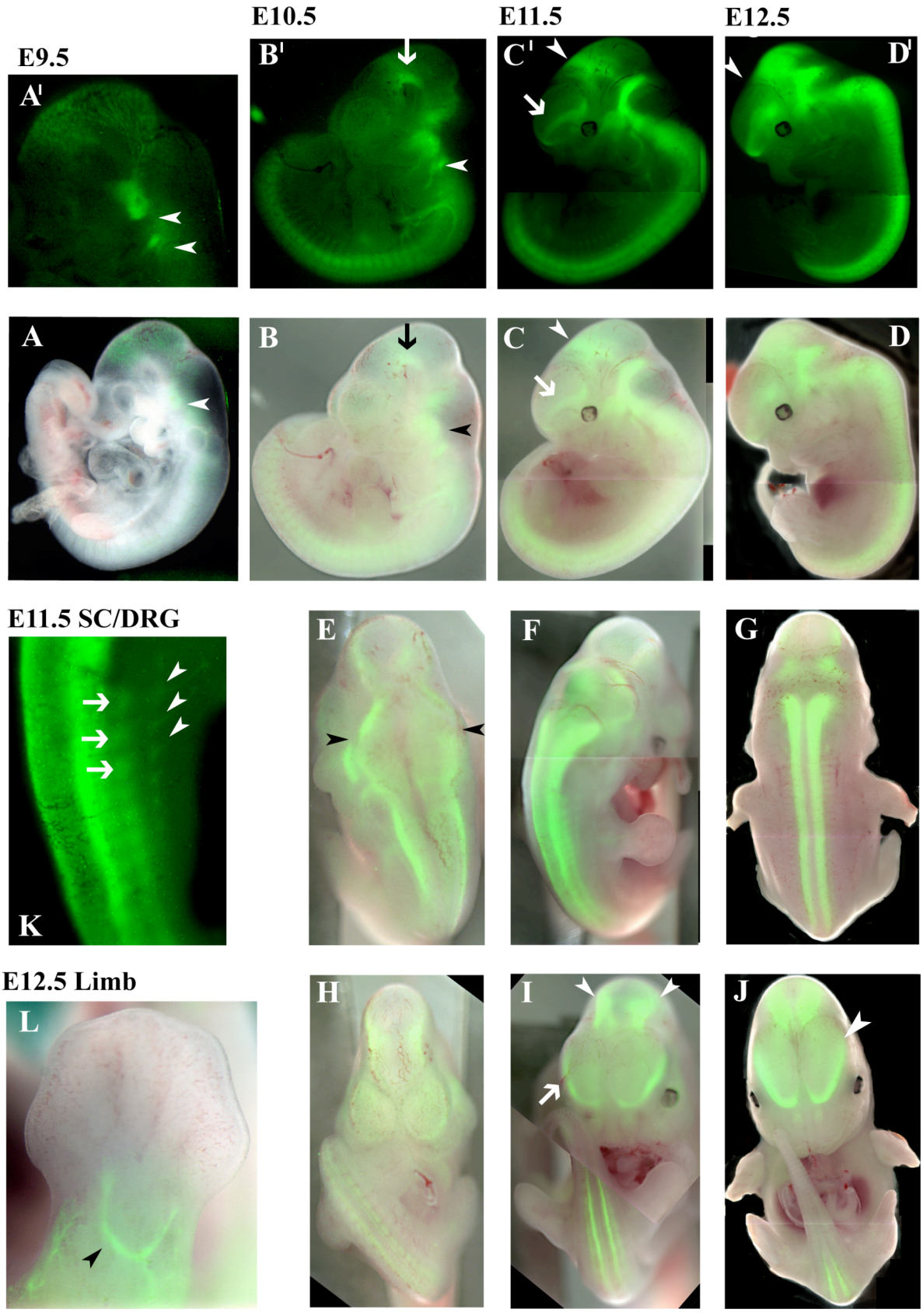

E9.5
E10.5
E11.5
E12.5
A'
B'
C'
D'
A
B
C
D
E11.5 SC/DRG
K
E
F
G
E12.5 Limb
L
H
I
J

Figure 17 (Previous page) **- βIIItubulin-GFP fluorescence in the *Tubb3*-GFP embryos.** (**A**-**L**) Unfixed whole mount *Tubb*3-GFP embryos pictures at different stages of development show GFP expression correlating with neurogenesis. (**A-J**) Overlay between transmitted and fluorescence light showing lateral (**A-D**), dorsal (**E-G)** and frontal view (**H-J**) of embryos at different stages of development. (**K**) Details of the developing dorsal root ganglia (arrows) and relative projecting axons (arrowheads) of E11.5 embryo. (**L**) Detail of the limb of E12.5 embryo. (**A'-D'**) Lateral views, green channel only, showing the increase of fluorescence concomitantly with the increase of the amount of neurons and the ventral-to-dorsal spreading of neurogenesis. SC = Spinal Cord; DRG = Dorsal Root Ganglia.

Analysis of sections of the developing CNS of the *Tubb3*-GFP mice showed thickening of the GFP-positive cell layer (i.e. neuronal layer) with the progression of neurogenesis (Fig. 18, A-C). Neurons could be detected in the E11.5 telencephalic ventricular zone (VZ) in the proximity of the ventricular surface (Fig. 18, D arrow), together with their neurites (Fig. 18, D arrowhead) Similar results were obtained by the analysis of the E12.5 *Tubb3*-GFP mouse retina where βIIItubulin-GFP fluorescence could be detected in the neuronal layer (Fig. 18, E, asterisk) and the neurites (Fig. 18, E, arrowhead). βIIItubulin-GFP was also a hallmark of the peripheral nervous system. βIIItubulin-GFP fluorescence could be detected in the developing dorsal root ganglia (Fig. 18, F and G arrowheads; fig. 17, K, arrows), including the bundles of projecting neurites (Fig. 18, F arrowheads; fig. 17, K, arrowheads), spinal cord (Fig. 18, G) and neurites innervating the limbs (E12.5, fig. 17, L arrowheads).

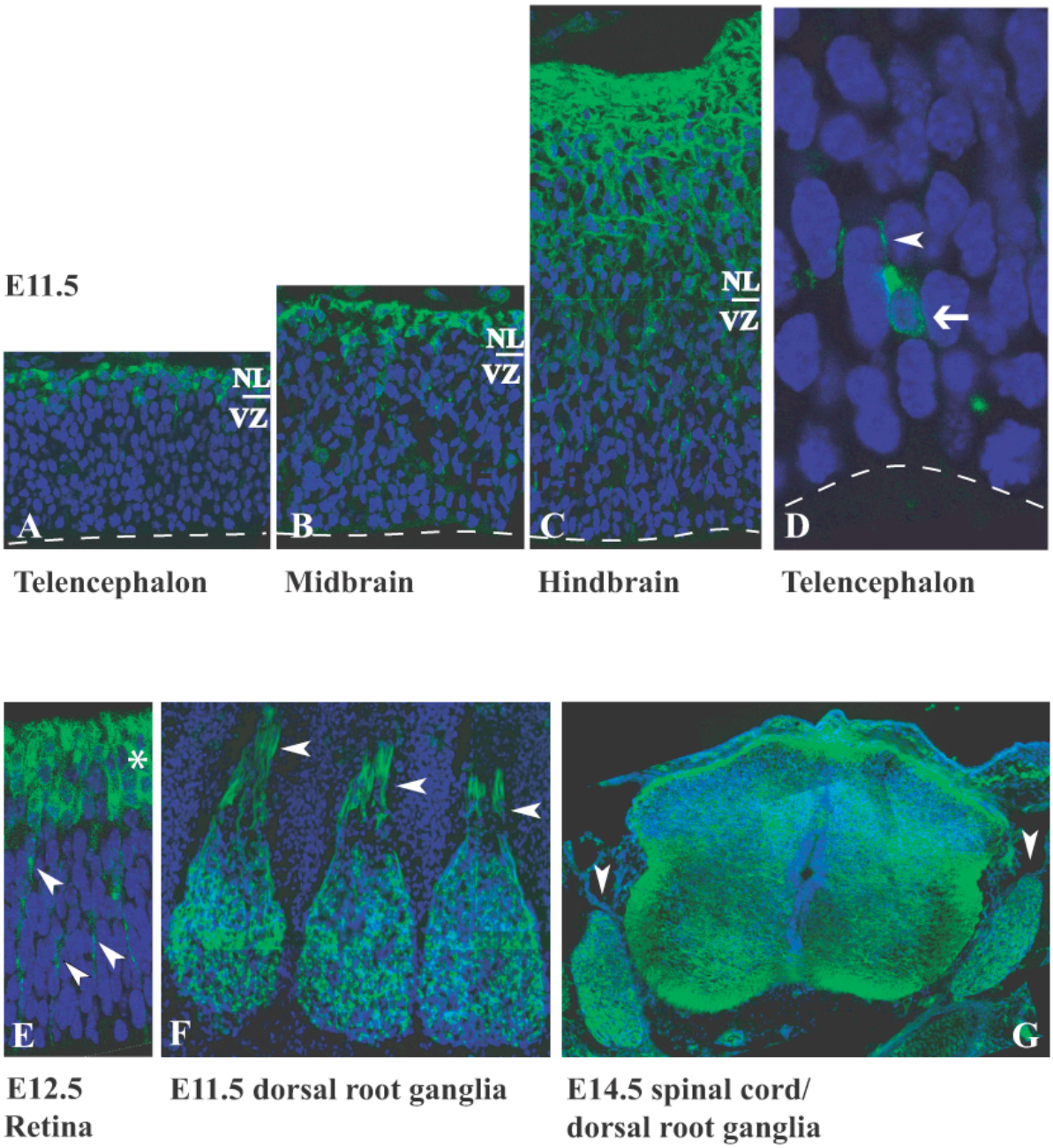


Figure 18 – βIIItubulin-GFP fluorescence at the cellular level. *Tubb*3-GFP embryos at different stages of development show GFP expression correlating with neurogenesis at the cellular level. (**A-G**) Cryosections, 12um thick, stained with Hoechst. Confocal scanning photomicrographs (single focal planes) of developing neural tissue of E11.5 and E12.5 embryos (**A**, telencephalon; **B**, midbrain; **C**, hindbrain; **D**, telencephalon; **E**, Retina). Note the increase in thickness of the GFP positive cell layer concomitantly with the progression of neurogenesis from telencephalon (**A**) to hindbrain (**C**). In **D** a neuron (arrow) whose soma is close to the ventricular surface is shown. The arrowhead points to a pial-directed green fluorescent process. (**E**) Section through the developing retina of an E12.5 embryo shows the somata of the neurons (asterisk) and their processes spanning the whole thickness of the epithelium (arrowheads). (**F-G**) Fluorescent wide field micrographs (mosaic of single high power views) showing βIIItubulin-GFP in the peripheral nervous system. (**F**) Three dorsal root ganglia of E11.5 embryo. The bundles of projecting axons (arrowheads) are evident. (**G**) Coronal section of the E14.5 spinal cord, with two Dorsal Root Ganglia (arrowheads). NL = Neuronal Layer; VZ = Ventricular Zone.

βIIItubulin-GFP was localized to the plasma membrane because of the GAP43 localization signal. However, the resolution of the light microscopy used for the quantification did not allow distinguishing between the plasma membrane and the thin layer of cytoplasm surrounding the nuclei or filling the processes. Therefore, in the following section, the word colocalization indicates colocalization at the light microscopy level, which in turn means that two markers that colocalize are localized to the same cell. To confirm that GFP expression was restricted to the neuronal population, immunolabelling experiments were performed in E11.5 *Tubb3*-GFP embryos using the neuronal markers βIIItubulin and Map2 [199, 200] and the progenitor marker Nestin [20]. After immunostaining βIIItubulin-GFP colocalized with Map2, showing that green fluorescence was restricted to the Map2 positive cell population in the neuronal layer (Fig. 19, A-C). βIIItubulin-GFP did not co-localize with Nestin, showing that green fluorescence was excluded from the progenitor cell population in the VZ (Fig. 19, D-F). However, higher magnification analysis showed an incomplete colocalization between the immunoreactivity for the anti βIIItubulin antibody and the intrinsic βIIItubulin-GFP fluorescence at the sub cellular level. A perinuclear structure was βIIItubulin-GFP fluorescent but not βIIItubulin immunoreactive (Fig. 19, G, arrowheads). A similar result was obtained by staining with the plasma membrane marker pancadherin (Fig. 19, H-J arrowheads). Such a βIIItubulin-GFP positive structure was the Golgi apparatus, as shown by co localization with giantin, a marker of the Golgi apparatus [201](Fig. 19, K-M arrowheads). A temporary accumulation of βIIItubulin-GFP in the Golgi apparatus was not unexpected since it is known that the GAP43 plasma membrane localization signal is palmitoylated [202]. The Golgi apparatus was fluorescent in the young neurons but later (P1) it was not detectable anymore.

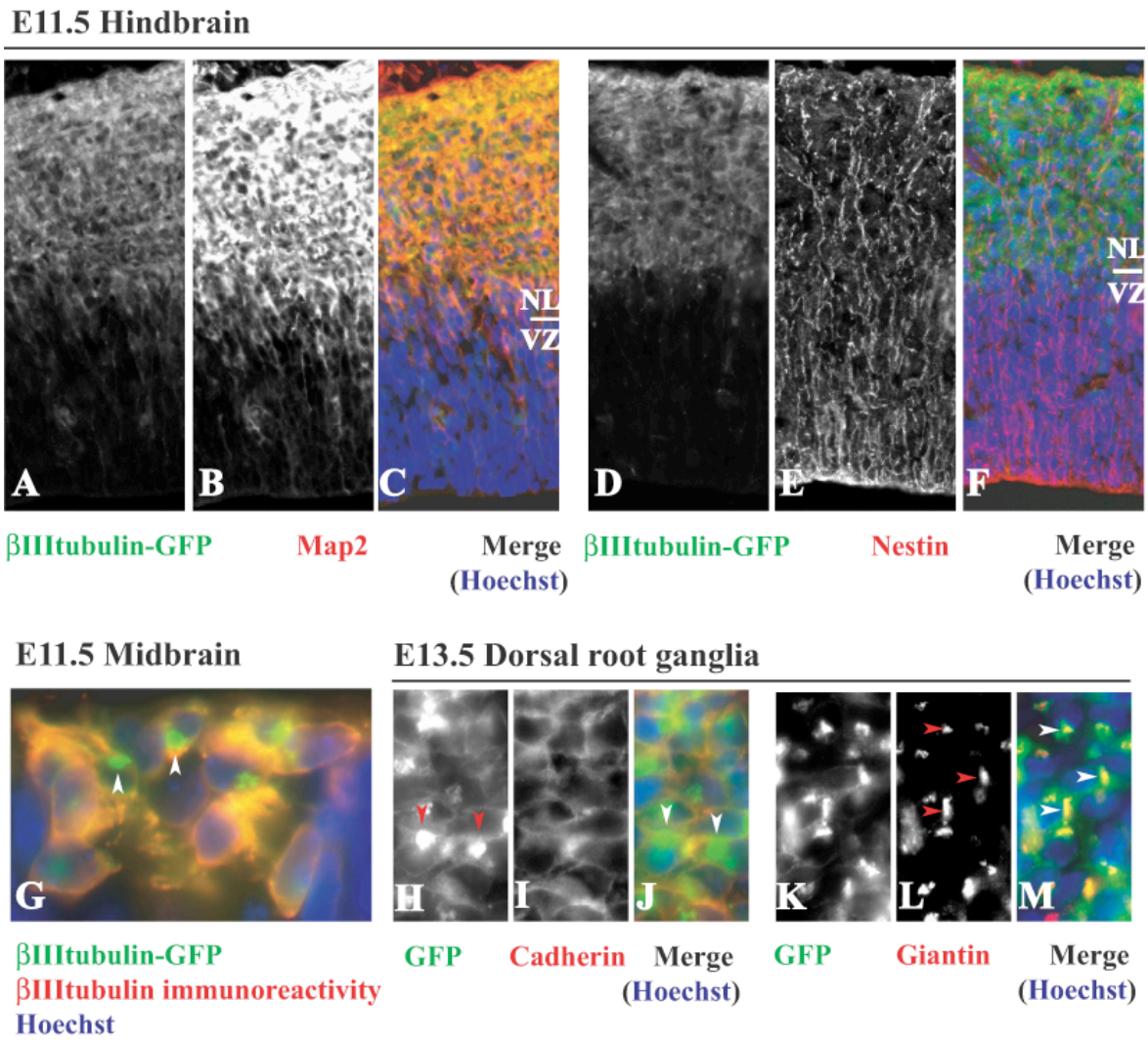


Figure 19 – βIIItubulin-GFP marks only the neurons in the developing neural tube. Fluorescent wide field photomicrographs of *Tubb*3-GFP embryos. Cryosections, 12um thick, stained with Hoechst and Map2 (**A-C**), Nestin (**D-F**), βIIItubulin (**G**), pancadherin (**H-J**) and giantin (**K-M**). βIIItubulin-GFP co localizes with immunoreactivity for the neuronal marker Map2 (**C**) but it does not colocalize with the progenitor marker Nestin (**F**). (**G**) Higher magnification showing the incomplete overlap of the endogenous βIIItubulin green fluorescent signal (arrowheads) with βIIItubulin immunoreactivity. (**I-J**) Immunolabelling with the plasma membrane marker pancadherin shows, similarly, a colocalization with βIIItubulin-GFP at the plasma membrane level and the non-colocalization at the perinuclear level (arrowheads). (**L-M**) Immunolabelling with giantin reveals an accumulation of βIIItubulin-GFP in the Golgi apparatus (arrowheads). NL = Neuronal Layer; VZ = Ventricular Zone; arrowheads = Golgi apparatus.

From these data we concluded that the βIIItubulin-GFP: (i) marks all the neurons, including neurons in the VZ, but (ii) is excluded from the progenitor population. Moreover, (iii) it is temporarily accumulated in the Golgi apparatus, at least during the early stages of neuronal differentiation.

II - 3.3.
The double transgenic TisTubb-GFP line allows detection of neurogenic progenitors and neurons

The newly characterized *Tubb3*-GFP mouse line was crossed with the existing *Tis21*-GFP line, in which the entirety of neurogenic progenitors are marked by nuclear GFP expression [28]. A mouse homozygous for the transgenic BAC *Tubb3*-GFP allele was crossed with a mouse homozygous for the *Tis21*-GFP knock in allele. The double heterozygous offspring was intercrossed until reaching a sufficient number of double homozygous (harbouring *Tubb3*-GFP alleles in both parental chromosomes together with GFP knocked into both parental *Tis21* loci) males. These males were crossed with C57Bl6 females that were sacrificed for embryo collection. In this way all the embryos collected were double heterozygous and no genotyping was necessary prior to imaging. The plasma membrane localization of the GFP in the *Tubb3*-GFP mouse line allowed to distinguish the two coexisting GFPs. The *βIIItubulin*-driven GFP is targeted to the plasma membrane of the neurons (Fig. 20, A and B, arrows), while the *Tis21*-driven GFP, targeted to the nuclei of the neurogenic progenitors (Fig. 20, A and B, arrowheads). This allowed detection of apical and basal neurogenic divisions and tracking of their daughters in time-lapse experiments.

The double mutant ("TisTubb-GFP") strain showed three different cell populations coexisting in the developing neuroepithelium and expressing GFP.

(i) Cells with a green fluorescent nucleus (Fig. 20, A-C arrowheads): the neurogenic progenitors; in these cells GFP is expressed under the control of the *Tis21* promoter.

(ii) Cells with a green fluorescent nucleus and a green fluorescent plasma membrane (Fig. 20, A-C solid arrows): the newborn neurons; in these cells nuclear GFP is inherited from the neurogenic progenitor mother and GFP targeted to the plasma membrane is driven by the *βIIItubulin* promoter.

(iii) Cells with a green fluorescent plasma membrane (Fig. 20, A-C empty arrows): the older neurons; in these cells nuclear GFP has been degraded and GFP targeted to the plasma membrane is driven by the *βIIItubulin* promoter.

In the TisTubb-GFP double mutant mouse strain, the level of green fluorescence was higher in neurons compared to neurogenic progenitors. This phenomenon could be explained by several factors. (i) Higher physiologic expression levels of the *βIIItubulin*

promoter compared to the *Tis21* promoter, or (ii) slow turnover of GFP in the neurons, or (iii) localization to the plasma membrane could cause GFP to appear brighter.

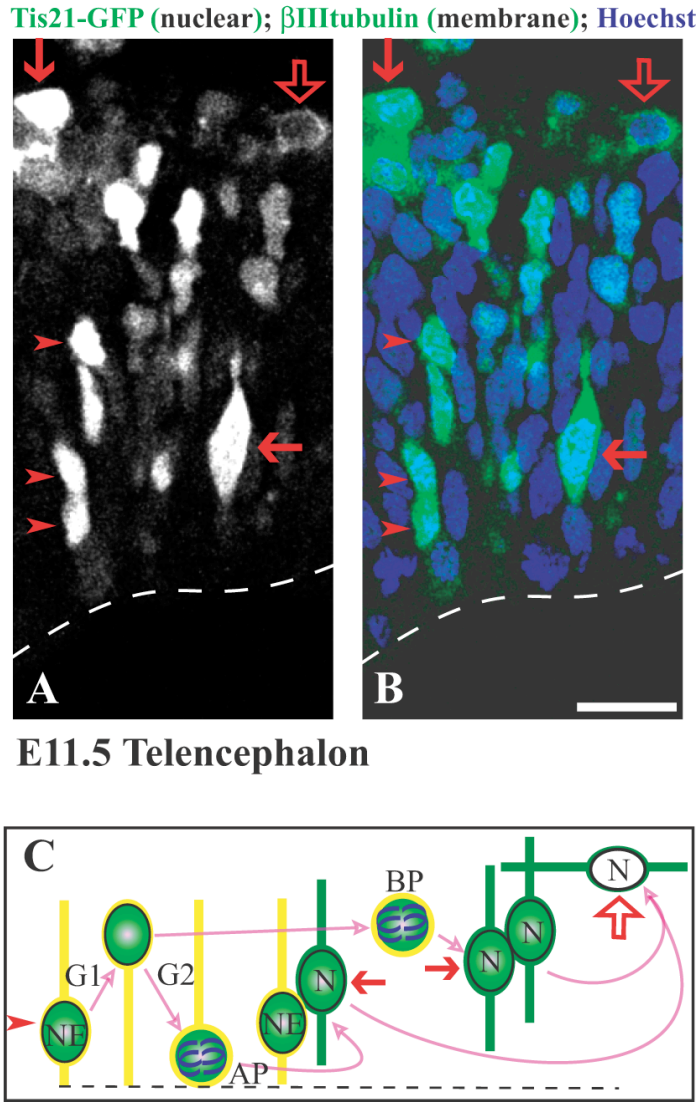


Figure 20 – The TisTubb-GFP mouse line at the cellular level. (**A-B**) Views of heterozygous TisTubb-GFP E11.5 telencephalon. Confocal scanning photomicrographs, single focal planes. Cryosections, 12um thick, stained with hoechst; GFP is detected by its own fluorescence. (**A**) βIIItubulin-GFP fluorescence only; (**B**) merge of βIIItubulin-GFP fluorescence and Hoechst. (**C**) Cartoon showing the different classes of green fluorescent cells detected in the double mutant mouse line. Pink arrows indicate the progression over time; dashed lines = ventricular surface; arrowheads = neurogenic progenitors; solid arrows = newborn neurons; empty arrows = older neurons; NE = neuroepithelial cells; N = neurons; AP = Apical progenitor; BP = Basal progenitor; G1 and G2 = phases of the cell cycle; scale bar = 10um.

II - 3.4.
High-resolution study of neuronal migration at the onset of neurogenesis

Thirty-six time-lapse two-photon experiments were carried out on acute brain slice culture of embryos ranging from E10.5 to E12.5. Each experiment was carried out on a single slice so that each experiment reflects a single embryo; all the experiments are independent from each other. Among these, 28 time-lapse movies were suitable for processing and statistical analysis; all the following data come from these movies (for details about statistics and processing see Material and methods).

We took advantage of the high level of fluorescence of the plasma membrane targeted βIIItubulin-GFP to investigate the behavior of young cortical neurons during early stages of neurogenesis (cortex E10.5). We detected several cases of neurite outgrowth toward the ventricular surface (Fig. 21, A, time points 0'-150', solid arrows). In 16 cases the neurites reaching the ventricular surface assumed a peculiar shape: after elongation towards the ventricle, the terminal portion of the process flattened, increasing its surface parallel to the ventricular surface (Fig. 21, A, time points 160'-250', arrowheads and asterisk). This flattened conformation persisted for a variable amount of time (10'-90') (Fig. 21, A, time points 160'-250', arrowhead) after which the process assumed its former elongated shape again and retracted (Fig. 21, A, 270'). In 4 cases the whole neuronal soma migrated towards the site of flattening and subsequently moved away back to the neuronal layer (Fig. 21, A, time points 230'-330', empty arrow) (Movie 5, supplementary CD).

The sub-cellular temporary accumulation of βIIItubulin-GFP allowed the localization of the Golgi apparatus to be followed during neuronal migration (n = 58). The Golgi apparatus was localized in the perinuclear region of the young neurons (Fig. 20, G, L-M and fig.21, B arrowheads); during migration the Golgi apparatus readily moved toward the future leading edge of the neurons before the onset of migration. We observed a precise sequence of events (including cases in which neurons were switching direction of migration during recording) (Movie 6, supplementary CD).

(i) Extension of the future leading process (Fig. 21, B, time points 130'-140' solid arrow).

(ii) Exploratory phase (this phase is not always observed), with multipolar neuronal processes and no movement of the soma (Fig. 21, B, time point 180' solid arrow).

(iii) Orientation phase, with movement of the Golgi apparatus towards the future leading direction (mostly keeping its perinuclear localization but also, in some cases, elongating into the process) (Fig. 21, B, time points 230'-240' solid arrow).

(iv) Migration of the soma (Fig. 21, B, time points 280'-370' empty arrow).

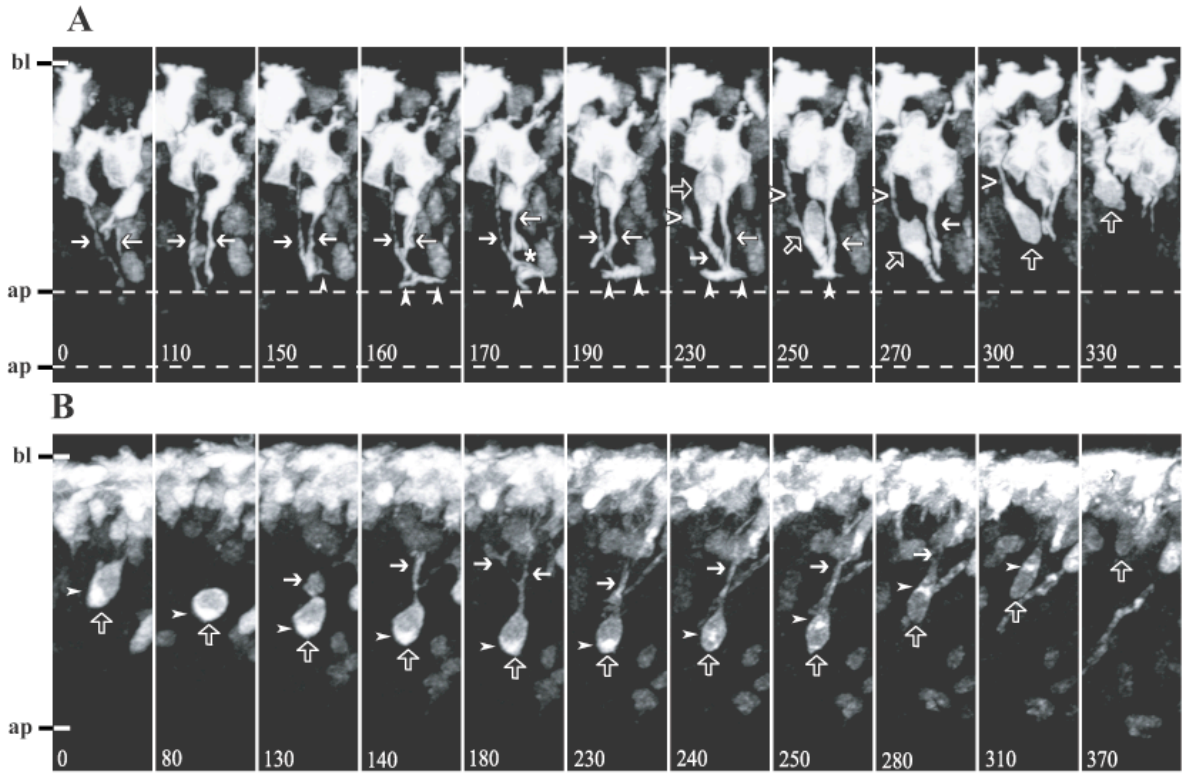


Figure 21 – Neuronal migration in the TisTubb-GFP neuroepithelium. Two-photon time-lapse scanning microscopy (slice cultures of TisTubb-GFP mouse E11.5 (**A**) and E10.5 (**B**) cortex) showing the migratory behavior of young neurons at the onset of neurogenesis. Each frame represents a single time point and it is the result of the three-dimensional reconstruction of several stacks (2.7um Z stack step, 10' interval between two frames). Embryos were collected, brains were dissected and sliced; culture was carried out in controlled environment while imaging was performed. (**A**) Two neuronal processes grow until reaching the apical surface (0'-150', solid arrows). The plasma membrane of one the two flattens (160', arrowheads) and keeps this particular shape for 90 minutes, in a dynamic fashion (160'-250', arrowheads). The second neuron shows this feature for a shorter time (70', asterisk). The soma of the first neuron migrates towards the apical surface (230'-250', empty arrow). In the meantime this neuron has elongated another process (230', open triangle) that becomes the leading process the neuron uses for its further migration (250'-330'). (**B**) A neuron (0', empty arrow) shows the bright perinuclear Golgi apparatus (arrowhead). After a pause (0'-130'), the neuron grows a process toward the basal side of the neuroepithelium (130'-140'). After an exploratory multipolar phase (180'-230'), the Golgi migrates towards the future leading direction of the neuron (240'-250'). When the Golgi apparatus has reached its final position, the whole neuronal soma migrated towards the neuronal layer (280'-370). Ap = apical side; Bl = basal side; in A the double Ap and the dashed lines indicate that the apical surface is not perpendicular to the plan of observation but rather concave.

From these data we concluded that the TisTubb-GFP mouse line allows detection and tracking of neurons from the onset of neurogenesis. Moreover, the temporary accumulation of βIIItubulin-GFP in the Golgi apparatus allows detection and tracking of this organelle in migrating neurons in living slices at very early stages of development.

II - 3.5.
Study of neurogenic divisions and tracking of neurons immediately after their birth.

Mitoses of apical (APs) and basal (BPs) neurogenic progenitors were imaged and daughter cells were tracked in slices of developing cortex as early as E10. 155 Tis21-GFP positive mitoses were imaged; the vast majority were detected at E10.5 (n=114), but also at E11.5 (n=15) and E12.5 (n = 26).

APs generated daughter cell pairs that migrated towards the basal side of the VZ with a different speed. The migration either followed the mitosis immediately or was preceded by period in which the nuclei of daughter cells stayed closely associated (Fig. 22, A, 30'-150'). The fast (leading) cells (Fig. 22, A, arrows), whose nucleus was more basally located, were the βIIItubulin-GFP expressing cells (Fig. 22, A, 160', arrow and arrowhead). The trailing cells, whose nuclei were more apically located (Fig. 22, A, asterisks), never expressed βIIItubulin-GFP for the whole duration of the movie (Movie 7, supplementary CD).

BPs generated daughter cell pairs whose nuclei kept their basal localization (Fig. 22, B), occasionally one of the two moved towards the apical side (never further than the half of the VZ thickness) for a short amount of time (Fig. 22, B, 24' to 72', left arrow). Both daughter cells expressed βIIItubulin-GFP (Fig. 22, B 216') either at the same time or with a non-significant time lag; βIIItubulin-GFP expression did not correlate with the relative position of the cell nuclei (Movie 8, supplementary CD). A single case of apical symmetric neurogenic division was observed (Fig. 22, C). In this case the apical division gave rise to two daughters whose nuclei stayed closely associated for 80'before one of the cells assumed a leading position and expressed βIIItubulin-GFP (310' after mitosis, data not shown). The second cells overcame the formerly leading cell, expressed the βIIItubulin-GFP (Fig. 22, C, 420'-610') and merged into the thin neuronal layer (Fig. 22, C, 660', asterisk). The cell that first expressed βIIItubulin-GFP formed a new basally directed process (Fig. 22, C, 680', red arrowhead), eventually reached the neuronal layer and could be observed there until the end of recording (Fig. 22, C, 830') (Movie 9, supplementary CD).

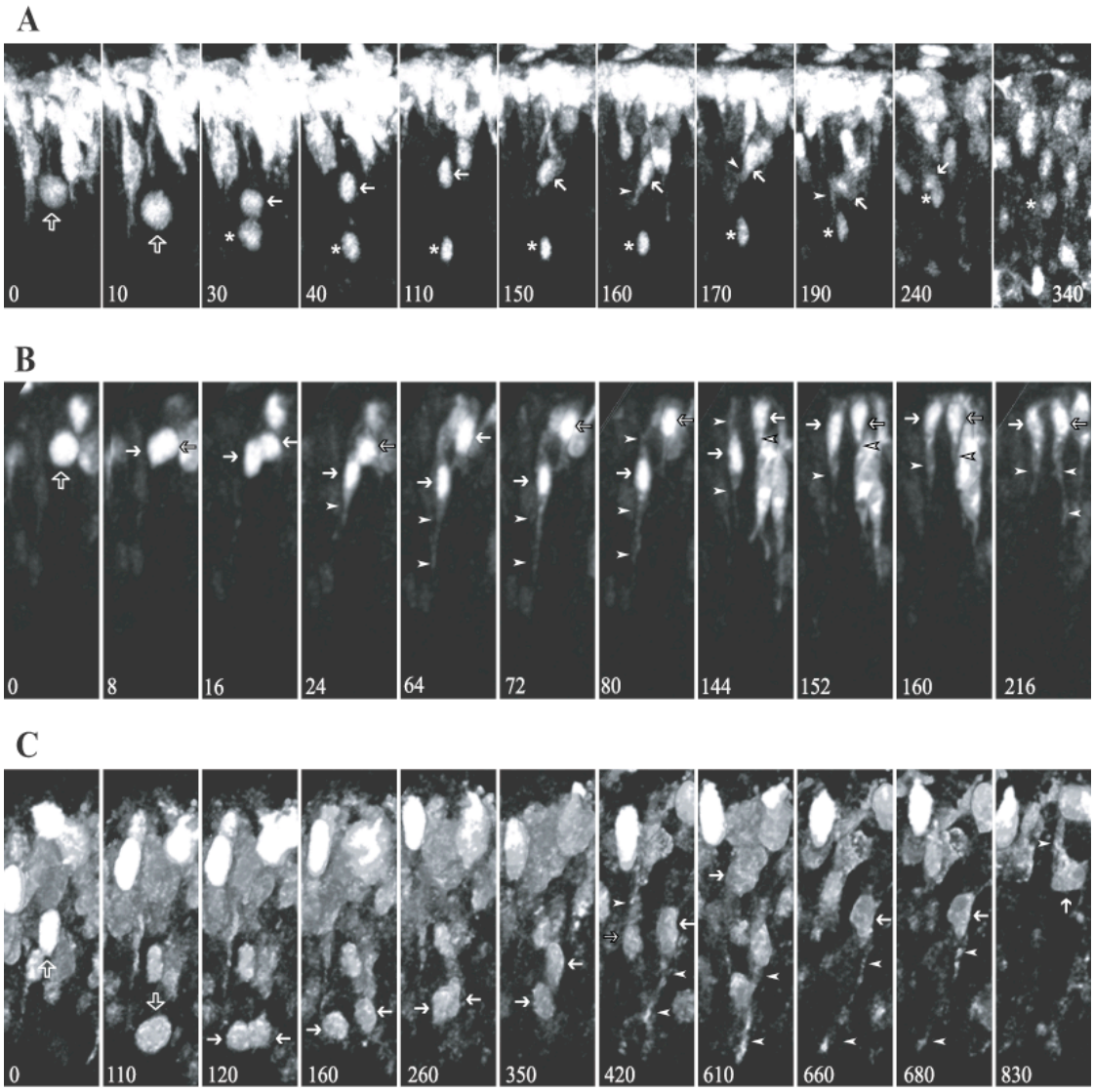


Figure 22 – Imaging neurogenic divisions and tracking daughter cells at the onset of neurogenesis. Two-photon time-lapse scanning microscopy (acute brain slice cultures of E11.5 (**A, C**) and E10.5 (**B**) TisTubb-GFP mouse developing cortex), showing: a sub apical asymmetric neurogenic division (**A**), a basal symmetric neurogenic division (**B**) and an apical symmetric neurogenic division (**C**). Embryos were collected, brains were dissected and sliced; culture was carried out in controlled environment while imaging was performed. Each frame represents a single time point and it is the result of the three-dimensional reconstruction of several stacks. (2.7um Z stack step, 8' (**B**) or 10' (**A, C**) interval between two frames). (**A**) The nucleus of a neurogenic cell (Tis21-GFP positive) (empty arrow) moves apically and divides, before reaching the apical surface (0'-30'). The nucleus of one of the daughters (arrow) moves towards the basal side faster than the nucleus of the other daughter (asterisk) (40'-150'). The leading daughter expresses βIIItubulin-GFP and displays it in the plasma membrane 140' after mitosis (160' arrowhead), then the cells migrates out from the imaged focal planes and disappear (170'-240'). The trailing daughter moves towards the basal side and it is lost after 340'. (**B**) The nucleus of a neurogenic cell (Tis21-GFP positive) is found on the basal side (0') (empty arrow) and there it divides (8'). One of the two daughters (left arrow) slightly migrates towards the apical side and it expresses βIIItubulin-GFP (24' arrowhead), then in migrates towards the forming neuronal layer (80'152'). The other daughter (right arrow) moves slightly towards the basal side (64'-80') and there it *–continues from previous page-* expresses βIIItubulin-GFP (144', arrowhead). (**C**) The nucleus of a neurogenic cell (Tis21-GFP positive) (empty arrow) moves apically, reaches the apical surface and divides (110'-120'). The two daughters stay close together until 260' and then one of the two (arrow) moves towards the basal side (350') and expresses βIIItubulin-GFP (not shown). The second daughter (asterisk) moves towards the basal side as well overcoming the first daughter and expressing βIIItubulin-GFP (420') (arrowhead), then it merges into the developing neuronal layer (610', asterisk). The daughter cell still in the VZ elongates a new process (680', arrowhead) and migrates towards the basal side of the VZ (830', arrow).

Out of 131 mitoses selected for analysis (see statistical analysis in the Material and methods section for details), 62 occurred at an apical or sub apical location while 69 occurred at a basal location (Fig. 23, A).

APs. Of the 62 cases of mitotic APs analyzed, three mitoses (3.2%) gave rise to two daughters, one of which expressed βIIItubulin-GFP while the other did not for the whole duration of the imaging (cells followed on average up to 263', StdDev 186') (Fig. 23, A, orange portion; B, yellow bars). In the rest of the cases, βIIItubulin-GFP was never detected in either of the daughters for the whole duration of the movie (cells followed on average up to 317', StdDev 165') (Fig. 23, A, blue portion; B, violet and magenta bars), either because the GFP was bleached or because the nucleus merged into the neuronal layer and could not be tracked thereafter. In all the cases observed, βIIItubulin-GFP was first expressed by the one leading (the most basally located cells) daughter.

BPs. Of the 69 cases of mitotic BPs analyzed, 17 mitoses (24.6%) gave rise to daughters both of which expressed βIIItubulin-GFP, either at the same time or with a non-significant (Fig24, A; $n = 17$; $P > 0.05$) time lag (Fig. 23, A yellow portion; C, yellow bars). In 13 cases (17.4%) of basal mitoses it was not possible to unequivocally assign the presence of GFP positive plasma membrane to both daughter cells: one of the daughters was lost in the GFP positive neuronal layer, lost by bleaching of the GFP or generally the quality of the imaging was not sufficient for an unequivocal determination (cells followed on average up to 204', StdDev 114'). The other daughters of the pair, whose nucleus could be unequivocally associated with a GFP positive plasma membrane (Fig. 23, A, red portion; C, yellow bars), expressed βIIItubulin-GFP at a time consistent with the 17 cases in which the both daughter cells were βIIItubulin-GFP positive (Fig. 24, A; $n = 13$; $p > 0.05$).

In the remaining 58% of cases it was not possible to observe any βIIItubulin-driven fluorescence appearance during the time of recording (cells followed on average up to 257', StdDev 163') (Fig. 23, A green portion; C, violet and magenta bars).

The similar amount of apical and basal mitoses detected (Fig. 23, A) indicated a bias of our system towards detection of basal mitoses, since at E10.5, when most of the mitoses analyzed took place, the number of mitotic BPs is approximately 1/4 of the mitotic APs [28]. However this result was not unexpected since the higher level of fluorescence of mitotic BPs makes them more easily detectable than mitotic APs.

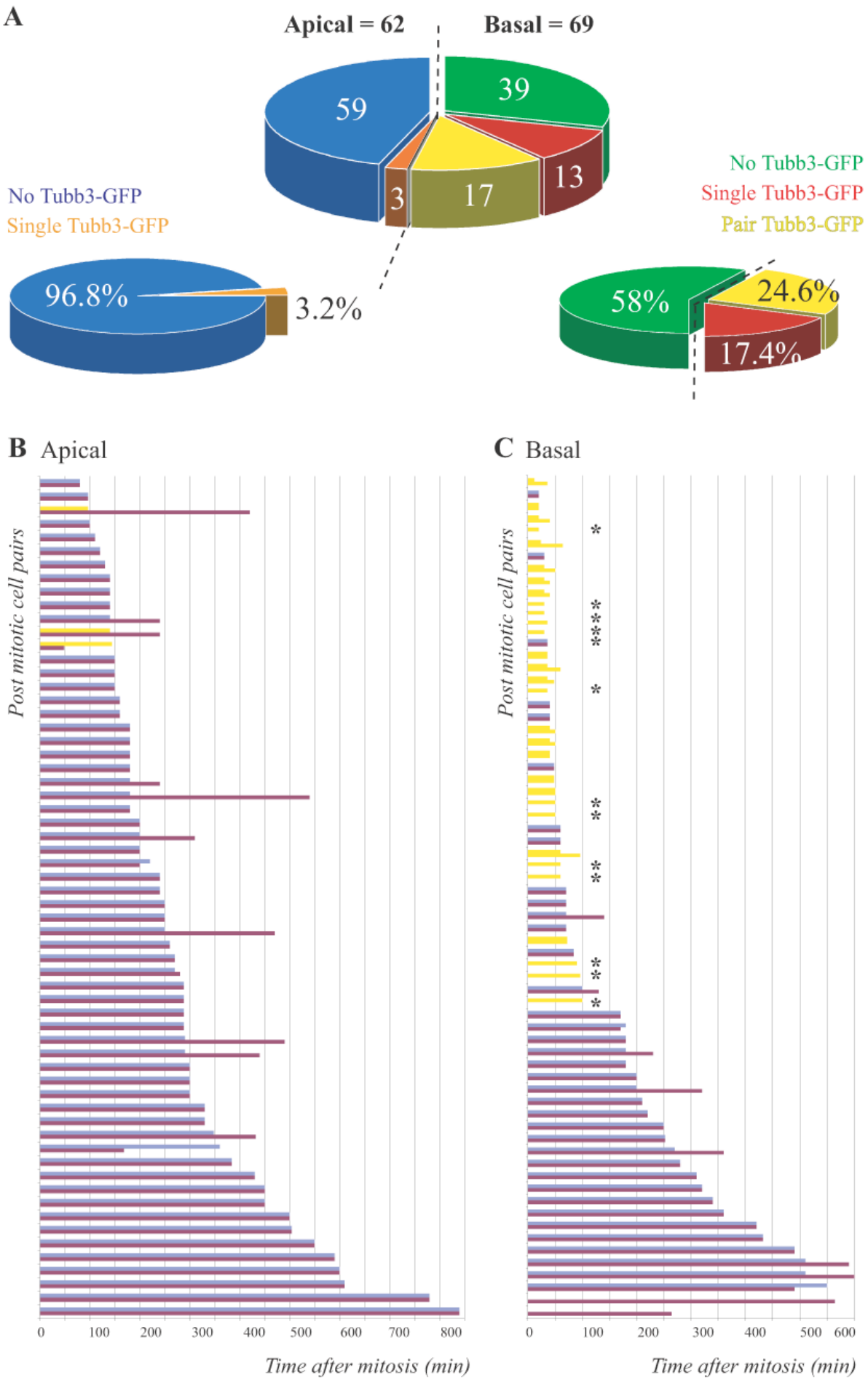

A
Apical = 62
Basal = 69
59
39
3
17
13
No Tubb3-GFP
Single Tubb3-GFP
No Tubb3-GFP
Single Tubb3-GFP
Pair Tubb3-GFP
96.8%
3.2%
58%
24.6%
17.4%
B Apical
C Basal
Post mitotic cell pairs
Post mitotic cell pairs
0 100 200 300 400 500 600 700 800
0 100 200 300 400 500 600
Time after mitosis (min)
Time after mitosis (min)

Figure 23 (Previous page) – **Distribution of neurogenic mitoses and βIIItubulin-GFP expression.** (**A**) Pie diagrams illustrating the distribution of all the mitoses grouped according to βIIItubulin-GFP expression. In the upper diagram the number of mitoses analyzed is shown. The lower left diagram shows the percentage of apical mitoses that gave rise to daughters that either never expressed βIIItubulin-GFP (blue) or only one of the daughters expressed βIIItubulin-GFP (orange). The lower right diagram shows the percentage of basal mitoses that gave rise to daughters that either never expressed βIIItubulin-GFP (green) or only one of the daughters could be unequivocally assigned to a βIIItubulin-GFP positive plasma membrane (red) or both daughters expressed βIIItubulin-GFP (yellow). (**B-C**) Bar diagrams illustrating the distribution of βIIItubulin-GFP expressing daughter cells grouped according to the location of their mitotic mother: (**B)** apical or (**C**) basal. All the tracked daughter cells are represented. Each horizontal bar represents a single cell, daughter cells are grouped as pairs (0'). Magenta and violet colors indicate absence of βIIItubulin-GFP expression, yellow color indicates βIIItubulin-GFP expression. Asterisks indicate the cases in which only one of the daughters could be unequivocally assigned to a βIIItubulin-GFP positive plasma membrane. Each vertical mark indicates 50 min after mitosis

All together these data leave open two interpretations. One of these is that the imaging set up does not allow to track all daughters of neurogenic progenitors long enough to observe appearance of βIIItubulin-GFP. Most of the newborn neurons express βIIItubulin-GFP when they are already out of the VZ and in the neuronal layer and since the neuronal layer is brightly green it is not possible to distinguish individual cells anymore. Another possible explanation of the data is that not all of the Tis21-GFP positive mitotic cells generate neurons. Some of the apical Tis21-GFP positive mitoses might generate BPs that will generate neurons in the next cell cycle; some of the basal Tis21-GFP positive mitoses might generate BPs, bringing up the possibility that Tis21 expression starts two cell cycles prior to the generation of neurons.

II - 3.6.
The kinetic of βIIItubulin-GFP expression differs between daughters of APs and BPs

In the cases of GFP expressing daughters of APs, βIIItubulin-GFP expression could be detected on average after 126.7' after mitosis (StdDev 26.6' n = 3 cells). The earliest βIIItubulin-GFP appearance was detected 96' after mitosis, the latest 144' after mitosis (Fig. 24, blue circles and bars). Interestingly, daughters of BPs expressed βIIItubulin-GFP on average 46' post mitosis (StdDev 20.7min; n = 46 cells). The earliest βIIItubulin-GFP appearance was 12' after mitosis, the latest 100' after mitosis (Fig. 24, red circles and bars). The lag between the first and the second βIIItubulin-GFP expressing daughters spanned from 0' to 48'. On average daughters of BPs expressed

βIIItubulin-GFP significantly faster than daughters coming from APs (Fig. 24; p > 0.001). The latest time point where βIIItubulin-GFP could be observed in our experiments was 470' after division in the only case of apical symmetric neurogenic division.

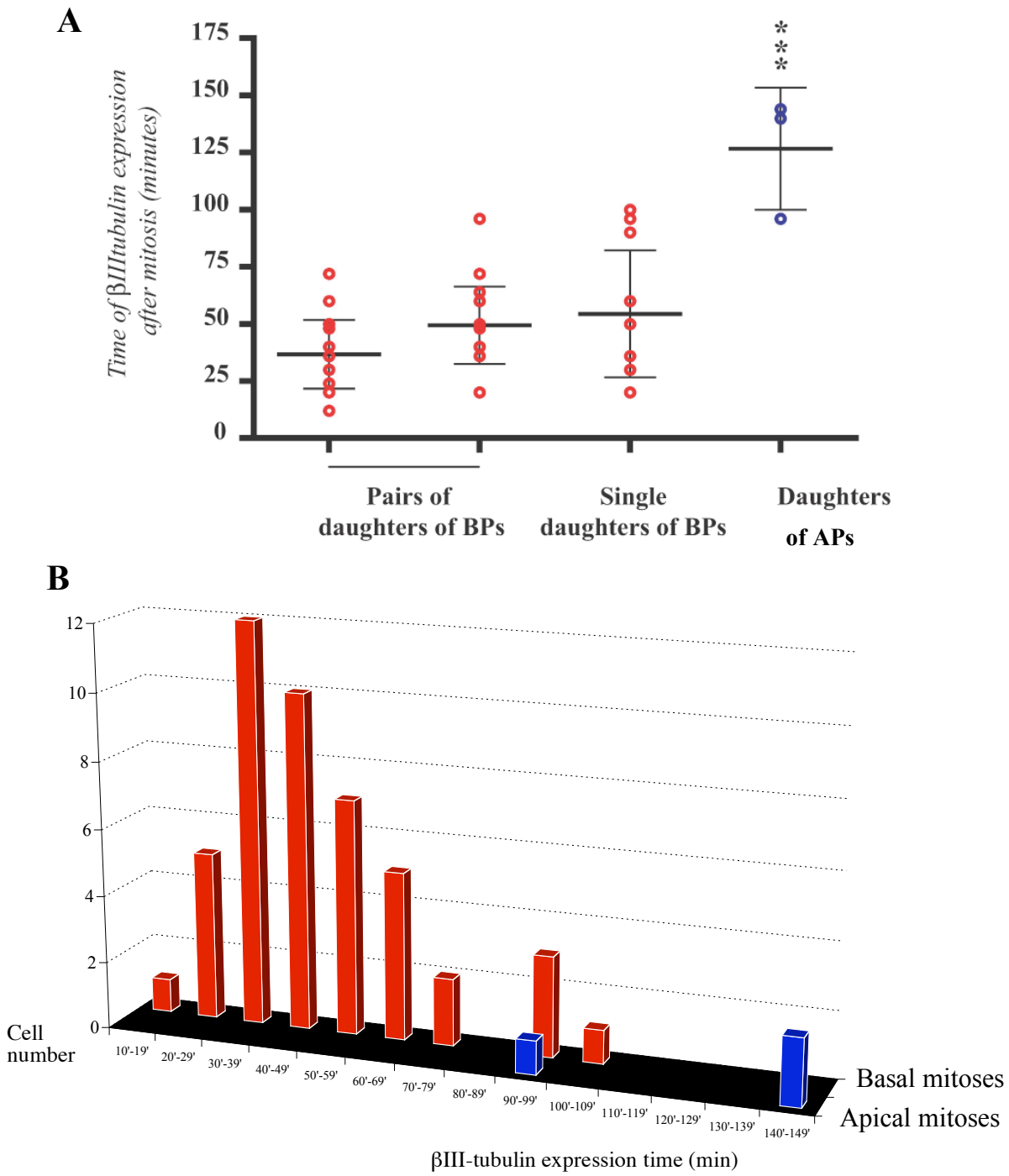


Figure 24 (Previous page) **–Daughters of BPs express βIIItubulin-GFP earlier than daughters of APs.** (**A** and **B**) Dot-plot and bar diagrams illustrating the distribution of βIIItubulin-GFP expression speed. (**A**) The daughters of BPs were grouped in three classes. Pairs, when both daughter originating from the same mother expressed βIIItubulin-GFP. Singles, when it was not possible to unequivocally assign to the both daughters a βIIItubulin-GFP positive plasma membrane. In such case only the unequivocally assigned daughter is represented. Each symbol (red circles for daughters of BPs and blue circles for daughters of APs) represents the time point of βIIItubulin-GFP expression after mitosis, cells with the same expression time are represented by one symbol. The three asterisks indicate a significant difference (ANOVA; $p < 0.001$) between the time of βIIItubulin-GFP expression of the daughters of APs and the other three groups independently. Thick horizontal black bars represent the average value, thin horizontal black bars represent the standard deviation. (**B**) Since they did not show any statistic difference (ANOVA; $p > 0.05$), all the daughter of BPs were pooled in a unique group and compared to daughters of APs. The height of each bar represents the number of the cells expressing βIIItubulin-GFP at a given time after mitosis. The time of βIIItubulin-GFP expression after mitosis is distributed in classes: 10 = from 10 to 19min and so on. Note the accumulation of daughters of BPs (n = 22) in the classes 30 and 40 (from 30 to 49min), while 2/3 of the daughters of APs fall in the class 140 (from 140 to 149min).

Taken together with the higher intensity of *Tis21*-driven fluorescence showed by BPs when compared to APs, these results show that an early step of neuronal differentiation, reflected by the expression of early markers, is accomplished in the neurons originating from BPs more quickly than in neurons originating from APs. This suggests that BPs are more strongly primed to neurogenesis than APs.

II - 4. Study of adult neurogenesis

The *Tis21*-GFP mouse line highlights *in vivo* all the neurogenic progenitor cells during embryonic development. This makes it a good candidate for a tool to study adult neurogenesis, eventually for *in vivo* applications, and to relate embryonic and adult mechanisms of neurogenesis. Since very little is known about *Tis21* expression in the adult, the aim of this part of the work is to characterize Tis21-GFP expression during adult neurogenesis. All the work of this section was carried out in collaboration with Dr. Klaus Fabel from the department of psychiatry of the Carl Gustav Carus clinic, Dresden.

II - 4.1.
Tis21-GFP is expressed in the adult neurogenic regions

Tis21-GFP presence, detected by its intrinsic fluorescence, was examined in the early postnatal (1 week after birth, fig. 25, A-B'), juvenile (2, 3 and 6 weeks after birth, fig. 25, C-D') and adult (9 and 18 weeks after birth, fig. 25, E-F') *Tis21*-GFP mouse, in the brain regions were neurogenesis is known to continue after birth: the DG of the Hippocampus and the SEZ. Tis21-GFP was detected in these regions at all the time points examined, as well as in another region where neurogenesis is known to continue shortly after birth: the early postnatal cerebellum (1 week after birth, fig. 25, G, G'). Furthermore, some of the Tis21-GFP positive cells divided (at least up to 6 weeks after birth), as indicated by staining for the antibody against PH3 (Fig. 25, G', arrowheads).

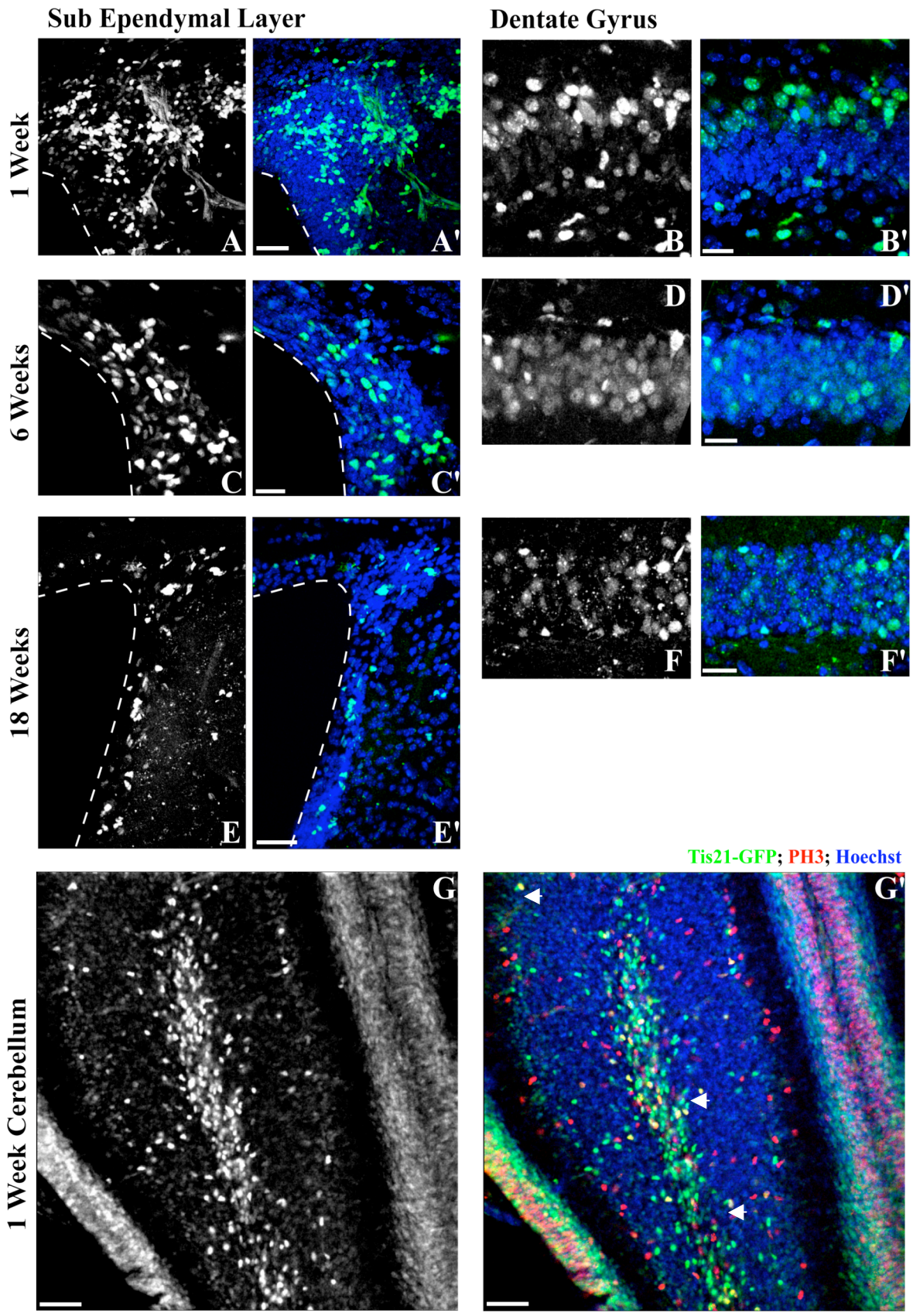

Sub Ependymal Layer
Dentate Gyrus
1 Week
6 Weeks
18 Weeks
1 Week Cerebellum
A
A'
B
B'
C
C'
D
D'
E
E'
F
F'
G
G'
Tis21-GFP; PH3; Hoechst

Figure 25 (Previous page) **–Tis21-GFP is found in the regions where neurons are generated in the adult.** Pictures showing the presence of Tis21-GFP positive cells in the postnatal mouse brain. Three-dimensional reconstructions, obtained from single confocal stacks, of 1 (**A-B'** and **G, G'**), 6 (**C-D'**) and 18 (**E-F'**) weeks old *Tis21*-GFP mouse dentate gyri, sub ependymal layers and cerebellum. The green channel (*Tis21*-GFP detected by its intrinsic fluorescence) is shown separately on the left of each series, blue is Hoechst and red, in G', is anti phospo-Histone 3 immunostaining. Please note the decrease in number of *Tis21*-GFP cells over time from 1 (**A**) to 18 weeks after birth (**F**). Arrowheads in G' indicate mitotic Tis21-GFP cells. Dashed lines indicate the ventricular surface, arrowheads indicate mtotic Tis21-GFP cells. Scale bars: 50um in A' and G', 40um in E' and 20um in B'- D' and F'.

The analysis of the adult Tis21-GFP expression mainly focused on the DG of the hippocampus for the following reasons.

(i) Astrocytes/stem cells, transit amplifying neuronal progenitors, immature and mature neurons are in close proximity with each other allowing an overview of all cell populations at different stages of maturation in a single field.

(ii) The cell lineage between astrocyte/stem cells and mature neurons is very well characterized by a panel of reliable markers, to which Tis21-GFP expression can be related.

(iii) There are many standard paradigms for inducing neurogenesis in this region, allowing variations of Tis21-GFP levels and possible re-expression to be tested.

Tis21-GFP positive cells were quantified over time, using single focal planes, and their number calculated as a percentage of the total number of cells in the DG (Granule and Sub granule cell layers, excluding hilus), as identified by Hoechst staining. The intensity of Tis21-GFP fluorescence was heterogeneous at all time points taken in analysis in both SEZ and DG. In the DG, the number of brightly fluorescent cells was variable (between 10% and 57% of the total amount of Tis21-GFP positive cells), however the progression of the Tis21-GFP bright cell population overtime did not show any significant difference from the progression of the whole Tis21-GFP positive population. The percentage of Tis21-GFP positive cells remained almost constant until the 9^{th} week of life, with fluctuations from about 30% to about 50%. The number of Tis21-GFP positive cells eventually decreased to about 12% at the end of the 18th week (Fig. 26)(ANOVA; $p<0.01$).

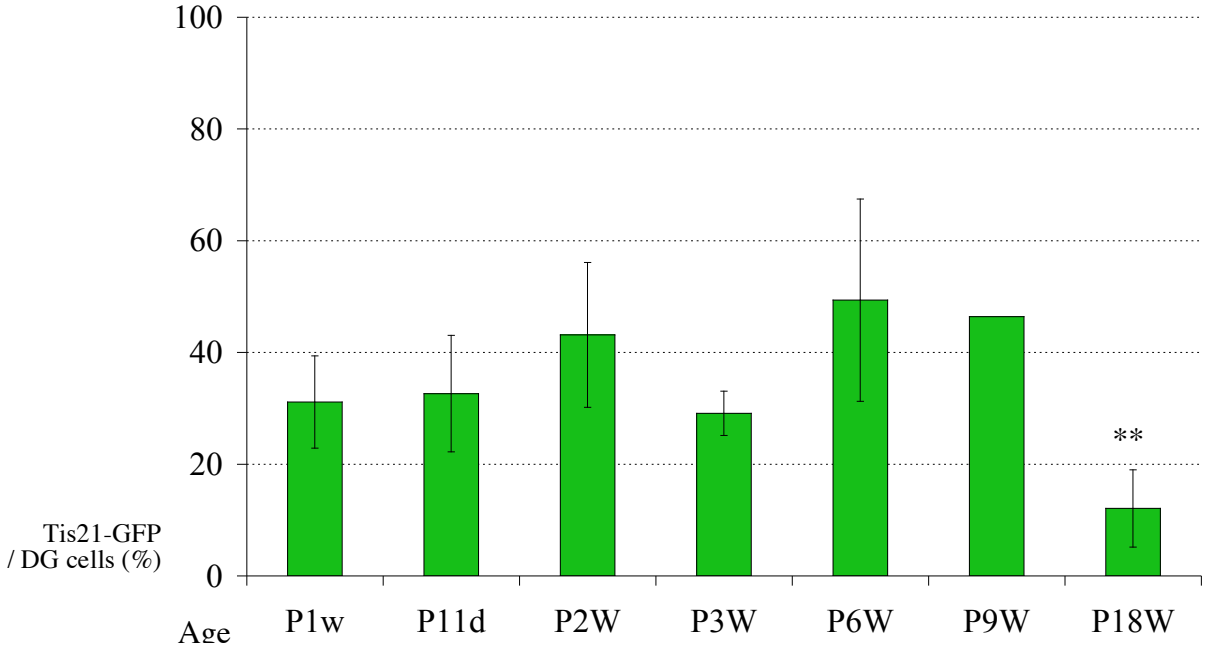


Figure 26 – The number of Tis21-GFP positive cells varies with age. Bar diagram illustrating the abundance of Tis21-GFP cells as a percentage of all cells in the DG of the hippocampus. Each count is the sum of different fields of different hippocampal regions (except one animal of the P2 weeks series in which only one field was counted). P1 and 3W = 4 animals; P11d = 2 animals; P2 and 6W = 5 animals; P9W = 1 animal; P18W = 3 animals. Total number of cells counted per animal between 166 and 2894, total number of Tis21-GFP positive cells counted per animal between 73 and 1220. Tis21-GFP was detected by its intrinsic fluorescence.

The data indicate that the proportion of Tis21-GFP positive cells keep constant during the juvenile and adult life of the animal n the DG. With aging, however, the proportion of Tis21-GFP positive cells decreases according to the known decrease in the level of neurogenesis that accompanies aging [172].

II - 4.2.
Tis21-GFP is first expressed in a subset of the transit amplifying progenitors and it is inherited by the young neurons

In order to determine if *Tis21*-GFP expression started in the astrocytes/stem cells, in the (neuronally committed) transit amplifying population or in the neurons, *Tis21*-GFP mice brain slices were stained with the following panel of markers.

A Presumptive stem cells with astroglial characteristics: Nestin and GFAP.

B Transit amplifying mitotic neuronal precursors: doublecortin (Dcx).

C Immature post mitotic neurons: NeuN and Prox1.

The data are presented here according to the temporal sequence in which these markers are known to be expressed during neuronal maturation in the DG: Nestin followed by Dcx followed by (and partially overlapping with) NeuN and Prox1. Tis21-GFP and Nestin or Dcx or NeuN or Prox1 single and double positive cells were quantified over time, using single focal planes images, and their number reported as a percentage of the total number of cells in the DG (granule and sub granule cell layers, excluding hilus), identified by Hoechst staining.

(**A**) Even at early stages (1 week after birth), no Nestin positive cell was also positive for Tis21-GFP (detected by its intrinsic fluorescence) in the SEZ and DG (Fig. 27). The same was true for GFAP in the SEZ: no double positive cell was found. In the DG, similarly, no Ti21-GFP positive cell was positive for GFAP staining; however, given the structure and the number of the astrocytes in this region, and the thickness of our slices, it was not detected a GFAP positive cell (including the nucleus), but only processes. From these data we concluded that *Tis21*-GFP is not expressed in the astrocyte/stem cell population.

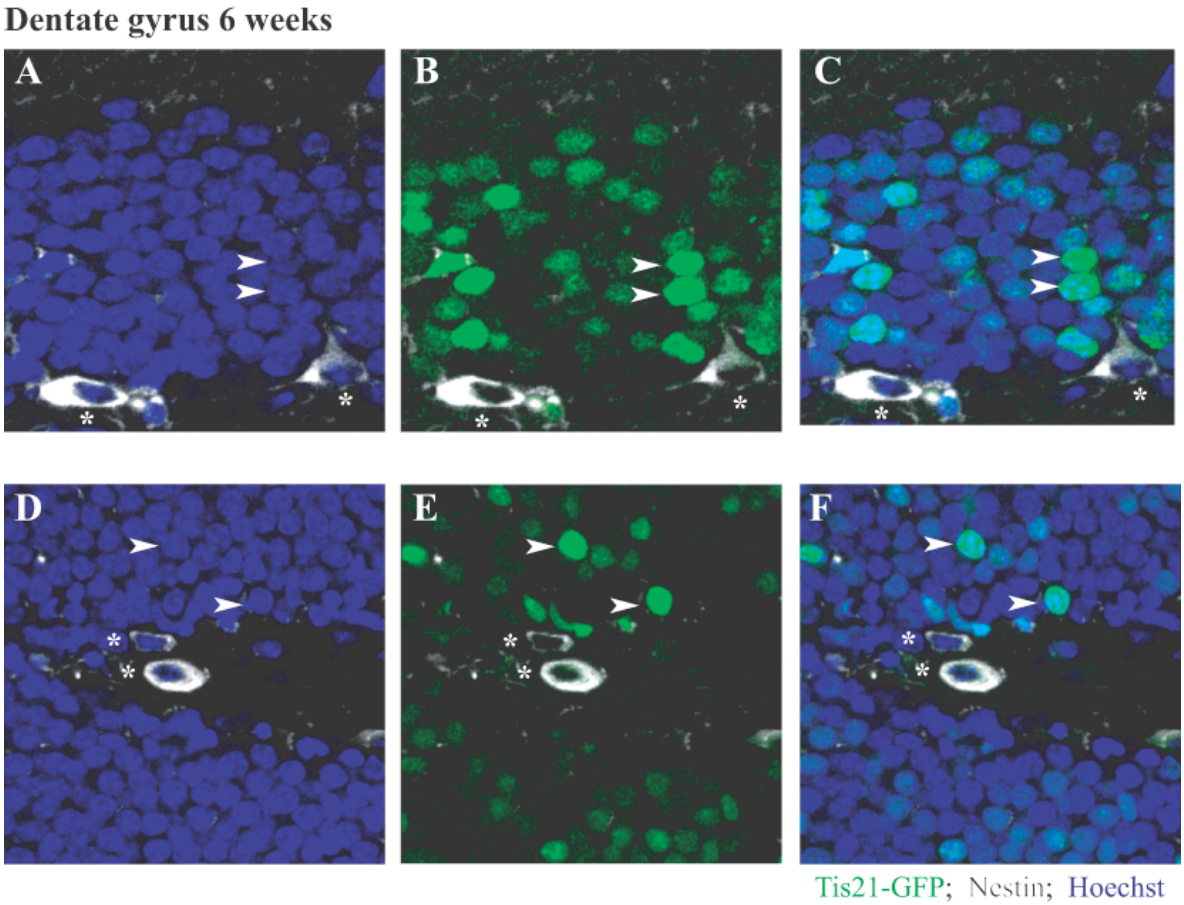


Figure 27 – Tis21-GFP is not found in the astrocytes/stem cells. (**A**-**F**) Examples of photomicrographs, used for quantification of the Nestin, Tis21-GFP and Tis21-GFP/Nestin positive cells. Single focal Z planes obtained from 40um thick brain slices of perfused and fixed 6 weeks-old Tis21-GFP animals. The single channels are shown in pairs: **A**-**D**, white (Nestin) and blue (Hoechst); **B**-**E**, green (Tis21-GFP) and white (Nestin); **C**-**E**, merge. Tis21-GFP was detected by its own fluorescence. Arrowheads = Tis21-GFP positive cells; asterisks = Nestin positive cells.

(**B**) Staining for doublecortin (Dcx)(Fig. 28. A-D, asterisks) in combination with Tis21-GFP (detected by its intrinsic fluorescence; fig. 28. A-D, arrowheads) showed that a small amount of Tis21-GFP positive cells is also positive for Dcx (Fig. 28. A-C, solid arrows), and this amount varies with time.

Early postnatally. 1 week after birth, the DG is being built by the second wave of migrating precursors, so that the majority of the cells of the DG were migrating Dcx positive transit amplifying precursors; out of these only about 30% showed Tis21-GFP expression (Tis21-GFP/doublecortin double positive (Tis21-GFP/Dcx), fig. 28, solid arrows)(Fig. 29, P1W).

Juvenile/adult. During the 2nd week, the number of Dcx positive cells decreased to about 30% of total DG cells (about 30% of the previous week); the number of Tis21-GFP/Dcx cells decreased more dramatically to about 4% (12.5% of the previous week) (Fig. 29,

P2W). This reflects the development of the DG and specifically the switch to the tertiary germinative matrix that will be the origin of all the neurons of the DG in the adult. From the 2nd to the 6th week after birth, the Tis21-GFP/Dcx positive cells remained as a subpopulation (constantly about 10%) of the Dcx positive cells. The Dcx and Tis21-GFP/Dcx positive cells continue decreasing with about the same speed from P2 to P6 weeks, while the number of Tis21-GFP positive-Dcx negative cells slightly increased (Fig. 29, P2 to P6W).

Aged. 18 weeks after birth the amount of neurogenesis in the hippocampus is low [172], as indicated by the low amount of Dcx positive cells. The extremely low levels of neurogenesis are reflected by the undetectable amount of Tis21-GFP/Dcx positive cells. The Tis21-GFP single positive cell population dropped to about 6% of all DG cells (Fig. 29, P18W).

SEZ. Doublecortin staining of the SEZ showed a different result: although the number of Tis21-GFP is high, and Tis21-GFP cells can be found in all the germinative layer, the double positive cells Tis21-GFP/Dcx were found only occasionally.

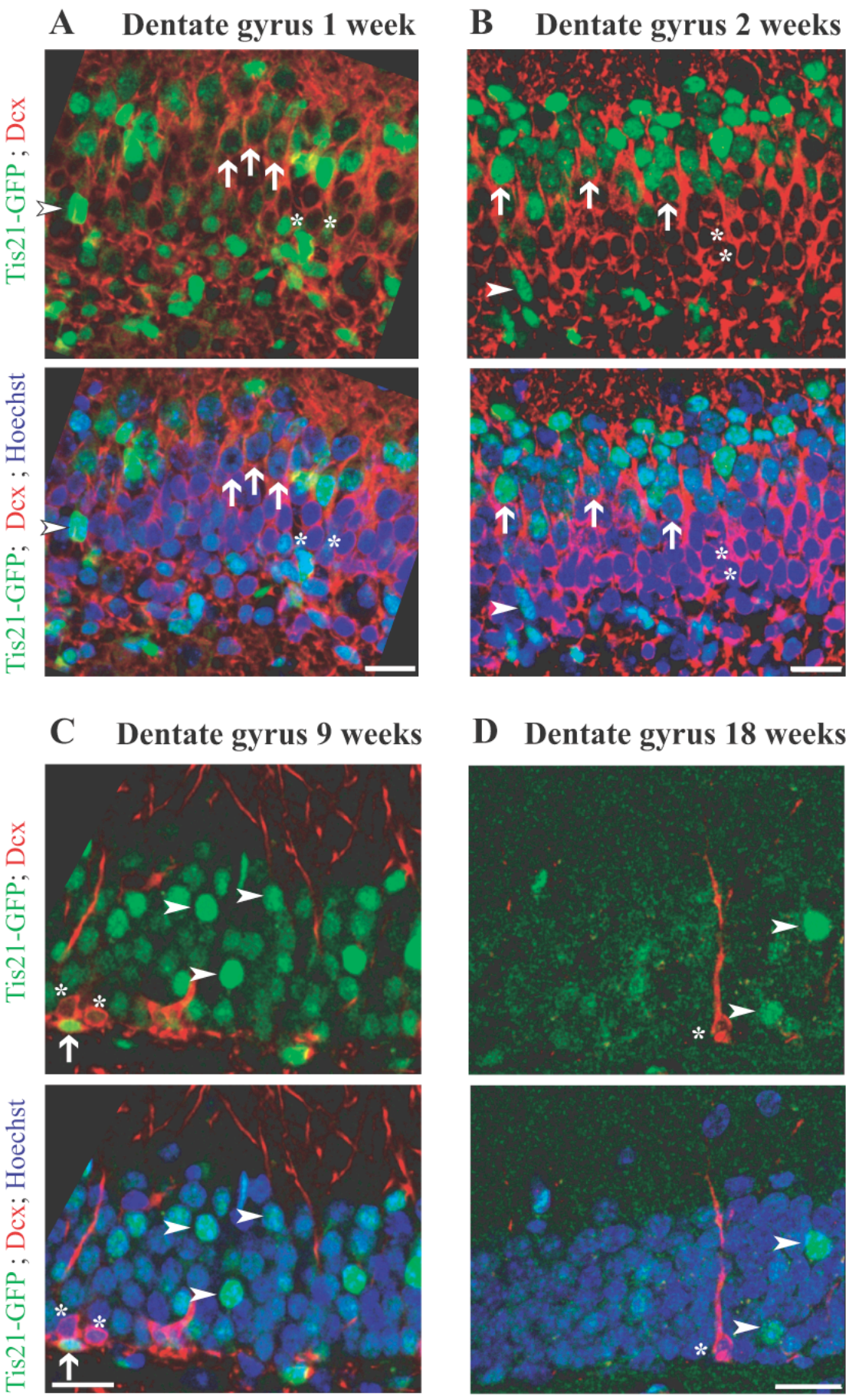

A Dentate gyrus 1 week
B Dentate gyrus 2 weeks
C Dentate gyrus 9 weeks
D Dentate gyrus 18 weeks
Tis21-GFP ; Dcx
Tis21-GFP; Dcx ; Hoechst
Tis21-GFP; Dcx
Tis21-GFP ; Dcx; Hoechst

Figure 28 (Previous page) **– Tis21-GFP is found only in a subpopulation of the transit amplifying cells.** (**A**-**D**) Examples of photomicrographs, used for quantification of the Dcx, Tis21-GFP and Tis21-GFP/Dcx positive cells. Single focal Z planes obtained from 40um thick brain slices of Tis21-GFP animals at various ages: 1 (**A**), 2 (**B**), 9 (**C**) and 18 (**D**) weeks after birth. The brains were either freshly dissected and fixed (**A** and **B**) or perfused and fixed (**C** and **D**). Upper panels show and overlay of the green (Tis21-GFP) and red (Dcx) channels, lower panels show the merge with the blue channel (Hoechst). Tis21-GFP was detected by its own fluorescence. Dcx positive cells were defined as a Hoechst positive nucleus completely surrounded by the Dcx staining, irrespective of the presence of an identifiable neuronal process. Arrowheads = Tis21-GFP positive cells; asterisks = Dcx single positive cells; solid arrows = Tis21-GFP/Dcx double positive cells. Scale bars = 20um

.

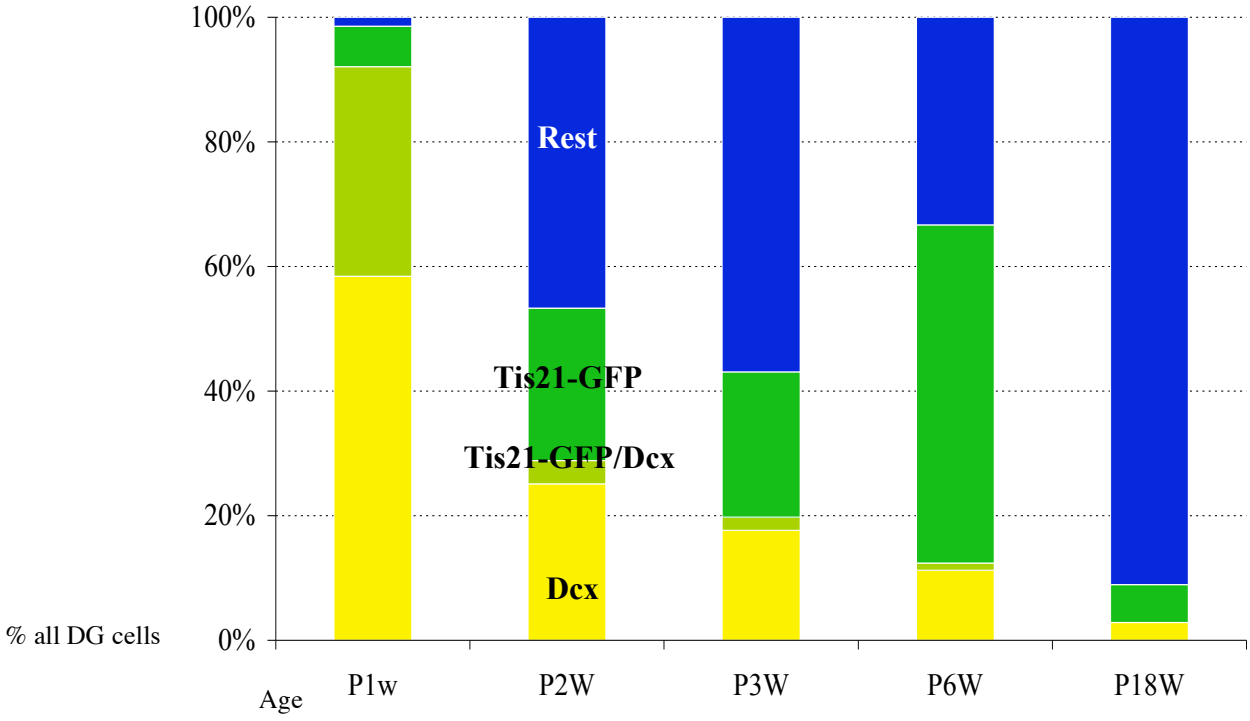


Figure 29 – The neurogenic cells decrease with time. Bar diagram illustrating the distribution over time of the Dcx (yellow bars, asterisks in fig. 28), Tis21-GFP (green bars, arrowheads in fig. 28) and Tis21-GFP/Dcx (light green, solid arrows in fig. 28) positive cells as a percentage of all cells in the DG of the Hippocampus (the rest of DG cells negative for Tis21-GFP and Dcx is represented by the blue bars). Each count is the sum of different fields of different hippocampal regions (except one animal of the P2 weeks series in which only one field was counted). P1 and 2W = 1 animal; P3 and 6W = 4 animals; P18W = 3 animals. The total number of cells counted per animal was between 341 and 1542; the total number of Tis21-GFP positive cells counted per animal was between 21 and 619; the total number of Dcx positive cells counted per animal was between 10 and 1420. Tis21-GFP was detected by its intrinsic fluorescence. Note that the total number of Dcx positive cells is represented by the sum of the yellow and light green bars, and the total number of Tis21-GFP positive cells is represented by the sum of the green and the light green bars.

(**C**) To identify granule cells, two different markers for post-mitotic neurons were used: NeuN (Fig. 30, B and E) and Prox1 (Fig. 30, D and E; G). NeuN is a marker of granule cells localized in the nucleus of mature neurons [203], while Prox1 is a marker for immature neurons. Prox1 is localized in the immature neurons nucleus as well, but its expression declines with time in mature neurons [204]. Staining for these markers showed a similar result: the majority of the Tis21-GFP positive cells is also positive for these markers but the proportion greatly varies with time (Fig. 31).

Early postnatal/juvenile. (1 to 6 weeks after birth). The number of NeuN positive cells increased with the development of the DG and the maturation of the neurons Tis21-GFP/NeuN double positive cells (some of which are also Dcx positive) increased concomitantly reaching a peak at 6 weeks after birth (Fig. 31, A, P1 to P6W). At this age the number of Tis21-GFP/NeuN double positive cells accounted for more than half the total number of NeuN positive cells.

Adult/aged. Later on (9 to 18 weeks after birth), while the number of NeuN positive cells remained constant the number of Tis21-GFP/NeuN cells decreased drastically to about 3.5% of the total number of cells (Fig. 31, A, P9 to P18W). Note that at this time point there are no longer Tis21-GFP/Dcx positive cells (Fig. 29, P18W).

The variation overtime of the Tis21-GFP/Prox1 double positive cells was not substantially different from the Tis21-GFP/NeuN double positive cells. The Tis21-GFP/Prox1 double positive cells increased until the 6th postnatal week (Fig. 31, B, P1 to P6W) and decreased at the end of the 18th week (Fig. 31, B, P18W).

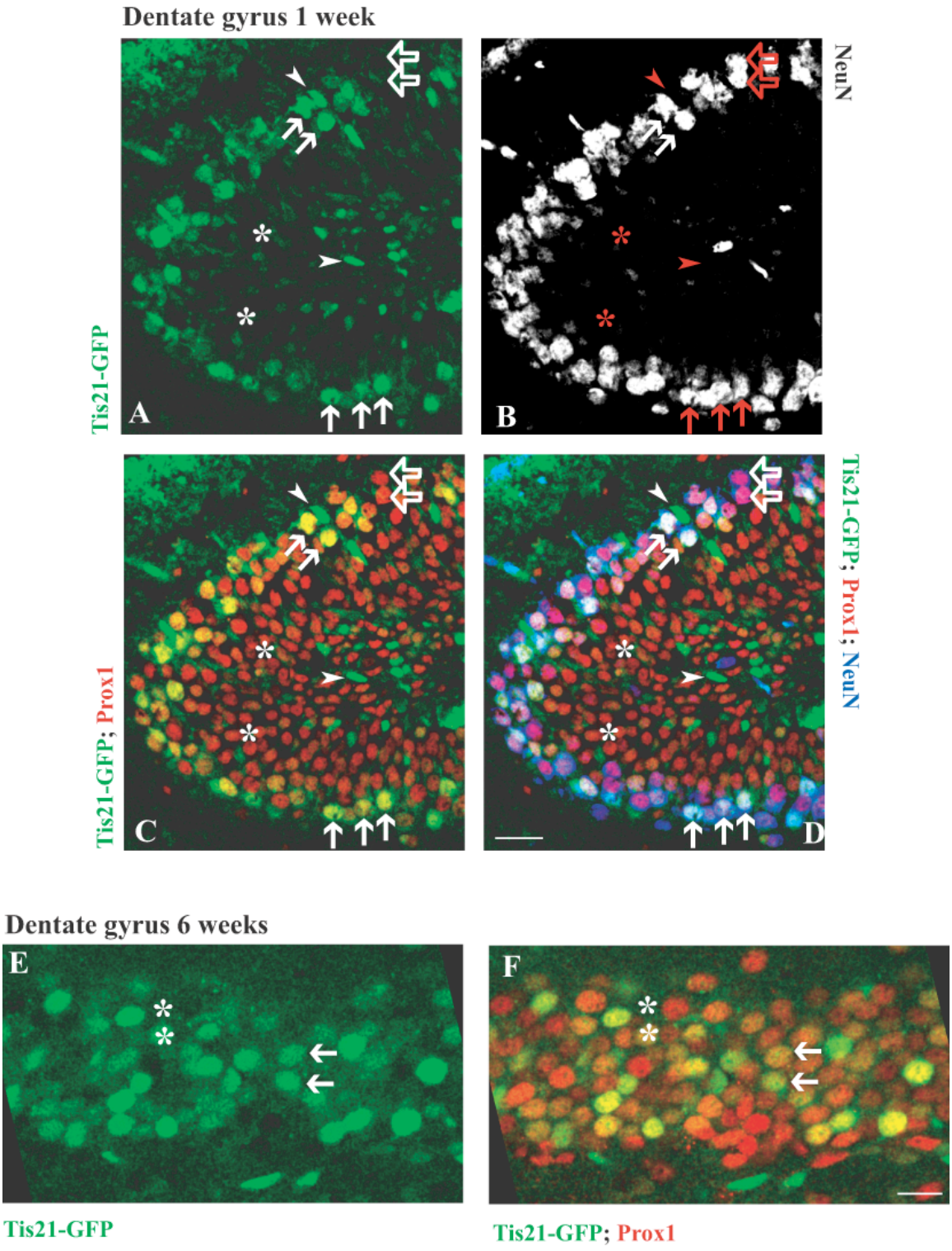


Figure 30 – Tis21-GFP is found in post-mitotic neurons. (**A-F**) Examples of pictures, used for quantification of the NeuN, Prox1, Tis21-GFP, Tis21-GFP/NeuN and Tis21-GFP/Prox1 positive cells. Single focal Z planes obtained from 40um thick brain slices of Tis21-GFP animals at various ages: 1 (**A-D**) and 6 (**E-F**) weeks after birth. The brains were either freshly dissected and fixed (**A-D**) or perfused and fixed (**E** and **F**). (**A**) single green (Tis21-GFP) channel; (**B**) single white (NeuN) channel; (**C**) overlay of the green (Tis21-GFP) and red (Prox1) channels; (**D**) merge of the green (Tis21-GFP), blue (NeuN) and red (Prox1) channels. Tis21-GFP was detected by its own fluorescence. Arrowheads = Tis21-GFP positive cells; asterisks = Prox1 single positive cells; empty arrows = NeuN/Prox1 double positive cells (Tis21-GFP negative); solid arrows = Tis21-GFP/NeuN/Prox1 triple positive cells. Scale bars = 20um

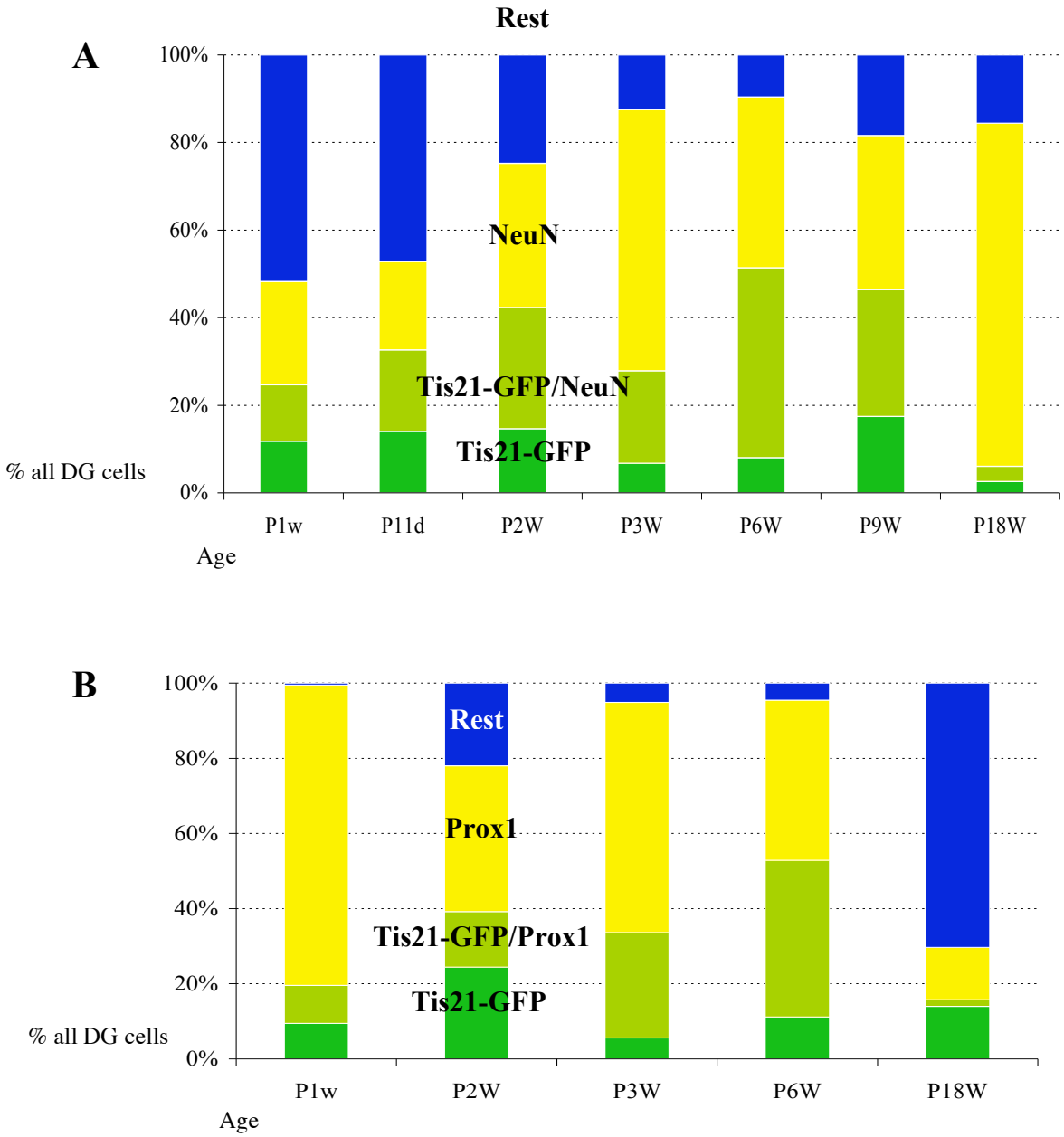


Figure 31 – Tis21-GFP is inherited by neurons and degraded with their maturation. (**A**) Quantification of the distribution of the NeuN (**A**, yellow bars) and Prox1 (**B**, yellow bars); Tis21-GFP (green bars); Tis21-GFP/NeuN (**A**, light green bars) and Tis21-GFP/Prox1 (**B**, light green bars) positive cells as a percentage of all cells in the DG of the Hippocampus (the rest of DG cells negative for Tis21-GFP and Dcx is represented by the blue bars), over time. Each count is the sum of different fields of different hippocampal regions (except A, P3 weeks and B, P18 weeks, in which only one field was counted in one of the animals). NeuN: P1W, P11d and P2W = 2 animals; P3W = 3 animals; P6W = 5 animals; P9W= 1 animal; P18W = 3 animals. The total number of cells counted per animal was between 461 and 2291; the total number of Tis21-GFP positive cells counted per animal was between 21 and 942; the total number of NeuN positive cells counted per animal was between 168 and 1767. Prox1: P1W = 2 animals; P2w = 3 animals; P3W = 3 animals; P6W = 5 animals; P18W = 3 animals. The total number of cells counted per animal was between 270 and 1116; the total number of Tis21-GFP positive cells counted per animal was between 55 and 278; the total number of Prox1 positive cells counted per animal was between 51 and 677. Tis21-GFP was detected by its intrinsic fluorescence. Note that the total number of NeuN or Prox1 positive cells is represented by the sum of the yellow and light green bars, and the total number of Tis21-GFP positive cells is represented by the sum of the green and the light green bars.

Taken together these data show that:

(i) Tis21-GFP does not mark the whole transit amplifying cell population in the DG but specifically a subpopulation.

(ii) Early after birth, the percentage of Dcx single positive cells decreases following a different kinetic than Tis21 GFP/Dcx double positive cells. The decrease of the Dcx single positive cells is slower than the decrease of the Tis21-GFP/Dcx double positive cells.

(iii) Tis21-GFP is inherited by young neurons.

(iv) Tis21-GFP is degraded in the mature neurons.

This suggests that not all the transit amplifying cells generate neurons directly but they first go through cycles of proliferation and then express Tis21-GFP and generate neurons (inheriting Tis21-GFP). So that the Dcx mitotic cells can be divided in two subsets: (i) a transit amplifying Dcx positive/ Tis21-GFP negative cell population that proliferate and (ii) a neurogenic Dcx/Tis21-GFP double positive cell population that divide (symmetrically or asymmetrically) to generate neurons.

II - 4.3.
The proliferation of Tis21-GFP cells overtime

To corroborate the results obtained using specific cell type markers, the mitotic behavior of Tis21-GFP cells was examined over time. In the DG and SEZ, mitotic cells were detected, using the anti PH3 antibody, and Tis21-GFP/PH3 double positive cells (scored by using confocal imaging) were plotted as a percentage of all mitotic cells. The percentage of Tis21-GFP mitotic cells changed dramatically over time in the hippocampus.

(i) It stayed almost constant early after birth, decreasing only 6% from 1 to 2 weeks after birth (Fig. 32, 1W_H and 2W_H); later on it decreased more dramatically.

(ii) A 30% decrease from 2 to 3 weeks and almost 20% from 3 to 6 weeks after birth was observed (Fig. 32, 2W_H and 4W_H).

(iii) It reached zero at 18 weeks after birth, when it was very rare to detect any dividing cell (Fig. 32, 18W_H).

Almost the totality of mitotic cells was Dcx positive (> 99%), so that all of the Tis21-GFP/PH3 double positive cells resulted to be also positive for Dcx.

The situation in the SEZ was different. In this region, the percentage of Tis21-GFP mitotic cells was constant (oscillating with a maximum of 8% difference) in the first 3 weeks of life (Fig. 32, 1W_SEZ to 3W_SEZ), and decreased later (6 weeks after birth, fig. 32, 6W_SEZ), reaching zero at the end of the 18th week after birth, when some mitotic cells can still be detected (Fig. 32, 18W_SEZ, asterisks).

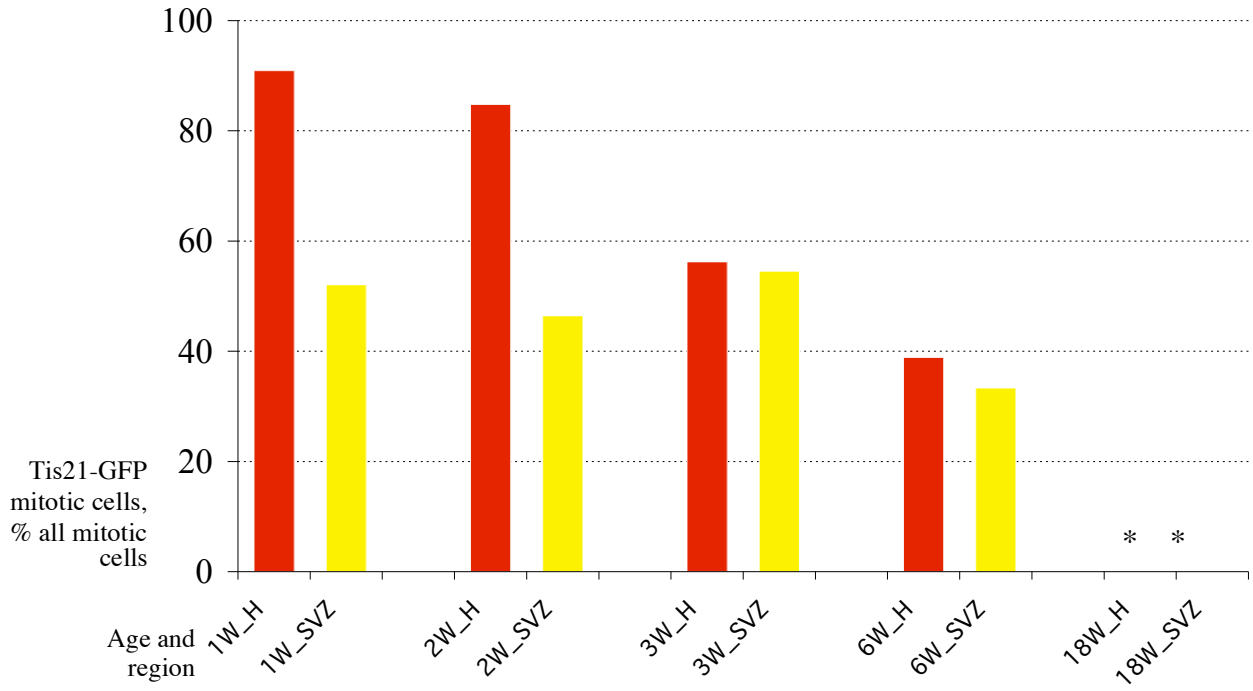


Figure 32 – Variation in the number of Tis21-GFP mitotic cells during adulthood in SEZ and DG. Bar diagram illustrating the distribution of the *Tis21*-GFP mitotic cells as percentage of the total number of mitotic cells in the DG of the hippocampus (red bars) and SEZ (yellow bars) over time. Each count is the sum of different fields of different hippocampal regions. Hippocampus counts: P1W, P3W and P18W = 1 animal; P2W = 2 animals; P6W = 3 animals. SEZ counts: one animal each. The total number of mitotic cells counted per animal was between 4 and 48; the total number of mitotic Tis21-GFP positive cells counted per animal was between 1 and 28. Tis21-GFP was detected by its intrinsic fluorescence. The asterisks indicate that, although no bars are present, the cells were counted and found to be 0.

These results are in accordance with the known gradients of neurogenesis in adult mice. Hippocampal neurogenesis declines during the whole postnatal life of animals under standard housing conditions, while generation of olfactory interneurons is steadier throughout life.

III Discussion

III–1. Tis21-GFP and the study of neurogenic cells

III – 1.1.
Tis21 is a pan-neurogenic marker

During embryonic development *Tis21* mRNA is specifically expressed in neurogenic progenitors, but it is excluded from proliferating progenitors or neurons, in all the regions of CNS and PNS [70, 180]. In the *Tis21*-GFP mouse line, green fluorescence appeared throughout the neural tube in exact correlation with the temporal and spatial gradients of neurogenesis. GFP expression was confined to the mitotically active layers: the VZ and the SVZ, where fluorescence became detectable in an increasing proportion of cells as more and more neurons were generated during development. In addition, many migrating neurons inherited GFP from the mother and were Tis21-GFP positive during their migration towards the cortical plate [28]. However, these findings did not prove that Tis21-GFP marks the entirety of the neurogenic progenitors. For this to be true, one condition must have been satisfied: all the neurons must have shown the inherited Tis21-GFP fluorescence immediately after their birth. Since the half-life of the Tis21-GFP protein in the neurons is not known, we aimed to identify neurons as early as possible after their birth, so that we could detect Tis21-GFP before its degradation. Neurons were identified by immunostaining using the earliest known marker for neurons, βIIItubulin [183]; in addition, only migrating neurons were selected. The criterion used to select migrating neurons was their position within the VZ. Although it is known that migrating neurons in the ventricular zone are not necessarily newborn neurons [40, 205], this was the best applicable criterion we could use in static images. The number of Tis21-GFP positive newborn and young neurons was scored in the telencephalon and hindbrain at the onset of neurogenesis. Neurons do not express Tis21-GFP but inherit it from the mother [70]; therefore, the finding that all the migrating neurons in the VZ were positive for Tis21-GFP (Table 1) shows that all neurons derive from a Tis21-GFP expressing cell. Consequently showing that Tis21-GFP is a pan-neurogenic marker. The fact that not all of the neurons scored are necessarily newborn, suggests that Tis21-GFP is not immediately degraded in the neurons, in accordance with the finding that Tis21-GFP is still present in some migrating neurons of the intermediate zone and cortical plate [28].

III – 1.2.
The early sub ventricular zone is neurogenic

Mitotic cells have been noticed previously, in the basal part of VZ, but their role has been unclear. Basal mitotic cells could have been the progenitors of the SVZ, which constitutes a distinct cell layer at later stages of development and which was thought to largely generate glia (Bayer, S. A. & Altman, J. (1991) *Neocortical development* (Raven Press, New York); Jacobson, M. (1991) *Developmental neurobiology* (Plenum Press, New York und London)). However, the increase in basal mitotic cells, in correlation with the progression of neurogenesis, suggested that these cells could contribute to neurogenesis [42, 206]. Furthermore, dividing SVZ cells and cortical neurons share expression of specific genes like *Manic-Fringe* [93], *SVET1* [94], *Cux1* and *2* [95, 96] and *Tbr2* [97], most of which are transcription factors. In addition mutants affecting SVZ development also affect the generation of upper-layer cortical neurons [94]. These observations were interpreted in favour of a role of dividing SVZ cells also in neurogenesis, but the proof came from imaging of acute brain slice cultures in which it was possible to show symmetric divisions of basally located progenitors giving rise to neurons [28, 40, 41].

In this doctoral work is shown that BPs outnumber APs during embryonic development (Fig. 10), constituting the predominant neurogenic population in the cortex. From this finding we deduced that BPs (or at least some of them) must initiate Tis21-GFP expression de novo, originating from a Tis21-GFP negative cell. Furthermore, considering that BPs generate twice as many neurons as APs, BPs are the major source of neurons generated in the cortex [28]. BPs constitute an additional mitotic zone (the SVZ), increasing the number of neurons generated *per* lumenal surface area in the neuroepithelium, in the region of the neural tube where the greatest number of neurons is generated, the cortex. This finding suggests that BPs could be one of the first steps to occur in mammals towards the "basalization" of neurogenesis. An increase in the importance of the basal side of the cortex in the generation of neurons is suggested to happen during evolution of the primate lineage, leading to the formation of thicker cortex, and seemingly linked to the increase in numbers of higher layers neurons [14, 42, 98].

III – 2. Study of neurogenic divisions

Real-time imaging studies of cells dividing at the apical surface of the neuroepithelium [47, 92, 207] and analyses of asymmetric distribution of cell fate determinants in mitotic NE cells [47, 208, 209] supported the idea that, during early neurogenesis, neurons are generated only by asymmetric differentiating divisions of NE cells. In contrast, retroviral lineage tracing studies in vivo [210-214] and in vitro analysis of the division patterns of cultured NE cells and their progeny documented the co-existence of asymmetric and symmetric neurogenic divisions of progenitors [68, 215, 216]. This discrepancy turned out to be apparent when, almost at the same time three different groups showed in slice culture the co-existence of apical asymmetric (APs) and basal symmetric (BPs) neurogenic progenitor cells divisions in the cortical neuroepithelium [28, 40, 41]. BPs are intermediate progenitors with a high neurogenic potential (they generate two neurons rather than one, as APs) but very low, if at all, self renewal potential (only about 10% of BPs were shown undergoing symmetric non-neurogenic divisions [28, 40]). Very little is known about BPs and we think, also in light of the findings related to evolution of the human lineage [14, 98], that it would be important to know more about the cell biology and the lineage of these intermediate progenitors that seem to have a crucial role especially during cortical neurogenesis. This doctoral work is therefore focused on the study of BPs.

III – 2.1.
The strategy and the new tool

The precise spatial segregation of APs and BPs in the neuroepithelium, suggests that the position in which the progenitors divide is of primary importance for the fate of their daughters. Therefore it is important to study the behaviour of the neurogenic precursors in a system that mimics as much as possible the physiologic environment. For this reason the use of acute brain organotypic slice culture is the best compromise to obtain cellular and sub cellular imaging resolution of the progenitors in an environment that resembles the physiologic one.

Two main approaches have been taken recently to investigate embryonic neurogenic divisions, *in-* or *ex-vivo*: random single cell labelling [40, 41, 92, 207, 217-219], or labelling of

entire specific cell populations [28, 39, 185, 220]. The use of a specific promoter driving GFP expression, labelling an entire cell population presents several advantages. (i) It makes possible to identify unequivocally the cell type during the imaging, without post-imaging analysis (immunostaining or single cell membrane potential recording). (ii) Neurogenesis can be investigated, without any manipulation of the embryo prior to imaging. (iii) The study of early neurogenesis is not limited by the technical difficulties of manipulating a young embryo *in* or *ex* utero. (iv) It excludes the bias towards labelling a cell subpopulation that is more susceptible to viral infection [221]. (v) In specific combination with a two-photon imaging system, allows collecting from a single experiment a greater amount of information compared to a single experiment of single cell labelling.

Having already a mouse in which all the neurogenic progenitors are marked, we sought to have a mouse line highlighting all neurons right after their generation since the onset of neurogenesis. Other transgenic lines expressing fluorescent proteins specifically in the neurons exist [222, 223]; however none of them was shown to mark all neurons immediately after their birth since the onset of neurogenesis, which conditions are crucial for our study. We, therefore, generated a new transgenic mouse line to identify the entirety of neurons immediately after their generation. For this purpose, the promoter of the earliest known neuronal marker, the βIIItubulin gene [183], was chosen to drive GFP expression. The new transgenic mouse line with a neuronal specific GFP expression was generated in a relatively short time combining the use of: (i) a BAC clone containing the whole *βIIItubulin* gene and large 3' and 5' flanking regions (Fig. 16, A), (ii) RED-ET-based BAC modification technology [197, 198] and (iii) male pronuclear injection. (This approach has recently been used to create a gene expression atlas of the central nervous system [224]). Targeting of the GFP to the plasma membrane using the GAP43 protein localization signal allowed to achieve a detailed labeling of the whole neuronal surface [225], and at the same time to distinguish the *βIIItubulin*-driven GFP from the *Tis21*-driven GFP during time-lapse experiments. The presence of the transgenic GFP does not cause any aberrant phenotype, and it reveals all the neurons including neurons migrating through the Ventricular Zone.

βIIItubulin-GFP fluorescence was (i) found in the central and peripheral nervous system (Fig. 17 and 18), it was (ii) confined to the neurons (Map2 and βIIItubulin positive

cells)(Fig. 19) and (iii) excluded from the progenitor cells (Nestin positive) (Fig. 19). (iv) It accumulated in the Golgi apparatus (Fig. 19), in young neurons (E10.5 cortex). This is in accordance with the known palmitoylation of the GAP43 plasma membrane localization [202] happening in this organelle.

The *Tubb3*-GFP line and the existing *Tis21*-GFP line were eventually crossed to obtain a double mutant, TisTubb-GFP, mouse line (Fig. 20). The newly generated TisTubb-GFP line allowed detection of neurogenic divisions and tracking of the daughters since the onset of neurogenesis. Moreover the plasma membrane βIIItubulin-GFP allowed us to study in detail neuronal migration and neurite outgrowth in the developing VZ at the onset of neurogenesis.

III – 2.2.
High-resolution study of neuronal migration at the onset of neurogenesis

Neurites extending towards the ventricle and neurons migrating towards the ventricular surface were detected in accordance with the results obtained by other groups [40, 205]. In addition, neurites assumed a flattened shape when close to the ventricular surface, in many cases (Fig. 21). Due to technical limitations of the imaging it was not possible to distinguish whether neurons contacted the ventricle or if, instead, this flattened conformation indicated growth cones unable to pass through the NE/RG cells junction barrier. However, the persistency of this peculiar flat conformation for a considerable amount of time (from 10' to 90'), the elongation of a long (often spanning the entire VZ) process and the migration of the whole soma towards the ventricle are suggestive of, at least a subset of neurons, seeking the ventricle. It is known that interneurons, migrating into the cortex from the GE migrate towards the ventricle; it has been suggested that they do so to synchronize their radial position with the position of projection neurons generated in that time and region [205]. It is not to be excluded that interneurons may also to take up some sort of diffusible signal from the luminal fluid. The βIIItubulin-GFP localization in the Golgi apparatus allowed us to image, for the first time, the migration pattern of the Golgi apparatus (presumably coupled with the centrioles and MTOC) in single neurons migrating in a tissue. Golgi apparatus moves towards the future leading edge of migrating neurons before the onset of somal migration (Fig. 21), keeping its leading position during migration. Such a migration of

the Golgi apparatus occurs as well when there was a switch in the direction of migration. Our results, obtained for the first time in organotypic slice culture, are in agreement with the observation of migrating neurons behaviour of other laboratories [226, 227].

III – 2.3.
Abundance of neurogenic divisions and kinetics of βIIItubulin expression

The TisTubb-GFP mouse line allowed us to image selectively all neurogenic divisions and track their progeny since early stages of neurogenesis (Fig. 22). The percentage of apical neurogenic mitoses giving rise to one βIIItubulin-GFP expressing daughter is unexpectedly low (around 3%) (Fig. 23), since it is known that all apical Tis21-GFP positive cells give rise to, at least, one neuron [28]. The observed low percentage can be justified by technical reasons. On the one hand, the high amount of energy delivered to the cells causes bleaching of the fluorescence, on the other hand track of many cells is lost while they merge into the (fluorescent) forming neuronal layer. This limits the time for which it is possible to track daughter cells of APs, thus not allowing the visualization of βIIItubulin-GFP expression in many cases. Despite the small number of cases observed, it is not to be excluded that the average time of onset of βIIItubulin-GFP expression (126'), observed after apical mitosis, would be an underestimation of the real average time of βIIItubulin-GFP expression. In other words the only cases observed of βIIItubulin-GFP expression in daughters of APs could be the fastest of the cells expressing βIIItubulin-GFP after apical mitosis. The same technical limitations apply to imaging of basal neurogenic mitoses. However, daughters of BPs express βIIItubulin-GFP earlier than daughters of APs; this makes the identification of βIIItubulin-GFP positive cells easier in our experimental set-up. This explains why the observed percentage of BPs giving rise to daughters, of which at least one was βIIItubulin-GFP positive, is close to 50% (Fig. 23).

In addition it should not be excluded the possibility that not all the Tis21-GFP positive cells generate neurons. While it has been shown that all the newborn neurons inherit Tis21-GFP, a lineage tracking of the Tis21-GFP expressing cells has never been carried

out, leaving open the possibility that Tis21-GFP positive precursors could divide without generating neurons. Tis21-GFP positive progenitors could divide either to self amplify to a limited extent or to generate BPs. This would imply that Tis21-GFP expression starts not just in the cell cycle previous the neuron generation but earlier; however, so far, it has not been possible to track Tis21-GFP positive progenitors long enough to solve this issue.

Most interestingly, we found that the kinetic of βIIItubulin-GFP expression varies between divisions of APs and divisions of BPs: daughters of BPs expressed βIIItubulin-GFP significantly faster than daughters of APs (ANOVA, $p < 0.001$) (Fig. 24). After a basal division, the earliest observed appearance of βIIItubulin-GFP was 12' and the latest was 100', with an average time of 46'. However, the distribution of βIIItubulin-GFP expression time after mitosis shows a peak, with half of the cells observed expressing βIIItubulin-GFP between 30' and 50' (Fig. 24). In contrast, daughters of APs express βIIItubulin-GFP slower than daughters of BPs. After an apical division, the earliest time after mitosis in which βIIItubulin-GFP could be detected is 96' and the latest is 144', with an average time of about 126'. Because of the small amount of cases observed it is not possible to infer about the distribution of speeds; however, it is worth to notice that two, out of the three cells observed, expressed βIIItubulin-GFP 140' post mitosis (Fig. 24), in accordance with the possibility that the real average time of βIIItubulin-GFP expression could be longer than observed. The use of ANOVA analysis correlated with Bonferroni cross correlation showed that daughter cells originated from BPs express βIIItubulin-GFP significantly early than daughters of APs (Fig. 24).

Taken in account together, the faster kinetic of βIIItubulin-GFP expression of daughters coming from BPs and the higher intensity of Tis21-driven fluorescence of BPs if compared to APs, these results suggest that BPs are intermediate progenitors more strongly primed to neurogenesis than APs. Moreover, these results are in agreement with the finding, from our and other laboratories, that BPs can be positive for early neuronal markers [28, 41, 93]. It is possible that BPs accumulate, already prior to mitosis some of the transcripts necessary for differentiation of the daughters, including the βIIItubulin mRNA. This would strongly suggest that a specific program is turned on in BPs before mitosis. In accordance with this hypothesis is the fact that BPs have a longer G2 cell cycle phase [85] and that they express specific transcription factors, like Tbr2 [97]

already in the G1 phase prior to mitosis. This specific program could be changing the NE/RG cells into BPs: intermediate progenitors with a higher neurogenic potential but a limited self-renewing capacity.

III – 2.4.
Loss of the apical contact of Basal Progenitors and evolution

We think that the loss of the apical contact prior mitosis of the BPs, showed by Miyata and coworkers [41] and confirmed in this work (Fig. 11), is of key importance in the determination of the fate of the BPs. Kosodo and coworkers found that the surface of apical plasma membrane of proliferating progenitors is roughly double the size of the apical plasma membrane of neurogenic progenitors; moreover apical membrane is asymmetrically distributed during asymmetric neurogenic division [71]. This strongly suggests that the apical plasma membrane, or the apical contact, is as a key regulator in maintaining the progenitors in the proliferative state. Keeping contact with the ventricle could allow signals coming from the ventricle to reach the progenitor cells, therefore maintaining the mitotic potential; for instance Shh might exert its action on the proliferating progenitors [52, 53] via Megalin [228], that is specifically localized in the apical plasma membrane. On the same line, loss of apical contact of BPs could explain the low rate of proliferation (only around 10% of the cells dividing on the basal aspect of the neuroepithelium don't generate neurons according to [28, 40]. Interestingly enough, BPs seem to have the highest neurogenic potential per cell division but they are very limited in self renewal (if they self renew at all!).

One can speculate that increasing the self-renewal potential of these basally dividing progenitors could as well increase the number of neurons generated per area. Interestingly Dehay and coworkers have shown that thalamo-cortical afferent axons (TCA) can regulate the cell cycle of progenitors (speeding it up) in monkey and mouse via a diffusible factor [229, 230] and that, in the OSVZ, the pattern of mitotic figures reflects their proximity to TCA (Dehay, C. personal communication). Ablation of the TCA projecting to visual area 17 in the monkey leads to a decrease in the number of mature neurons in the targeted area [229] moreover, OSVZ progenitors of area 17 showed a cell cycle shorter than progenitors of area 18. This implies a further amplification of the progenitors pool before neurogenesis in the area 17 compared to the area18 [84]. The

earlier appearance of the outer fiber layer in the monkey [98] compared to the mouse [231] suggests that TCA reach their cortical targets earlier in the monkey than in the mouse. It is not to be excluded that the early growth of the TCA in the monkey could lead to an increase in the size of the basal germinative layer prior to or at the onset of neurogenesis, ultimately leading to the appearance of the OSVZ. In the mouse, conversely, later growth of TCA could either not induce a sufficient proliferation or induce it too late, when neurogenesis is declining. This is an intriguing possibility that would combine an intrinsic genetic program of the progenitors to divide generating a defined lineage to an environmental control of the proliferation by the factor(s) secreted by the TCA.

A second interesting possibility is that apical contact, rather than granting access to the ventricle, would give anchorage to the cells to complete INM or to segregate specific proteins to the junctions. Conditional deletion of the *Cdc42* gene by Cappello et al. [195] showed misorganization of the neuroepithelial tissue concomitantly with an increase in the number of: abventricular dividing cells, Tbr2-positive cells and number of neurons. Taken together, these results suggested an increase in the abventricular, symmetric neurogenic mitoses. In addition this correlated with the loss, during neurogenesis, of immunoreactivity for the proteins of the junction complex and an increase in the number of progenitors lacking apical contact (this work, fig. 15), suggesting a causal link between loss of apical junctions, collapse of apical contact and increase of abventricular progenitors [195]. However, further studies are required to confirm that this abventricular mitotic cells divide symmetrically to generate neurons and so that they are *bona fide* BPs.

It has still to be elucidated if loss of apical contact is the trigger for the cells to divide on the basal side or rather the consequence of a program that requires basal localization for symmetric neurogenic division. However, the finding that both neurogenic and non-neurogenic basal dividing cells miss the apical contact (Fig. 12; table 2; fig. 13) indicate that a limited self renewal capacity is independent from the contact with the ventricle, as suggested by the presence of a small amount of basally-dividing, symmetric, non-neurogenic progenitors. Furthermore, it is not likely that apical contact loss is the only trigger for the switch to basal symmetric neurogenic divisions. This is confirmed by the presence of a small amount of basally-dividing, symmetric, non-neurogenic progenitors that lack apical contact as well.

III - 3. The Tis21-GFP mouse and the study of adult neurogenesis

The study of adult neurogenesis has been carried out mostly using methods that allow marking of proliferating cells and tracking of daughter cells. These methods, including use base analogs like BrdU and viruses, however, present several disadvantages; among these the need to fix the tissue for detection (BrdU), the non-specific marking of cells (BrdU and viruses). In general these methods are not very selective; they target either all cells in S phase (BrdU) or random cells (virus). This has made difficult the study of specific cell subpopulations in vivo. Targeting with a genetically encoded reporter a specific cell type would allow studying the behavior of entire cell populations over time eventually *in vivo*. In this context, the *Tis21*-GFP mouse line seems to be a very interesting tool, because, during embryonic development, it offers the possibility to label specifically all the neurogenic progenitors and to track, to a limited extent, the newborn neurons [28] To exploit these characteristics for the study of adult neurogenesis, Tis21-GFP expression was characterized in postnatal, juvenile and adult mice.

III – 3.1.
Tis21-GFP in the lineage of adult progenitors

The sequential expression of the markers chosen for this analysis in the DG (Nestin/GFAP > Dcx > Prox1/NeuN; with some overlap between Dcx and Prox1/NeuN see fig. 33) allowed us to position onset of Tis21-GFP expression in the known lineage of DG adult neurogenesis (Fig. 33) [134]

Tis21-GFP is not expressed in the astrocytes/stem cells, as shown by the absence of Tis21-GFP Nestin or GFAP double positive cells (Fig 27).

Tis21-GFP is first expressed in a subpopulation of the Dcx positive cells, as shown by the fact that only a subset of Dcx positive cells is also positive for Tis21-GFP (Fig. 28 and 29).

Tis21-GFP is inherited by the neurons and then degraded. Two lines of evidences point towards the passive inheritance of Tis21-GFP by the neurons (Fig. 30 and 31). During embryonic development, *Tis21* is not expressed in the neurons but inherited [70] and Tis21-GFP persist in the neurons for a limited time their birth [28] Furthermore, in the adult a substantial portion, but not all, of the Prox1 and NeuN positive cells are positive

for Tis21-GFP. However, when at older age (18weeks), the rate of generation of new neurons decreases, the number of Tis21-21/Prox1 and Tis21-GFP/NeuN positive cells decreases as well; in contrast to the number of NeuN positive cells that stays constant.

A similar result was obtained in the SEZ. Tis21-GFP/Nestin or GFAP double positive cells were never detected confirming that the astrocytes/stem cells do not express *Tis21*. In coronal sections of the SEZ, Tis21-GFP/Dcx double positive cells were found very seldom. The percentage of Tis21-GFP/Dcx positive cells was not quantified, but it seems that these cells are more rare in the SEZ than in the DG. This could be explained by the fact that Dcx cells migrate away from the SVZ along the RMS, so that Tis21-GFP/Dcx double positive cells might be along the RMS distal from the SEZ and closer to the OB. However, a copious amount of Tis21-GFP cells was found in the SEZ suggesting that Tis21-GFP expression starts already in progenitors located in the SEZ. The Tis21-GFP expression in the SEZ will be further characterized by checking the progenitors close to the OB along the RMS and staining for the early fate specification marker Dlx2.

III – 3.2.
Tis21-GFP expression marks the neurogenic subpopulation of the mitotic doublecortin positive cells in the dentate gyrus

The fact that Tis21-GFP is found in a subpopulation of the Dcx, but not in the Nestin/GFAP positive cells, together with the finding that Tis21-GFP/Dcx cells are mitotic, show that mitotic doublecortin cells are divided in two subpopulations.

The transit amplifying cells: a proliferating cell population that is Dcx positive and Tis21-GFP negative (Fig. 33).

The neurogenic progenitors: a neurogenic cell population that is Dcx positive and Tis21-GFP positive (Fig. 33).

This implies that progenitors transit-amplify for a limited number of cell cycles and then express Tis21-GFP and generate neurons. However, it is not known if Tis21-GFP self amplify as well as if they generate one (asymmetric division) or two (symmetric division) neurons per division. This adult cell lineage recalls the embryonic cell lineage; a stem cell proliferate to give rise to neurogenic progenitors that eventually generate neurons in which, at the single cell level, proliferative proceeds neurogenic phase.

However, there are at least two differences from the embryo. During embryonic development cells go sequentially through a Nestin positive, a Nestin/Tis21-GFP double positive stage and eventually post mitotic Dcx/Tis21-GFP neurons. In the adult Dcx starts being expressed before mitosis so that the expression sequence becomes: Nestin> Dcx> Dcx/Tis21-GFP> post mitotic Tis21-GFP>NeuN. Furthermore, during embryonic development the NE cells go from a stage in which only proliferative divisions take place to a stage in which proliferative and neurogenic divisions coexist and eventually only neurogenic (and gliogenic) divisions occur. In the adult DG proliferation and neurogenesis seem to coexist at all times after birth and both decrease with aging at a similar rate (Fig. 29). The only time in which the decline of Tis21-GFP/Dcx double positive cells is faster than the decline of the single Dcx positive cells is between 1 and 2 weeks after birth (Fig. 29). Dcx positive cells number decreases 3 fold, from about 90% to about 30% of the cells of the DG, while Tis21-GPF/Dcx double positive cells decreased 9 fold, from about 33% to about 4% of the cells of the DG. This shows that, between the 1st and 2nd week, the number of Dcx positive cells (mostly transit amplifying cells but also migrating immature neurons) is reflecting the massive 1st and 2nd waves of SVZ progenitors migration. The actual number of neurogenic cells at the end of the 2nd week is best indicated by the Tis21-GFP/Dcx cells that reflect the 3rd germinative matrix. In other words the number of Dcx positive cells, at the end of the 2nd week, still reflects the build-up phase of the DG while the Tis21-GFP/Dcx double positive cells already shows the adult level of neurogenesis. Later on, the proportion of Dcx and Tis21-GFP/Dcx positive cells stays proportional and proportionally the two population decrease (Fig. 29), probably until the end of the life of the animal.

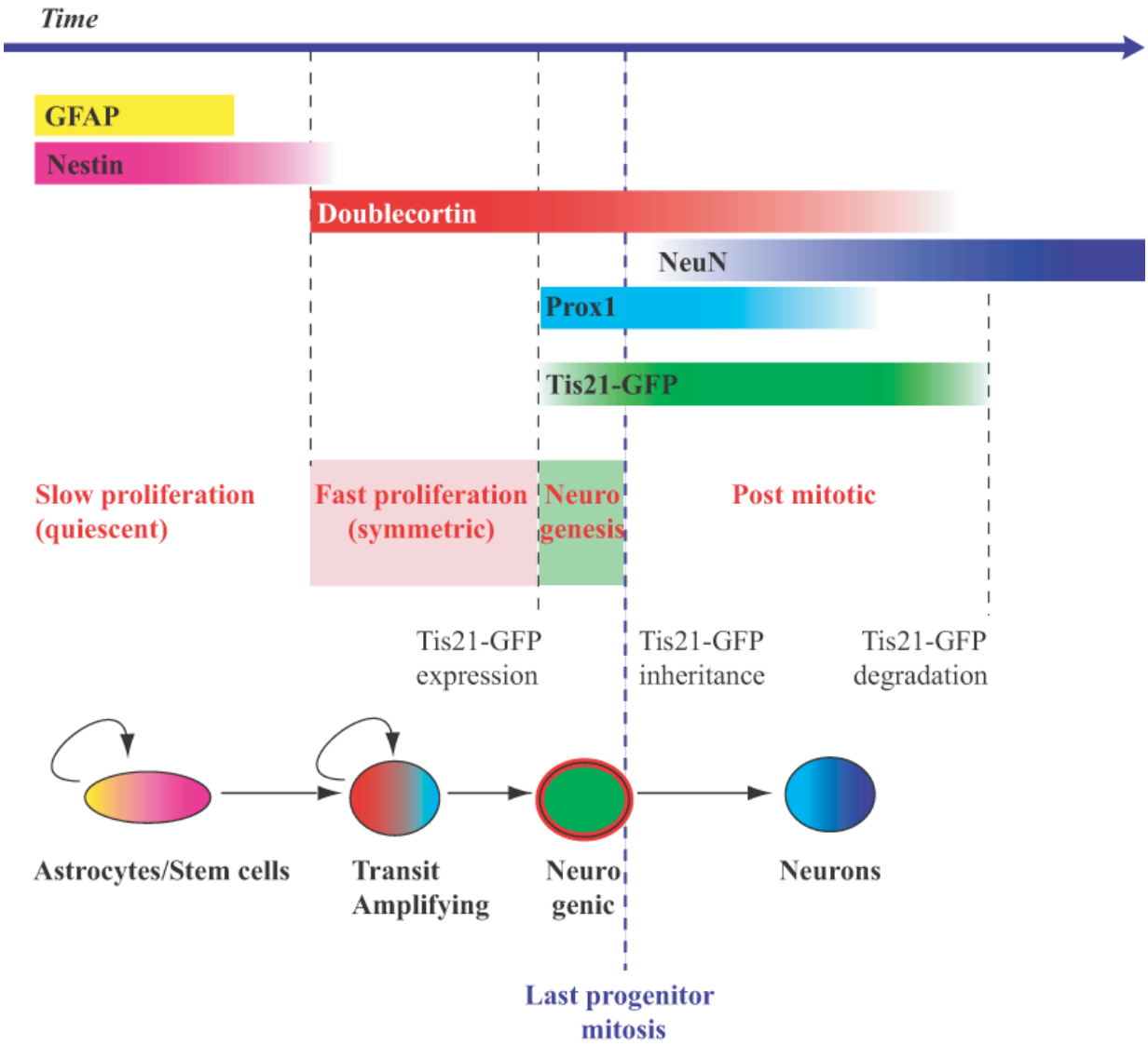


Figure 33 – Tis21-GFP marks the neurogenic adult cells. Schematic representation of the expression of Tis21-GFP with other cell lineage markers at single cell level in the adult mouse DG. Note that it is not known if Tis21-GFP/Dcx double positive cells self renew, and divide symmetrically or asymmetrically. The colors in the schematic cell representation indicate the markers expressed in that stage.

III – 3.3.
Tis21-GFP correlates with the level of neurogenesis in the dentate gyrus

The finding that Tis21-GFP is not transcribed in neurons [70] but it is inherited by the neurons and then degraded [28] in the embryo, seem to be true also in the adult. Although an in situ hybridization must be carried out in the adult to confirm the lack of Tis21 expression in the neurons, two lines of evidences point in the direction of the passive inheritance and degradation. On the one hand, the finding that not the totality of NeuN positive post mitotic neurons are Tis21-GFP positive. On the other hand, the finding that, at later ages, when neurogenesis is almost undetectable (P18W, fig 29), the amount of NeuN/Tis21-GFP double positive cells decreases (degradation of the GFP) while the number of NeuN positive cells stays constant (active transcription of NeuN). So that at each time point examined, the number of post mitotic Tis21-GFP cells reflects the steady state of the balance between the input of new neurons that inherit Tis21-GFP from the mother, and an output to which death of neurons and degradation of Tis21-GFP contribute to a variable extent. This scenario is confirmed by the Prox1 staining with two obvious differences at the 1st and 18th weeks after birth. Prox1 marks immature post mitotic neurons as well as neuronal progenitors (Kempermann G., personal communication), but it is not expressed in mature neurons and this is the reason why the decrease of Prox1 at 18 weeks after birth correlates with the decrease of Tis21-GFP. Thus, considering that the number of Tis21-GFP/Dcx cycling cells (the cells that express Tis21-GFP) is a small proportion of the total number of Tis21-GFP cells, the number of Tis21-GFP positive cells reflects, with a delay that has still to be quantified, the variations of neurogenesis in physiological conditions. Specifically, while the number of mitotic Tis21-GFP/Dcx cells reflects the neurogenic progenitors, the number of post mitotic Tis21-GFP cells reflects the number of newborn and young post mitotic neurons that survive in the DG.

III – 4. Perspectives

The study of the genetic programs and signaling molecules involved in the generation of BPs is of crucial importance; however, a marker of BPs has not been found to present. The TisTubb-GFP mouse line is, in this context, a good tool for screening for factors influencing the generation of BPs, since it allows detection and identification of BPs by the fate of the progeny. The TisTubb-GFP mouse line could be used as a reporter to be crossed with any other line of interest. In a growing amount of cases (as the Cdc42 conditional knock-out of Cappello and coworkers [195]), the increase of abventricular mitoses is correlated with an increase of prematurely and ectopically generated neurons; however, it is not clear if these neurons originate from asymmetric or symmetric divisions. Live imaging of neurogenic mitoses in the TisTubb-GFP strain could clarify that. Furthermore, single cells coming from the TisTubb-GFP mouse line (phenotypically normal) could be transplanted into other mice with any other phenotype to study the influence of a mutant environment on wild type progenitors in the generation of BPs and ultimately neurons. In addition, when an accurate fax sorting would be set up, the TisTubb mouse could result in an extremely fast and precise read-out for the variation in numbers of neural stem cells (unstained nucleus), neurogenic progenitors (GFP positive nucleus) and neurons (GFP positive plasma membrane, occasionally together with GFP positive nucleus).

The advantages offered by the Tis21-GFP mouse line in the study of adult neurogenesis are related on one hand to the possibility to identify the neurogenic progenitors, and on the other hand to the possibility to identify the newborn neurons that inherit Tis21-GFP fluorescence. The possibility to identify in vivo all the neurogenic progenitors opens the way to the study of several cell biological aspects of neurogenic progenitors. It is not known if there is any (and if it plays any role) asymmetric distribution of cell fate determinants during adult neurogenic division. Comparative analysis of mitotic proliferating and neurogenic cells could identify interesting candidates for asymmetric distribution during mitosis. It is not known if neurogenic progenitors in the adult divide symmetrically or asymmetrically. Time-lapse imaging of neurogenic progenitors in living hippocampal slice culture could offer an answer to this question. While it is known that astrocyte/stem cells have a slower cell cycle than transit amplifying progenitors, nothing is known about the difference between the cell cycle length of

transit amplifying and neurogenic progenitors. In addition, increase or decrease of Tis21-GFP/Dcx double positive cells could be used as a read-out to analyze the effect of any kind of manipulation, specifically on the neurogenic population, discriminating variations that could be otherwise averaged in the whole transit amplifying population. A careful measurement of the half-life of Tis21-GFP in neurons is still required, however, it is clear that Tis21-GFP is inherited by the neurons and degraded with maturation. This makes it a marker of the newborn-young neurons, in the DG, so that changes in the number of Tis21-GFP positive cells could reveal a change in the number of newborn neurons after any treatment of choice; discriminating, in addition, between generation of neurons and proliferation of astrocytes (side effect of many experimental models of brain injury), that are often much more abundant than neurons.

IV Materials and methods

IV – 1. Materials

IV - 1.1. Antibodies

Antibody I	*Kind*	*Dilution*	*Source*
anti-BrdU	Mouse, monoclonal, IgG	1:500	Hybridoma cell line
anti-Cadherin	Rabbit, polyclonal, IgG	1:300	DAKO
anti-Dcx	Goat, polyclonal, IgG	1:100	Santa Cruz Biotechnology
anti DIG-AP	Sheep, polyclonal, IgG	1:20000	Roche
anti-GFAP	Mouse, monoclonal, IgG	1:200	Chemicon
anti-GFP	Rabbit, polyclonal, IgG	1:200	Molecular Probes
anti-Giantin	Mouse, monoclonal, IgG	1:1000	Alexis Biochemicals
anti-Map2	Mouse, monoclonal, IgG	1:1000	Sigma
anti-MPM2	Mouse , Monoclonal, IgG	1:6000	Upstate
anti -Nestin	Mouse, monoclonal, IgG	1:200	USBio
anti -NeuN	Mouse , monoclonal, IgG	1:1000	Chemicon
anti -PH3	Rabbit, polyclonal, IgG	1:400	Upstate
anti -Prox1	Rabbit, Monoclonal	1:2000	Chemicon

Antibody II	*Kind*	*Dilution*	*Source*
anti -Goat Cy3	Donkey, polyclonal IgG	1:1000	Jacksons immunoresearch
anti -Mouse Cy3	Goat, polyclonal IgG	1:1000	Jacksons immunoresearch
anti -Mouse Cy5	Goat, polyclonal IgG	1:1000	Jacksons immunoresearch
anti -Rabbit Cy2	Donkey, polyclonal IgG	1:1000	Jacksons immunoresearch
anti -Rabbit Cy3	Goat, polyclonal IgG	1:1000	Jacksons immunoresearch
anti -Rabbit Cy5	Goat, polyclonal IgG	1:1000	Jacksons immunoresearch

IV - 1.2. Bacterial and mouse strains

TOP10 (Invitrogen):

f- mcrA D(mrr-hsdRMS-mcrBC) f80lacZDM15 DlacX74 deoR recA1 araD139 galU D(ara-leu)7697 galK rpsL (Str^R) endA1 nupG.

Embryos and tissues were taken from C57/Bl6 inbreed animals. The animals were kept in a controlled 12h day-night cycle. The genetic background of all the transgenic animals was C57Bl6, all the embryos and brains used were heterozygous. For staging of the embryos: E0 equals 0h:00 of the vaginal plug day.

IV - 1.3. Buffers and culture media

10X DNA loading buffer	50mM Tris/Hcl, pH7.6 2.5mg/ml Bromophenol Blue 2.5mg/ml Xylene Cyanol 60% Glycerol in H_2O
10X TBE	0.89 Tris 0.89 Boric Acid 20mM EDTA pH8.0 in H_2O
Immunofluorescence:	
(i) Permeabilization	0.25% Triton X 100 in PBS
(ii) Quenching	10mM NH_4Cl in PBS
(iii) Blocking and antibody incubation	5% Bovine Serum Albumine 5% Foetal Calf Serum 0.25% Triton X 100 in PBS
LB	10mg/ml NaCl 10mg/ml Bacto-Tryptone (Difco) 5mg/ml Bacto-Yeast extract (Difco)
LB-Agar	15mg/ml Bacto-Agar (Difco) in LB
Moviol	6.9g Glycerol 2.4g Moviol 120ul 200mM Tris/HCl pH8.5 in 6ml H_2O
PB1	10% Foetal calf Serum 1X Penicillin/Streptomycin in PBS
PBS	137mM NaCl 2.7mM KCl 8mM Na_2HPO_4 1.5mM KH_2PO_4
Penicillin/Streptomycin (100X)	10.000U/ml Penicillin 10.000U/ml Streptomycin in PBS

Pronuclear injection buffer		5mM Tris 0.1mM EDTA, pH 7.6 in H_2O
Slice culture		
(i)	Collagen	2.5ml Cellmatrix (Nitta gelatin Japan) 1ml 5X DMEM/F12 (GibcoBRL) 0.5ml reconstitution buffer 1ml H_2O
(ii)	Medium	Neurobasal Medium (GibcoBRL) 1X N2 (GibcoBRL) 1X B27 (GibcoBRL) 10% Freshly centrifuged mouse serum (Harlan) 1X Penicillin/Streptomycin
(iii)	Reconstitution buffer 0.05N NaOH	2.2g $NaHCO_4$ 200mM HEPES in 100ml H_2O
Southern blot hybridization		
(i)	Denaturation buffer	0.5N NaOH 1.5M NaCl in H_2O
(ii)	Neutralization buffer	0.5M Tris HCl, pH 7.5 3M NaCl in H_2O
(iii)	20X SSC	3M NaCl 300mM Tri-sodim-cytrate pH 7.0 in H_2O
(iv)	Wash buffer 1	2X SSC 0.1% SDS in H_2O
(v)	Wash buffer 2	0.5X SSC 0.1% SDS in H_2O
Tail lysis buffer		50mM Tris/HCl pH 8.0 100mM EDTA 100mM NaCl 1% SDS in H_2O
Tyrod		16g NaCl 0.4g KCl 0.4g $CaCl_2$ 0.42g $MgCl_2 \cdot 6H_2O$ 0.114g $NaH_2PO_4 \cdot 2H_2O$ 2g $NaHCO_3$ 2g Glucose pH 7.4

	in H_2O
Whole embryo culture Medium Japan)	Freshly centrifuged rat serum (Charles River 1X Penicillin/Streptomycin 2mg/ml Sucrose

IV - 1.4. Chemicals, enzymes, DNA standards and films

For routine work, standard chemicals from the companies Merck, Roth and Sigma were used.

Digoxygenin labelling and detection systems	Roche	
DNA standards	MBI Fermentas NEB	
Films	Amersham Hyperfilm	
Glutamine	GibcoBRL	
Penicillin/Streptomycin	GibcoBRL	
Restriction enzymes and ligases	MBI Fermentas NEB Roche	
Southern hybridization buffer	Roche	Easy Hyb granules

IV - 1.5. Devices and computer applications

Computer software	Adobe	Photoshop Illustrator Image ready
	Biorad	Laser view 2000
	Bitplane AG	Imaris 4.1
	Diagnostic instruments Inc.	Spot Advanced 3.5.9
	Improvision	Volocity
	Microsoft	Office for Mac
	Scanalytics Inc.	IpLab 3.5.5
	Zeiss	LSM image
examiner		
Crosslinker	Stratagene	Stratalinker 2400
Centrifuges	Eppendorf	5417R 5415R
	Beckmann Coulter	Avanti J-25
Cryostat	Microm	HM560
Developer	Kodak	M35X-OMAT-Processor

Electroporator	Genetronics	BTX®-ECM®830
Electrophoresis chambers	EMBL	
Heating block	Eppendorf	Thermostat 5320
Heating chamber	Saur	Bachoffer Chamber
Microscopes	Olympus	BX61 SZX12 Fluoroview FV1000
	Zeiss	LSM510
	Nikon	TE300
Two-photon set up:		
(i) Beam conditioning unit and Scanning head	Biorad	Radiance 2100MP
(ii) Laser	Verdi	10W
(iii) Modelock unit	Coherent	Mira 900
Objective heater	Bioptecs	
Peristaltic pump	Gilson	Minipulse 3
pH Meter	Radiometer Analytical	MeterLab PHM210
Spectrophotometer	Pharmacia	Ultrospec III
Steril Hood	The Baker Company	SteriGard Hood
Thermal Cycler	MJ Research	PTC-200
Timer	Oregon scientific	
Tissue Chopper	Ted Pella	Vibratome 600
Vibratome	Leica	VT 1000 S

IV - 1.6. Kits

Digoxygenin labelling and detection systems		Roche	
DNA preparation			
(i)	Maxiprep	Quiagen	Endofree Plasmid Maxi Kit
(ii)	Miniprep	Quiagen	QUIAprep spin Miniprep Kit
(iii)	Tail preparation	Quiagen	DNAeasy Tissue Kit
DNA transfer		Schlecker & Schuell	Turbo blotter

IV - 1.7. Oligonucleotides

Genotyping of the *Tubb3*-GFP strain.

(i) GFP detection:	Q-EGFP-F1	ACCAGCAGAACACCCCCATCG
	Q-EGFP-R1	CGGTCACGAACTCCAGCAGGA
(ii) Southern probe:	Probe Tubbac F2	CAATCGGTTCCCCTCAATCAC
	Probe Tubbac B19	TGGCTTCAACACCTGGATGC

Genotyping of the TisTubb-GFP strain.
Combined detection of Tis21, βIIItubulin and GFP

Tubb Geno Close 5'	TCCGCCTGCCTTTTCGTC
Egfp Start 3'	GCTCCTCGCCCTTGCTCAC
Tis21 34 F	GAGTGGTATGAAAGGCGCAGC
Tis21 167 R	TTCCAGACCCCGACGTGTGCTCAC

Genotyping of the $Cdc42^{floxex2}$ strain.

Cdc42 1	TTGTTATGTAGTGTCTGTCCATTGG
Cdc42 2	TGTCCTCTGCCATCTACACATACAC

IV- 1.8. Plasmids

pCS2-GAP43GFP	GAP43-GFP mammalian expression vector (CMV promoter)
pCAGGs-GAP43GFP	GAP43-GFP mammalian expression vector (CAGGs promoter)
pCAGGS-mRFP	mRFP mammalian expression vector (CAGGs promoter)
pCAGGS-Prominin1GFP	Mammalian expression vector (CAGGs promoter) expressing a Prominin1-GFP fusion protein

IV - 2.1. BAC modification

A Bacterial Artificial Chromosome clone containing the full length sequence of the βIIItubulin gene and 50Kb up- and downstream genomic sequence (Celera: RP23-214J5) was chosen for the modification. The BAC modification was carried out by Gene Bridges. All the following modifications were achieved using the RED-ET based recombination method [197, 198] The DNA fragments to be inserted were PCR-amplified using oligonucleotides including a sequence identical to the locus of insertion; by use of a sequence-specific recombinase, the DNA fragment was inserted precisely into the target locus. A floxed hygromicin cassette was inserted downstream the MycTAG-GAP43-GFP-polyA sequence. The MycTAG-GAP43-GFP-polyA-flHygro fragment was then inserted after the first ATG on the βIIItubulin ORF, in the BAC. This construct could be possibly used for production of βIIItubulin-GFP ES cell lines. Hygromicin was excised by coexpression of the Cre recombinase in the same bacterial strain. The final βIIItubulin-GFP BAC construct used for pronuclear injection contained the bacterial backbone and the following sequences, from N to COOH terminal. 50Kb-long 5' upstream βIIItubulin genomic sequence; 3 Myc TAGs for immunolocalization of the recombinant protein; the GAP43 plasma membrane localization signal; EGFP ORF; SV40 polyadenilation sequence; 50Kb-long 3' downstream βIIItubulin genomic sequence.

IV - 2.2. DNA preparation

Plasmid and genomic DNA from mouse tails was prepared used commercially available Kits from Quiagen, according to the manufacturer instructions. For details and buffer composition refer to the manufacturer handbooks.

IV - 2.2.1. **Miniprep (**QUIAprep spin Miniprep Kit)

A single bacterial colony was picked with a sterile toothpick and used to inoculate 5ml of LB, auditioned with the appropriate concentration of the appropriate antibiotic. The culture was grown overnight in a shaking incubator at 37^{o}. The bacteria were harvested by centrifugation (5' at 13.000 rpm, room temperature) and resuspended in 250ul of buffer P1, then lysed by addition of 250ul of buffer P2. The lysed suspension was neutralized after 5' by addition of 350ul of buffer N3 and centrifuged for 10' at 13.000 rpm. The supernatant was applied on the QUIAprep column and centrifuged for 1' at 13.000 rpm. The column was washed twice by addition of 750ul of buffer PE and centrifugation for 1' at 13.000 rpm. The DNA was eluted by addition of 50ul of buffer EB and centrifuged for 1' at 13.000 rpm.

IV - 2.2.2. **Maxiprep (**Endofree Plasmid Maxi Kit)

A single bacterial colony was picked with a sterile toothpick and used to inoculate 5ml LB, additioned with the appropriate concentration of the appropriate antibiotic. The

culture was grown overday in a shaking incubator at 37°. 500ul of the culture were used to inoculate 250ml LB, additioned with the appropriate concentration of the appropriate antibiotic. The bacteria were harvested by centrifugation (15' at 6.000g, 4^0) and resuspended in 10ml of buffer P1, then lysed by addition of 10ml of buffer P2. The lysate was neutralized after 5' by addition of 10ml of cold buffer P3. The lysate was poured into the QUIAfilter cartridge and filtered after 10' incubation. The filtered lysate was incubated for 30' with the endotoxin removal buffer ER, then applied onto the QUIGEN-tip 500 column and allowed to elute by gravity flow. The column was washed twice by addition of 30ml of buffer QC. The DNA was eluted into a corex tube by addition of 15ml of buffer QN. The eluate was precipitated by addition of 10.5ml (0.7 volumes) of isopropanol and centrifugation (30' at 15.000g, 4^O). The DNA pellet was washed by addition of 5ml 70% endotoxin free ethanol and centrifugation (15' at 15.000g, 4^O). The pellet was air-dried and resuspended in 100ul of cell culture-grade PBS. The DNA solution was centrifuged once more for 10' at 13.000 rpm to clear it from possible debris.

IV - 2.2.3. Genomic DNA preparation from a tail biopsy

A tail biopsy (approximately 0.5 cm long) was cut from a 4 weeks old mouse and dissolved (overnight in a shaking incubator at 55°) in a mixture of 180ul of buffer ATL and 20ul of proteinase K (Merck) solution (15mg/ml). 400ul of freshly prepared mixture (1:1) of buffer AL and ethanol were added to the dissolved tail. The solution was applied on the DNeasy spin column and centrifuged for 1' at 13.000 rpm. The column was washed twice by addition of 500ul of buffer AW1 and centrifugation for 1' at 13.000 rpm. The column was washed again twice by addition of 500ul of buffer AW2 and centrifugation for 1' at 13.000 rpm. The DNA was eluted by addition of 200ul of buffer AE and centrifuged for 1' at 13.000 rpm.

IV - 2.3. Embryo electroporation

Using a glass capillary, wild type or transgenic mice embryos (from 10.5 to E12.5) were injected (*in* or *ex* utero) into the developing telencephalic vesicle with 1-2ul of an endotoxin-free DNA solution (pCAGGs-GAP43GFP, pCS2-GAP43GFP, pCAGGs-mRFP or pCAGGs-Prominin1GFP; concentrations ranging from 0.3ug/ul to 1ug/ul in PBS) containing a vital dye (Fastgreen in PBS, 10%). 5-7 unidirectional squared electrical pulses (25-30 V, 50 ms each at 1-s intervals), were delivered through platinum electrodes (2 mm diameter, 1 mm space between the electrodes), using a BTX®-ECM®830 electroporator. The orientation of the electric field was used to direct the uptake of the plasmid to cortical cells with an apical contact. The embryos were allowed to develop 16h to 1 day, then collected and checked for fluorescence, prior to fixation, with a dissection steromicroscope equipped with a fluorescence lamp (Olympus SZX12).

IV - 2.3.1. *In utero* electroporation

In utero electroporation of mouse embryos was performed as described in [[232] except that the topology of the embryos was determined using illumination and a dissecting microscope rather than ultrasound microscopy. Pregnant mice 12 days post coitum were

anesthetized with isofluorane vapour and their uteri exposed. 1-2 µl of the DNA solution described above were injected, through the uterine wall, into the lumen of the telencephalic vesicles. Immediately after injection, electrical pulses were delivered as described above. After electroporation, the uterus was relocated into the peritoneal cavity and the abdomen sutured. The mice were sacrificed either 24h or 48h after this procedure and embryos collected for further analysis.

IV - 2.3.2. *Ex utero* electroporation and whole embryo culture

Ex utero electroporation and whole embryo culture were performed as described in [193,194] The uteri were collected from time-mated females killed by cervical dislocation, dissected in PB1 or Tyrod solution. E10.5 embryos, were freed from uterine walls, decidua capsularis and Reichert's membrane; they were then cultured with their open amnion, yolk sac and ectoplacental cone for approximately one hour to allow equilibration with the culture conditions. The culture was carried out in glass bottles (two embryos were cultured together in the same bottle) containing 1.5 ml of whole embryo culture medium. To ensure proper oxygenation the bottles were kept in continuous rotation (30 rpm) with a continuous oxygen flow (from 60% to 95% O_2, 5% CO_2 in N_2) going from 50cm^3/min (60% O_2) to 50 cm^3/min (95% O_2) according to the developmental stage. After equilibration, the embryos were transferred to the electroporation station and immobilized. 1-2 µl of the DNA solution described above were injected into the lumen of the telencephalic vesicles. Immediately after injection, electrical pulses were delivered as described above. The embryos were transferred back to the culture bottle and analyzed 16-20hrs later.

IV - 2.4. Genotyping

The mice were genotyped by Southern blot hybridization or PCR. The presence of the two BAC transgenic alleles in the Tubb3-GFP and TisTubb-GFP mouse stains was checked *via* back crossing with C57Bl6 mice.

IV - 2.4.1. Genotyping via Polymerase Chain Reaction

An aliquot of the genomic DNA tail preparation was used for amplification via Polymerase Chain Reaction. The recombinant TAQ DNA polymerase, made in house by D. Drechsel, had a proofreading activity. The amplification products were run on a 2% agarose gel containing Ethidium Bromide, 0.5mg/ml. The gel was prepared in TBE and the gel was run with a TBE Ethidium Bromide containing buffer.

PCR Mix

Reaction Buffer (10x)	3ul
dNTPs (10mM)	0.3ul
Oligonucleotides (100um)	0.3ul
Template DNA	5ul
"super" TAQ (5U/ul)	0.3ul
ddH_2O up to	30ul

Thermal Cycler Program

Cycle(s)	Temperature	Time
1	95^0C	5'
10	95^0C	30"
	0.1^0C/ sec down to	
	55^0- 65^0C	45"
	72^0 C	1'/Kb
20	95^0C	30"
	55^0- 65^0C	45"
	72^0 C	1'/Kb
1	72^0 C	10'

IV - 2.4.2 Genotyping *via* Southern blot hybridization

The following procedure was carried out accordingly to the Roche suggested protocol. 3-10ug of genomic DNA tail preparation were digested overnight with 10-30U of the appropriate restriction enzyme. The unpurified digestion reaction was run on a 0.8% TBE-agarose gel. The gel was washed twice for 20' with denaturation buffer and twice for 20' with neutralization buffer. The DNA was transferred overnight on a nylon membrane using the Schlecker and Schuell system. The DNA was crosslinked to the membrane by UV irradiation (1200uj/cm^2, stratalinker). The membrane was blocked by 1h incubation at 68^0C with the Easy Hyb solution (Roche), then it was hybridized overnight with the DIG marked DNA (30ng/ul in Easy Hyb solution) probe (see later for details). To avoid unspecific probe binding, the membrane was washed twice for 5' at room temperature with the washing solution 1 and twice for 15' at 68^0 with the washing solution 2. The membrane was equilibrated in Maleic acid and blocked by incubation in blocking buffer for 30'. After 30' of further incubation with anti DIG-AP (1:20000), the membrane was washed twice in wash buffer for 15'. The membrane was soaked with detection buffer and then with CDP-star to allow development of the enzymatic reaction. The membrane was exposed to a film for typically 5'-30'. The probe was generated by marking with Digoxygenin a PCR product obtained by a linearized template according to the following procedure.

PCR Mix		*Thermal Cycler Program*		
Reaction Buffer (10x)	5ul	Cycle(s)	Temperature	Time
Unlabeled dNTPs (200uM)	5ul	1	95^0C	5'
DIG-labeled dNTPs (200uM)	5ul	30	95^0C	30"
Oligonucleotides (100um)	0.75ul		55^0- 65^0C	45"
Template DNA	5ul		72^0 C	1'/Kb
Enzyme Mix (3U/ul)	0.75ul	1	72^0 C	10
ddH_2O up to	50ul			

IV - 2.5. Immunofluorescence

The cryosections were surrounded with a layer of hydrophobic compound (PAP-pen). Then kept in a humidified chamber and treated according to the following protocol. The stained slides were mounted in moviol and stored in the dark always at 4^0 C. The thick (40um) slices were stained while floating according to the following protocol and then mounted on coated glass slides
(Histobond Marienfeld).

Permeabilization	15' incubation in PBS, 0.25% TritonX100
Quenching of free aldehyd groups	15' incubation in PBS, 10mM NH_4Cl
Wash	3x 5' in PBS
Blocking	1h in PBS, 5%BSA, 5%FCS, 0.1% TritonX100
Primary antibody	1h in blocking solution
Wash	3x 5' in PBS
Secondary antibody	1h in blocking solution
Wash	1x 5' in PBS
DNA staining	1x 5' in PBS, Hoechst 1ug/ml
Wash	1x 5' in PBS

Wash	1x in ddH_2O

IV - 2.6. Mice handling, embryos, organ collection and cryosectioning

The mice were always handled according to the german legislation.
For brain collection, the pups were killed by cutting the head off; adult mice were anesthetized with an intraperitoneal injection of a mixture of Ketamine and Xylazine and then intracardiacally perfused with NaCl 0.9% followed by cold freshly prepared 4% PFA (in phosphate buffer, pH 7.4). The brains were fixed in freshly depolymerized 4% PFA overnight, then transferred in a sucrose solution (30% in PBS) for cryopreservation. For cryosectioning the brains were embedded in Tissue Tek (Sakura), deep frozen (on dry ice) then stored at -20^0 C until cutting. Cryosections (10-20um-thick) were cut with a cryostat (Microm, HM560) and collected on coated glass slides (Histobond Marienfeld); slides were kept at -20^0 C in the dark until staining. For thick sectioning, the brains were placed on a freezing platform and frozen without embedding; 40um-thick sections were cut and stored at 4^0 in PBS, 50% Glycerol, 0.05% NaN_3.

IV - 2.7. Microscopy

IV - 2.7.1. Confocal microscopy

Different confocal microscopes were used for imaging (see "Devices and computer applications" section). The different fluorophores in the 10 to 40um-thick sections were excited with the following laser lines. Pinhole size was always kept to 1 Airy unit.

Hoechst	405 or 364
GFP	488
mRFP	594
Cy3	633
Cy5	688

IV - 2.7.2. Stereomicroscopy

Dissection of embryos was always carried out at room temperature using either prewarmed (37^0C) PB1, in case of preparation for whole embryo or slice culture, or ice-cold PBS in case of preparation for fixation. An Olympus SZX12 dissecting scope equipped with a 130W mercury lamp was used for dissection and fluorescence detection.

IV - 2.7.3. Two-photon microscopy

High resolution two-photon microscopy was carried out on fixed 250um-thick cortical slices electroporated with GAP43-GFP. The slices were quenched with 10mM NH_4Cl then mounted directly on a coverslip using cell culture glass rings and 50-70% glycerol. The pump laser was modelocked and tuned to 890nm manually. The laser power was tuned to the maximum possible output, then, *via* the software regulation, it was tuned down to the minimum possible level compatible with imaging. Gain and offset vary between experiments, the other parameter were set as follows.

Width of the optical cube:	200um
Z step:	0.5um

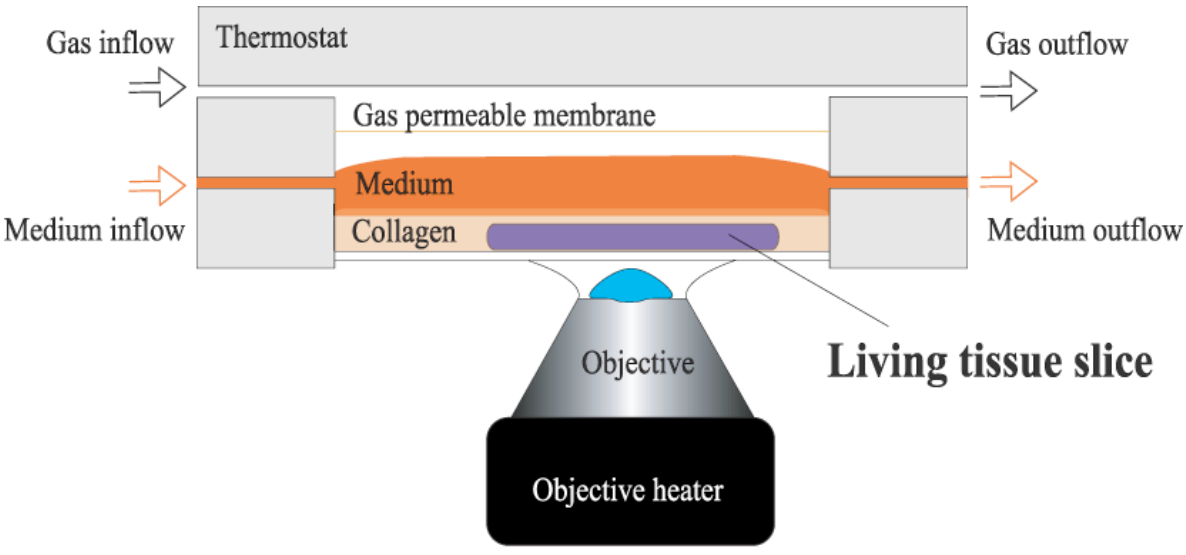
Resolution: 1024x1024 pixels
Scan speed: 166 lines per second
The Z stacks were reconstructed with the software Imaris (Bitpalne A.G.). The mode used for three-dimensional reconstruction was maximum intensity projection; presence or absence of apical contact was scored manually.

IV - 2.7.4. Two-photon time-lapse microscopy

Time lapse microscopy was carried out in acute brain slices culture according to the previously published methods [28, 92] that were combined in this doctoral work.

(i) Organotypic Slice Culture

E10.5, E11.5, E12.5 and E12.5+16-24h *in* utero development heads were cut, then ectoderm, skin, meninges and skull (when present) were removed using the stereomicroscope. If necessary, presence of fluorescence was assessed, the whole procedure was carried out at room temperature using prewarmed (37^0C) PB1 or Tyrod. The brains were embedded in 3% low-gelling agarose (in PBS) and cut using a manual tissue chopper to 300-500um thick slices. The orientation of the cut was kept orthogonal to the longitudinal axis of the brain (transverse cut), only intact (including ganglionic eminences) telencephalic slices were selected for imaging. The slices were collected and transferred to the culture medium at 37^0C. A solution of collagen (Type I-A, Cellmatrix, Nitta Gelatin, Japan) was prepared according to the manufacturer's instructions, the concentration was adjusted to 1.5mg/ml. The slices were resuspended in the ice-cold collagen solution and this mixture was poured onto the coverslip of a POC incubation chamber (Saur, bachhoffer chamber set up) (Fig.34). The slices were oriented such that the major axis of the NE/RG cells would be parallel to the imaging plane. The collagen was allowed to solidify in a cell culture incubator (37^0C, 20% O_2, 5% CO_2) for 40' to 1h. The culture was carried out in a thermostated chamber (37^0C) (Fig.34); slice culture medium (5ml) was kept recirculating by a peristaltic pump (Gilson. Minipulse 3); oxygenation was insured by a continuous flow of a gas mixture (40% O_2, 5% CO_2, 55%N_2) (Fig.34). The stable temperature of the imaged slice was insured by using an immersion objective equipped with an objective heater (Bioptecs) (Fig.34).



Multiphoton microscope

Figure 34 *(previous page)* – Cartoon showing the acute brain culture set up together with the imaging set up used. The slices were embedded in collagen (directly into the POC chamber) and kept at 37^0C, with a continuous oxygen flow and medium recirculation. Imaging was performed while culturing the slices.

(ii) Two-photon time-lapse microscopy

The pump laser was modelocked and tuned to 890nm manually. The laser power was tuned to the maximum possible output, then, *via* the software regulation, it was tuned down to the minimum possible level compatible with imaging. Gain and offset vary between experiments, the other parameter were set as follows.

Width of the optical cube:	100-180um
Z step:	2.7um
Resolution:	521x521 pixels
Interval between two following time points:	8'-12'
Scan speed:	500 lines per second

The Z stacks were reconstructed in four dimensional movies (three-dimensional reconstructions of several time points) with the software Imaris (Bitplane A.G.). The modes used for reconstruction were either maximum intensity projection or blend. All analysis of the movies was carried out in the four dimensional format allowing free three-dimensional rotation of the virtual tissue reconstruction. The movies were exported in the Quicktime format.

IV - 2.8. Pronuclear injection and transgenesis

The modified BAC (*Tubb3*-GFP) including the bacterial backbone, were linearized and diluted to the final concentration of 2ug/ml in pronuclear injection buffer. 820 oocytes were injected and transferred into pseudo-pregnant foster mother; 10 fertilized oocytes were transferred per each horn of the uterus. Of the 65 pups born, 2 chimeras showed βIIItubulin-GFP integration in the genome (checked by southern and PCR). Of these chimeras only one male showed germ line transmission and gave rise to green fluorescent pups. Homo- and heterozygous animals did not show any obvious phenotype and breed normally. The colony was maintained in the homozygous state and only heterozygous animals were used fro the experiments. The animals used for the experiments were a minimum of 75% C57Bl6 genetic background.

IV - 2.9. Restriction analysis

To analyze DNA sequences by restriction, a DNA fragment (0.5-1ug) was digested with the appropriate restriction enzyme (2U/ug) in 30ul. The reaction was incubated overnight and then 15ul of the reaction mix were loaded on a 0.7-2% agarose gel containing Ethidium Bromide, 0.5mg/ml. The gel was prepared in TBE and the gel was run with a TBE Ethidium Bromide containing buffer.

IV - 2.10. Statistical analysis of the data

155 Tis21-GFP positive mitoses were imaged (E10.5, n = 114; E11.5, n = 15; E12.5, n = 26). The divisions were subdivided in apical and basal classes; statistical analysis of the two classes was performed independently; the only example of apical symmetric neurogenic division was not taken in account for the analysis.

(i) Apical mitoses

All the mitoses whose daughters were lost either immediately or up to 40' after mitosis before expressing βIIItubulin-GFP were excluded from the analysis. Furthermore, another cutoff was applied to increase the stringency of the results. Average and standard deviation of the βIIItubulin-GFP expression time were calculated (n = 3; Avg 126.67; StDev 26.63). All the mitoses whose daughters were lost (before expressing any βIIItubulin-GFP) before a time equivalent to the average time of βIIItubulin-GFP expression minus twice the StDev were excluded from the analysis. In this way 62 apical mitoses and daughter pairs were analyzed.

(ii) Basal mitoses

The same cutoff applied to the apical mitoses was applied to the basal mitoses. Average and standard deviation of the βIIItubulin-GFP expression time were calculated (n = 3; Avg 46; StDev 20.64) All the mitoses whose daughters were lost (before expressing any βIIItubulin-GFP) before a time equivalent to the average time of βIIItubulin-GFP expression minus twice the StDev were excluded from the analysis. In this way 69 basal mitoses and daughter pairs were analyzed.

Pairs of daughters coming from a basal mitosis and expressing βIIItubulin-GFP were grouped in two classes. Mitoses (17 cases) giving rise to daughters both of which expressed βIIItubulin-GFP. Mitoses (13 cases) where it was not possible to unequivocally assign the presence of GFP positive plasma membrane to both daughter cells. In this way we obtained 3 groups of βIIItubulin-GFP expressing cells; (i) early and (ii) late βIIItubulin-GFP expressing cells of couples of daughters both of which expressed βIIItubulin-GFP and (iii) βIIItubulin-GFP expressing cells of couples of daughters in which it was not possible to unequivocally assign the presence of GFP positive plasma membrane to both daughter cells.

Use of one-way ANOVA test showed that there is no significant difference between the 3 classes of daughters of BPs ($p > 0.05$) while there is a significant difference between the 3 classes of daughters of BPs and the daughters of APs ($p < 0.001$)

V REFERENCES

V References

1. Hill, R. S. & Walsh, C. A. Molecular insights into human brain evolution. Nature 437, 64-7 (2005).
2. Gross, C. G. Neurogenesis in the adult brain: death of a dogma. Nat Rev Neurosci 1, 67-73 (2000).
3. Ming, G. L. & Song, H. Adult neurogenesis in the mammalian central nervous system. Annu Rev Neurosci 28, 223-50 (2005).
4. Marin, O. & Rubenstein, J. L. Cell migration in the forebrain. Annu Rev Neurosci 26, 441-83 (2003).
5. Kornack, D. R. & Rakic, P. Changes in cell-cycle kinetics during the development and evolution of primate neocortex. Proceedings Of The National Academy Of Sciences Of The United States Of America 95, 1242-6 (1998).
6. Caviness, V. S., Jr., Takahashi, T. & Nowakowski, R. S. Numbers, time and neocortical neuronogenesis: a general developmental and evolutionary model. Trends Neurosci 18, 379-83. (1995).
7. Gilbert, S. L., Dobyns, W. B. & Lahn, B. T. Genetic links between brain development and brain evolution. Nat Rev Genet 6, 581-90 (2005).
8. Smith, J. L. & Schoenwolf, G. C. Notochordal induction of cell wedging in the chick neural plate and its role in neural tube formation. J Exp Zool 250, 49-62 (1989).
9. Keller, R., Shih, J., Sater, A. K. & Moreno, C. Planar induction of convergence and extension of the neural plate by the organizer of Xenopus. Dev Dyn 193, 218-34 (1992).
10. Rallu, M., Corbin, J. G. & Fishell, G. Parsing the prosencephalon. Nat Rev Neurosci 3, 943-51 (2002).
11. Houart, C., Caneparo, L., Heisenberg, C., Barth, K., Take-Uchi, M. & Wilson, S. Establishment of the telencephalon during gastrulation by local antagonism of Wnt signaling. Neuron 35, 255-65 (2002).
12. Shimamura, K. & Rubenstein, J. L. Inductive interactions direct early regionalization of the mouse forebrain. Development 124, 2709-18 (1997).
13. Matise, M. P. & Joyner, A. L. Gli genes in development and cancer. Oncogene 18, 7852-9 (1999).
14. Monuki, E. S. & Walsh, C. A. Mechanisms of cerebral cortical patterning in mice and humans. Nat Neurosci 4 Suppl, 1199-206. (2001).
15. Bertrand, N., Castro, D. S. & Guillemot, F. Proneural genes and the specification of neural cell types. Nat Rev Neurosci 3, 517-30. (2002).
16. Muzio, L. & Mallamaci, A. Emx1, emx2 and pax6 in specification, regionalization and arealization of the cerebral cortex. Cereb Cortex 13, 641-7 (2003).
17. Muzio, L., DiBenedetto, B., Stoykova, A., Boncinelli, E., Gruss, P. & Mallamaci, A. Conversion of cerebral cortex into basal ganglia in Emx2(-/-) Pax6(Sey/Sey) double-mutant mice. Nat Neurosci 5, 737-45 (2002).
18. Wilson, S. W. & Rubenstein, J. L. Induction and dorsoventral patterning of the telencephalon. Neuron 28, 641-51 (2000).
19. Sur, M. & Rubenstein, J. L. Patterning and plasticity of the cerebral cortex. Science 310, 805-10 (2005).
20. Lendahl, U., Zimmerman, L. B. & McKay, R. D. CNS stem cells express a new class of intermediate filament protein. Cell 60, 585-95. (1990).

21. Weigmann, A., Corbeil, D., Hellwig, A. & Huttner, W. B. Prominin, a novel microvilli-specific polytopic membrane protein of the apical surface of epithelial cells, is targeted to plasmalemmal protrusions of non-epithelial cells. Proc. Natl. Acad. Sci. USA 94, 12425-12430 (1997).
22. McCarthy, R. A., Barth, J. L., Chintalapudi, M. R., Knaak, C. & Argraves, W. S. Megalin functions as an endocytic sonic hedgehog receptor. J Biol Chem 277, 25660-7 (2002).
23. Aaku-Saraste, E., Hellwig, A. & Huttner, W. B. Loss of occludin and functional tight junctions, but not ZO-1, during neural tube closure - remodeling of the neuroepithelium prior to neurogenesis. Dev. Biol. 180, 664-679 (1996).
24. Zhadanov, A. B., Provance, D. W., Jr., Speer, C. A., Coffin, J. D., Goss, D., Blixt, J. A., Reichert, C. M. & Mercer, J. A. Absence of the tight junctional protein AF-6 disrupts epithelial cell-cell junctions and cell polarity during mouse development. Curr Biol 9, 880-888 (1999).
25. Manabe, N., Hirai, S., Imai, F., Nakanishi, H., Takai, Y. & Ohno, S. Association of ASIP/mPAR-3 with adherens junctions of mouse neuroepithelial cells. Dev Dyn 225, 61-69. (2002).
26. Wodarz, A. & Huttner, W. B. Asymmetric cell division during neurogenesis in *Drosophila* and vertebrates. Mech. Dev. 120, 1297-1309 (2003).
27. Sauer, M. E., & Walker, B. E. Radiographic study of interkinetic nuclear migration the neural tube. Proc. Soc. Exp. Biol. Med. 101, 557-560 (1959).
28. Haubensak, W., Attardo, A., Denk, W. & Huttner, W. B. Neurons arise in the basal neuroepithelium of the early mammalian telencephalon: A major site of neurogenesis. Proc. Natl. Acad. Sci. USA 101, 3196-3201 (2004).
29. Götz, M. & Huttner, W. B. The cell biology of neurogenesis. Nat Rev Mol Cell Biol 6, 777-88 (2005).
30. Aaku-Saraste, E., Hellwig, A. & Huttner, W. B. Cell polarity in the mouse neuroepithelium: distribution of viral envelope proteins. Eur. J. Cell Biol. Suppl., 210 (1995).
31. Aaku-Saraste, E., Oback, B., Hellwig, A. & Huttner, W. B. Neuroepithelial cells downregulate their plasma membrane polarity prior to neural tube closure and neurogenesis. Mech. Dev. 69, 71-81 (1997).
32. Marzesco, A. M., Janich, P., Wilsch-Brauninger, M., Dubreuil, V., Langenfeld, K., Corbeil, D. & Huttner, W. B. Release of extracellular membrane particles carrying the stem cell marker prominin-1 (CD133) from neural progenitors and other epithelial cells. J Cell Sci 118, 2849-58 (2005).
33. Gadisseux, J. F. & Evrard, P. Glial-neuronal relationship in the developing central nervous system. A histochemical-electron microscope study of radial glial cell particulate glycogen in normal and reeler mice and the human fetus. Dev Neurosci 7, 12-32 (1985).
34. Shibata, T., Yamada, K., Watanabe, M., Ikenaka, K., Wada, K., Tanaka, K. & Inoue, Y. Glutamate transporter GLAST is expressed in the radial glia-astrocyte lineage of developing mouse spinal cord. J Neurosci 17, 9212-9 (1997).
35. Hartfuss, E., Galli, R., Heins, N. & Gotz, M. Characterization of CNS precursor subtypes and radial glia. Dev Biol 229, 15-30. (2001).
36. Misson, J.-P., Edwards, M. A., Yamamoto, M. & Caviness Jr., V. S. Identification of radial glia cells within the developing murine central nervous system: studies based upon a new histochemical marker. Dev. Br. Res. 44, 95-108 (1988).
37. Feng, L., Hatten, M. E. & Heintz, N. Brain lipid-binding protein (BLBP): a novel signaling system in the developing mammalian CNS. Neuron 12, 895-908 (1994).

38. Levitt, P. & Rakic, P. Immunoperoxidase localization of glial fibrillary acidic protein in radial glial cells and astrocytes of the developing rhesus monkey brain. Journal Of Comparative Neurology 193, 815-40 (1980).
39. Malatesta, P., Hartfuss, E. & Gotz, M. Isolation of radial glial cells by fluorescent-activated cell sorting reveals a neuronal lineage. Development 127, 5253-5263. (2000).
40. Noctor, S. C., Martinez-Cerdeno, V., Ivic, L. & Kriegstein, A. R. Cortical neurons arise in symmetric and asymmetric division zones and migrate through specific phases. Nat Neurosci 7, 136-144 (2004).
41. Miyata, T., Kawaguchi, A., Saito, K., Kawano, M., Muto, T. & Ogawa, M. Asymmetric production of surface-dividing and non-surface-dividing cortical progenitor cells. Development 131, 3133-3145 (2004).
42. Smart, I. H. M. Proliferative characteristics of the ependymal layer during the early development of the mouse neocortex: a pilot study based on recording the number, location and plane of cleavage of mitotic figures. J. Anat. 116, 67-91 (1973).
43. Sauvageot, C. M. & Stiles, C. D. Molecular mechanisms controlling cortical gliogenesis. Curr Opin Neurobiol 12, 244-9 (2002).
44. Takahashi, T., Nowakowski, R. S. & Caviness, V. S., Jr. The cell cycle of the pseudostratified ventricular epithelium of the embryonic murine cerebral wall. J Neurosci 15, 6046-6057. (1995).
45. Takahashi, T., Nowakowski, R. S. & Caviness, V. S., Jr. The leaving or Q fraction of the murine cerebral proliferative epithelium: a general model of neocortical neuronogenesis. J Neurosci 16, 6183-6196. (1996).
46. Knoblich, J. A. Asymmetric cell division during animal development. Nat Rev Mol Cell Biol 2, 11-20 (2001).
47. Chenn, A. & McConnell, S. K. Cleavage orientation and the asymmetric inheritance of Notch1 immunoreactivity in mammalian neurogenesis. Cell 82, 631-641. (1995).
48. Huttner, W. B. & Kosodo, Y. Symmetric versus asymmetric cell division during neurogenesis in the developing vertebrate central nervous system. Curr Opin Cell Biol 17, 648-57 (2005).
49. Heins, N., Cremisi, F., Malatesta, P., Gangemi, R. M., Corte, G., Price, J., Goudreau, G., Gruss, P. & Gotz, M. Emx2 promotes symmetric cell divisions and a multipotential fate in precursors from the cerebral cortex. Mol Cell Neurosci 18, 485-502. (2001).
50. Estivill-Torrus, G., Pearson, H., van Heyningen, V., Price, D. J. & Rashbass, P. Pax6 is required to regulate the cell cycle and the rate of progression from symmetrical to asymmetrical division in mammalian cortical progenitors. Development 129, 455-466. (2002).
51. Heins, N., Malatesta, P., Cecconi, F., Nakafuku, M., Tucker, K. L., Hack, M. A., Chapouton, P., Barde, Y. A. & Gotz, M. Glial cells generate neurons: the role of the transcription factor Pax6. Nat Neurosci 5, 308-315 (2002).
52. Dahmane, N., Sanchez, P., Gitton, Y., Palma, V., Sun, T., Beyna, M., Weiner, H. & Ruiz i Altaba, A. The Sonic Hedgehog-Gli pathway regulates dorsal brain growth and tumorigenesis. Development 128, 5201-12 (2001).
53. Palma, V. & Ruiz i Altaba, A. Hedgehog-GLI signaling regulates the behavior of cells with stem cell properties in the developing neocortex. Development 131, 337-45 (2004).
54. Aubert, J., Dunstan, H., Chambers, I. & Smith, A. Functional gene screening in embryonic stem cells implicates Wnt antagonism in neural differentiation. Nat Biotechnol 20, 1240-5 (2002).

55. Chenn, A. & Walsh, C. A. Regulation of cerebral cortical size by control of cell cycle exit in neural precursors. Science 297, 365-369. (2002).
56. Haegele, L., Ingold, B., Naumann, H., Tabatabai, G., Ledermann, B. & Brandner, S. Wnt signalling inhibits neural differentiation of embryonic stem cells by controlling bone morphogenetic protein expression. Mol Cell Neurosci 24, 696-708 (2003).
57. Sato, N., Meijer, L., Skaltsounis, L., Greengard, P. & Brivanlou, A. H. Maintenance of pluripotency in human and mouse embryonic stem cells through activation of Wnt signaling by a pharmacological GSK-3-specific inhibitor. Nat Med 10, 55-63 (2004).
58. Viti, J., Gulacsi, A. & Lillien, L. Wnt regulation of progenitor maturation in the cortex depends on Shh or fibroblast growth factor 2. J Neurosci 23, 5919-27. (2003).
59. Israsena, N., Hu, M., Fu, W., Kan, L. & Kessler, J. A. The presence of FGF2 signaling determines whether beta-catenin exerts effects on proliferation or neuronal differentiation of neural stem cells. Dev Biol 268, 220-31 (2004).
60. Hirabayashi, Y., Itoh, Y., Tabata, H., Nakajima, K., Akiyama, T., Masuyama, N. & Gotoh, Y. The Wnt/beta-catenin pathway directs neuronal differentiation of cortical neural precursor cells. Development 131, 2791-801 (2004).
61. Louvi, A. & Artavanis-Tsakonas, S. Notch signalling in vertebrate neural development. Nat Rev Neurosci 7, 93-102 (2006).
62. Gaiano, N., Nye, J. S. & Fishell, G. Radial glial identity is promoted by Notch1 signaling in the murine forebrain. Neuron 26, 395-404. (2000).
63. Mizutani, K. & Saito, T. Progenitors resume generating neurons after temporary inhibition of neurogenesis by Notch activation in the mammalian cerebral cortex. Development 132, 1295-304 (2005).
64. Ishibashi, M., Moriyoshi, K., Sasai, Y., Shiota, K., Nakanishi, S. & Kageyama, R. Persistent expression of helix-loop-helix factor HES-1 prevents mammalian neural differentiation in the central nervous system. EMBO J. 13, 1799-1805 (1994).
65. Guo, M., Jan, L. Y. & Jan, Y. N. Control of daughter cell fates during asymmetric division: interaction of numb and Notch. Neuron 17, 27-41 (1996).
66. Zhong, W., Jiang, M. M., Weinmaster, G., Jan, L. Y. & Jan, Y. N. Differential expression of mammalian Numb, Numblike and Notch1 suggests distinct roles during mouse cortical neurogenesis. Development 124, 1887-1897 (1997).
67. Li, H. S., Wang, D., Shen, Q., Schonemann, M. D., Gorski, J. A., Jones, K. R., Temple, S., Jan, L. Y. & Jan, Y. N. Inactivation of Numb and Numblike in embryonic dorsal forebrain impairs neurogenesis and disrupts cortical morphogenesis. Neuron 40, 1105-18 (2003).
68. Shen, Q., Zhong, W., Jan, Y. N. & Temple, S. Asymmetric Numb distribution is critical for asymmetric cell division of mouse cerebral cortical stem cells and neuroblasts. Development 129, 4843-4853. (2002).
69. Sun, Y., Goderie, S. K. & Temple, S. Asymmetric distribution of EGFR receptor during mitosis generates diverse CNS progenitor cells. Neuron 45, 873-86 (2005).
70. Iacopetti, P., Michelini, M., Stuckmann, I., Oback, B., Aaku-Saraste, E. & Huttner, W. B. Expression of the antiproliferative gene TIS21 at the onset of neurogenesis identifies single neuroepithelial cells that switch from proliferative to neuron-generating division. Proc Natl Acad Sci U S A 96, 4639-4644. (1999).
71. Kosodo, Y., Röper, K., Haubensak, W., Marzesco, A.-M., Corbeil, D. & Huttner, W. B. Asymmetric distribution of the apical plasma membrane during

neurogenic divisions of mammalian neuroepithelial cells. EMBO J. 23, 2314-2324 (2004).
72. do Carmo Avides, M. & Glover, D. M. Abnormal spindle protein, Asp, and the integrity of mitotic centrosomal microtubule organizing centers. Science 283, 1733-5 (1999).
73. do Carmo Avides, M., Tavares, A. & Glover, D. M. Polo kinase and Asp are needed to promote the mitotic organizing activity of centrosomes. Nat Cell Biol 3, 421-4 (2001).
74. Bond, J., Roberts, E., Mochida, G. H., Hampshire, D. J., Scott, S., Askham, J. M., Springell, K., Mahadevan, M., Crow, Y. J., Markham, A. F., Walsh, C. A. & Woods, C. G. ASPM is a major determinant of cerebral cortical size. Nat Genet 32, 316-320 (2002).
75. Bond, J., Scott, S., Hampshire, D. J., Springell, K., Corry, P., Abramowicz, M. J., Mochida, G. H., Hennekam, R. C., Maher, E. R., Fryns, J. P., Alswaid, A., Jafri, H., Rashid, Y., Mubaidin, A., Walsh, C. A., Roberts, E. & Woods, C. G. Protein-truncating mutations in ASPM cause variable reduction in brain size. Am J Hum Genet 73, 1170-1177 (2003).
76. Fish, J. L., Kosodo, Y., Enard, W., Paabo, S. & Huttner, W. B. Aspm specifically maintains symmetric proliferative divisions of neuroepithelial cells. Proc Natl Acad Sci U S A 103, 10438-43 (2006).
77. Feng, Y. & Walsh, C. A. Mitotic spindle regulation by Nde1 controls cerebral cortical size. Neuron 44, 279-93 (2004).
78. Calegari, F. & Huttner, W. B. An inhibition of cyclin-dependent kinases that lengthens, but does not arrest, neuroepithelial cell cycle induces premature neurogenesis. J Cell Sci 116, 4947-4955 (2003).
79. Tarui, T., Takahashi, T., Nowakowski, R. S., Hayes, N. L., Bhide, P. G. & Caviness, V. S. Overexpression of p27Kip1, Probability of Cell Cycle Exit, and Laminar Destination of Neocortical Neurons. Cereb Cortex (2005).
80. Malatesta, P., Gotz, M., Barsacchi, G., Price, J., Zoncu, R. & Cremisi, F. PC3 overexpression affects the pattern of cell division of rat cortical precursors. Mech Dev 90, 17-28. (2000).
81. Canzoniere, D., Farioli-Vecchioli, S., Conti, F., Ciotti, M. T., Tata, A. M., Augusti-Tocco, G., Mattei, E., Lakshmana, M. K., Krizhanovsky, V., Reeves, S. A., Giovannoni, R., Castano, F., Servadio, A., Ben-Arie, N. & Tirone, F. Dual control of neurogenesis by PC3 through cell cycle inhibition and induction of Math1. J Neurosci 24, 3355-3369 (2004).
82. Lukaszewicz, A., Savatier, P., Cortay, V., Kennedy, H. & Dehay, C. Contrasting effects of basic fibroblast growth factor and neurotrophin 3 on cell cycle kinetics of mouse cortical stem cells. J Neurosci 22, 6610-6622 (2002).
83. Hodge, R. D., D'Ercole, A. J. & O'Kusky, J. R. Insulin-like growth factor-I accelerates the cell cycle by decreasing G1 phase length and increases cell cycle reentry in the embryonic cerebral cortex. J Neurosci 24, 10201-10 (2004).
84. Lukaszewicz, A., Savatier, P., Cortay, V., Giroud, P., Huissoud, C., Berland, M., Kennedy, H. & Dehay, C. G1 phase regulation, area-specific cell cycle control, and cytoarchitectonics in the primate cortex. Neuron 47, 353-64 (2005).
85. Calegari, F., Haubensak, W., Haffner, C. & Huttner, W. B. Selective lengthening of the cell cycle in the neurogenic subpopulation of neural progenitor cells during mouse brain development. J Neurosci 25, 6533-8 (2005).
86. Tsai, J. W., Chen, Y., Kriegstein, A. R. & Vallee, R. B. LIS1 RNA interference blocks neural stem cell division, morphogenesis, and motility at multiple stages. J Cell Biol 170, 935-45 (2005).

87. Faulkner, N. E., Dujardin, D. L., Tai, C. Y., Vaughan, K. T., O'Connell, C. B., Wang, Y. & Vallee, R. B. A role for the lissencephaly gene LIS1 in mitosis and cytoplasmic dynein function. Nat Cell Biol 2, 784-791. (2000).
88. Smith, D. S., Niethammer, M., Ayala, R., Zhou, Y., Gambello, M. J., Wynshaw-Boris, A. & Tsai, L. H. Regulation of cytoplasmic dynein behaviour and microtubule organization by mammalian Lis1. Nat Cell Biol 2, 767-75. (2000).
89. Karfunkel, P. The activity of microtubules and microfilaments in neurulation in the chick. J Exp Zool 181, 289-301 (1972).
90. Messier, P.-E. & Auclair, C. Effect of Cytochalasin B on interkinetic nuclear migration in the chick embryo. Dev. Biol. 36, 218-223 (1974).
91. Murciano, A., Zamora, J., Lopez-Sanchez, J. & Frade, J. M. Interkinetic nuclear movement may provide spatial clues to the regulation of neurogenesis. Mol Cell Neurosci 21, 285-300 (2002).
92. Miyata, T., Kawaguchi, A., Okano, H. & Ogawa, M. Asymmetric inheritance of radial glial fibers by cortical neurons. Neuron 31, 727-741 (2001).
93. Ishii, Y., Nakamura, S. & Osumi, N. Demarcation of early mammalian cortical development by differential expression of fringe genes. Brain Res Dev Brain Res 119, 307-20 (2000).
94. Tarabykin, V., Stoykova, A., Usman, N. & Gruss, P. Cortical upper layer neurons derive from the subventricular zone as indicated by Svet1 gene expression. Development 128, 1983-93. (2001).
95. Nieto, M., Monuki, E. S., Tang, H., Imitola, J., Haubst, N., Khoury, S. J., Cunningham, J., Gotz, M. & Walsh, C. A. Expression of Cux-1 and Cux-2 in the subventricular zone and upper layers II-IV of the cerebral cortex. J Comp Neurol 479, 168-80 (2004).
96. Zimmer, C., Tiveron, M. C., Bodmer, R. & Cremer, H. Dynamics of Cux2 expression suggests that an early pool of SVZ precursors is fated to become upper cortical layer neurons. Cereb Cortex 14, 1408-20 (2004).
97. Englund, C., Fink, A., Lau, C., Pham, D., Daza, R. A., Bulfone, A., Kowalczyk, T. & Hevner, R. F. Pax6, Tbr2, and Tbr1 are expressed sequentially by radial glia, intermediate progenitor cells, and postmitotic neurons in developing neocortex. J Neurosci 25, 247-51 (2005).
98. Smart, I. H., Dehay, C., Giroud, P., Berland, M. & Kennedy, H. Unique morphological features of the proliferative zones and postmitotic compartments of the neural epithelium giving rise to striate and extrastriate cortex in the monkey. Cereb Cortex 12, 37-53. (2002).
99. Carroll, S. B. Genetics and the making of Homo sapiens. Nature 422, 849-57 (2003).
100. Marin-Padilla, M. Ontogenesis of the pyramidal cell of the mammalian neocortex and developmental cytoarchitectonics: a unifying theory. J Comp Neurol 321, 223-40 (1992).
101. Ponting, C. & Jackson, A. P. Evolution of primary microcephaly genes and the enlargement of primate brains. Curr Opin Genet Dev 15, 241-8 (2005).
102. Woods, C. G., Bond, J. & Enard, W. Autosomal recessive primary microcephaly (MCPH): a review of clinical, molecular, and evolutionary findings. Am J Hum Genet 76, 717-28 (2005).
103. Monuki, E. S., Porter, F. D. & Walsh, C. A. Patterning of the dorsal telencephalon and cerebral cortex by a roof plate-Lhx2 pathway. Neuron 32, 591-604. (2001).
104. Altman, J. & Das, G. D. Autoradiographic and histological evidence of postnatal hippocampal neurogenesis in rats. J Comp Neurol 124, 319-35 (1965).

105. Altman, J. & Das, G. D. Autoradiographic and histological studies of postnatal neurogenesis. I. A longitudinal investigation of the kinetics, migration and transformation of cells incorporating tritiated thymidine in neonate rats, with special reference to postnatal neurogenesis in some brain regions. Journal Of Comparative Neurology 126, 337-89 (1966).
106. Altman, J. Autoradiographic and histological studies of postnatal neurogenesis. IV. Cell proliferation and migration in the anterior forebrain, with special reference to persisting neurogenesis in the olfactory bulb. Journal Of Comparative Neurology 137, 433-57 (1969).
107. Cayre, M., Malaterre, J., Scotto-Lomassese, S., Strambi, C. & Strambi, A. The common properties of neurogenesis in the adult brain: from invertebrates to vertebrates. Comp Biochem Physiol B Biochem Mol Biol 132, 1-15 (2002).
108. Gould, E., McEwen, B. S., Tanapat, P., Galea, L. A. & Fuchs, E. Neurogenesis in the dentate gyrus of the adult tree shrew is regulated by psychosocial stress and NMDA receptor activation. J Neurosci 17, 2492-8 (1997).
109. Kornack, D. R. & Rakic, P. The generation, migration, and differentiation of olfactory neurons in the adult primate brain. Proc Natl Acad Sci U S A 98, 4752-7. (2001).
110. Pencea, V., Bingaman, K. D., Freedman, L. J. & Luskin, M. B. Neurogenesis in the subventricular zone and rostral migratory stream of the neonatal and adult primate forebrain. Exp Neurol 172, 1-16 (2001).
111. Eriksson, P. S., Perfilieva, E., Bjork-Eriksson, T., Alborn, A. M., Nordborg, C., Peterson, D. A. & Gage, F. H. Neurogenesis in the adult human hippocampus. Nat Med 4, 1313-7 (1998).
112. Grandel, H., Kaslin, J., Ganz, J., Wenzel, I. & Brand, M. Neural stem cells and neurogenesis in the adult zebrafish brain: Origin, proliferation dynamics, migration and cell fate. Dev Biol (2006).
113. Nottebohm, F. The road we travelled: discovery, choreography, and significance of brain replaceable neurons. Ann N Y Acad Sci 1016, 628-58 (2004).
114. Lois, C. & Alvarez-Buylla, A. Long-distance neuronal migration in the adult mammalian brain. Science 264, 1145-1148 (1994).
115. Cameron, H. A. & McKay, R. D. Adult neurogenesis produces a large pool of new granule cells in the dentate gyrus. J Comp Neurol 435, 406-17 (2001).
116. Kempermann, G., Wiskott, L. & Gage, F. H. Functional significance of adult neurogenesis. Curr Opin Neurobiol 14, 186-91 (2004).
117. Luskin, M. B. Restricted proliferation and migration of postnatally generated neurons derived from the forebrain subventricular zone. Neuron 11, 173-89 (1993).
118. Carleton, A., Petreanu, L. T., Lansford, R., Alvarez-Buylla, A. & Lledo, P. M. Becoming a new neuron in the adult olfactory bulb. Nat Neurosci 6, 507-18 (2003).
119. Altman, J. & Bayer, S. A. Migration and distribution of two populations of hippocampal granule cell precursors during the perinatal and postnatal periods. J Comp Neurol 301, 365-81 (1990).
120. van Praag, H., Schinder, A. F., Christie, B. R., Toni, N., Palmer, T. D. & Gage, F. H. Functional neurogenesis in the adult hippocampus. Nature 415, 1030-4 (2002).
121. Brazel, C. Y., Romanko, M. J., Rothstein, R. P. & Levison, S. W. Roles of the mammalian subventricular zone in brain development. Prog Neurobiol 69, 49-69 (2003).

122. Tramontin, A. D., Garcia-Verdugo, J. M., Lim, D. A. & Alvarez-Buylla, A. Postnatal development of radial glia and the ventricular zone (VZ): a continuum of the neural stem cell compartment. Cereb Cortex 13, 580-7 (2003).
123. Doetsch, F., Caille, I., Lim, D. A., Garcia-Verdugo, J. M. & Alvarez-Buylla, A. Subventricular zone astrocytes are neural stem cells in the adult mammalian brain. Cell 97, 703-716 (1999).
124. Seri, B., Garcia-Verdugo, J. M., McEwen, B. S. & Alvarez-Buylla, A. Astrocytes give rise to new neurons in the adult mammalian hippocampus. J Neurosci 21, 7153-7160 (2001).
125. Machold, R., Hayashi, S., Rutlin, M., Muzumdar, M. D., Nery, S., Corbin, J. G., Gritli-Linde, A., Dellovade, T., Porter, J. A., Rubin, L. L., Dudek, H., McMahon, A. P. & Fishell, G. Sonic hedgehog is required for progenitor cell maintenance in telencephalic stem cell niches. Neuron 39, 937-950 (2003).
126. Nakatomi, H., Kuriu, T., Okabe, S., Yamamoto, S., Hatano, O., Kawahara, N., Tamura, A., Kirino, T. & Nakafuku, M. Regeneration of hippocampal pyramidal neurons after ischemic brain injury by recruitment of endogenous neural progenitors. Cell 110, 429-41 (2002).
127. Lois, C., Garcia-Verdugo, J. M. & Alvarez-Buylla, A. Chain migration of neuronal precursors. Science 271, 978-81 (1996).
128. Alvarez-Buylla, A., Garcia-Verdugo, J. M. & Tramontin, A. D. A unified hypothesis on the lineage of neural stem cells. Nat Rev Neurosci 2, 287-293. (2001).
129. Doetsch, F. A niche for adult neural stem cells. Curr Opin Genet Dev 13, 543-50 (2003).
130. Seri, B., Garcia-Verdugo, J. M., Collado-Morente, L., McEwen, B. S. & Alvarez-Buylla, A. Cell types, lineage, and architecture of the germinal zone in the adult dentate gyrus. J Comp Neurol 478, 359-78 (2004).
131. Doetsch, F., Garcia-Verdugo, J. M. & Alvarez-Buylla, A. Regeneration of a germinal layer in the adult mammalian brain. Proc Natl Acad Sci U S A 96, 11619-11624 (1999).
132. Garcia, A. D., Doan, N. B., Imura, T., Bush, T. G. & Sofroniew, M. V. GFAP-expressing progenitors are the principal source of constitutive neurogenesis in adult mouse forebrain. Nat Neurosci 7, 1233-1241 (2004).
133. Doetsch, F., Garcia-Verdugo, J. M. & Alvarez-Buylla, A. Cellular composition and three-dimensional organization of the subventricular germinal zone in the adult mammalian brain. J Neurosci 17, 5046-61. (1997).
134. Kempermann, G., Jessberger, S., Steiner, B. & Kronenberg, G. Milestones of neuronal development in the adult hippocampus. Trends Neurosci 27, 447-52 (2004).
135. Galli, R., Fiocco, R., De Filippis, L., Muzio, L., Gritti, A., Mercurio, S., Broccoli, V., Pellegrini, M., Mallamaci, A. & Vescovi, A. L. Emx2 regulates the proliferation of stem cells of the adult mammalian central nervous system. Development 129, 1633-44 (2002).
136. Maekawa, M., Takashima, N., Arai, Y., Nomura, T., Inokuchi, K., Yuasa, S. & Osumi, N. Pax6 is required for production and maintenance of progenitor cells in postnatal hippocampal neurogenesis. Genes Cells 10, 1001-14 (2005).
137. Machold, R., Hayashi, S., Rutlin, M., Muzumdar, M. D., Nery, S., Corbin, J. G., Gritli-Linde, A., Dellovade, T., Porter, J. A., Rubin, L. L., Dudek, H., McMahon, A. P. & Fishell, G. Sonic hedgehog is required for progenitor cell maintenance in telencephalic stem cell niches. Neuron 39, 937-50 (2003).
138. Palma, V., Lim, D. A., Dahmane, N., Sanchez, P., Brionne, T. C., Herzberg, C. D., Gitton, Y., Carleton, A., Alvarez-Buylla, A. & Ruiz i Altaba, A. Sonic

hedgehog controls stem cell behavior in the postnatal and adult brain. Development 132, 335-44 (2005).
139. Ahn, S. & Joyner, A. L. In vivo analysis of quiescent adult neural stem cells responding to Sonic hedgehog. Nature 437, 894-7 (2005).
140. Stump, G., Durrer, A., Klein, A. L., Lutolf, S., Suter, U. & Taylor, V. Notch1 and its ligands Delta-like and Jagged are expressed and active in distinct cell populations in the postnatal mouse brain. Mech Dev 114, 153-9 (2002).
141. Chambers, C. B., Peng, Y., Nguyen, H., Gaiano, N., Fishell, G. & Nye, J. S. Spatiotemporal selectivity of response to Notch1 signals in mammalian forebrain precursors. Development 128, 689-702. (2001).
142. Gage, F. H. Mammalian neural stem cells. Science 287, 1433-8 (2000).
143. Temple, S. The development of neural stem cells. Nature 414, 112-7. (2001).
144. Alvarez-Buylla, A. & Lim, D. A. For the long run: maintaining germinal niches in the adult brain. Neuron 41, 683-6 (2004).
145. Lie, D. C., Dziewczapolski, G., Willhoite, A. R., Kaspar, B. K., Shults, C. W. & Gage, F. H. The adult substantia nigra contains progenitor cells with neurogenic potential. J Neurosci 22, 6639-49 (2002).
146. Pencea, V., Bingaman, K. D., Wiegand, S. J. & Luskin, M. B. Infusion of brain-derived neurotrophic factor into the lateral ventricle of the adult rat leads to new neurons in the parenchyma of the striatum, septum, thalamus, and hypothalamus. J Neurosci 21, 6706-17 (2001).
147. Rallu, M., Machold, R., Gaiano, N., Corbin, J. G., McMahon, A. P. & Fishell, G. Dorsoventral patterning is established in the telencephalon of mutants lacking both Gli3 and Hedgehog signaling. Development 129, 4963-74 (2002).
148. Kleber, M. & Sommer, L. Wnt signaling and the regulation of stem cell function. Curr Opin Cell Biol 16, 681-7 (2004).
149. Lee, S. M., Tole, S., Grove, E. & McMahon, A. P. A local Wnt-3a signal is required for development of the mammalian hippocampus. Development 127, 457-67. (2000).
150. Lie, D. C., Colamarino, S. A., Song, H. J., Desire, L., Mira, H., Consiglio, A., Lein, E. S., Jessberger, S., Lansford, H., Dearie, A. R. & Gage, F. H. Wnt signalling regulates adult hippocampal neurogenesis. Nature 437, 1370-5 (2005).
151. Song, H., Stevens, C. F. & Gage, F. H. Astroglia induce neurogenesis from adult neural stem cells. Nature 417, 39-44. (2002).
152. Bachiller, D., Klingensmith, J., Kemp, C., Belo, J. A., Anderson, R. M., May, S. R., McMahon, J. A., McMahon, A. P., Harland, R. M., Rossant, J. & De Robertis, E. M. The organizer factors Chordin and Noggin are required for mouse forebrain development. Nature 403, 658-61. (2000).
153. Lim, D. A., Tramontin, A. D., Trevejo, J. M., Herrera, D. G., Garcia-Verdugo, J. M. & Alvarez-Buylla, A. Noggin antagonizes BMP signaling to create a niche for adult neurogenesis. Neuron 28, 713-26 (2000).
154. Louissaint, A., Jr., Rao, S., Leventhal, C. & Goldman, S. A. Coordinated interaction of neurogenesis and angiogenesis in the adult songbird brain. Neuron 34, 945-60 (2002).
155. Jin, K., Zhu, Y., Sun, Y., Mao, X. O., Xie, L. & Greenberg, D. A. Vascular endothelial growth factor (VEGF) stimulates neurogenesis in vitro and in vivo. Proc Natl Acad Sci U S A 99, 11946-50 (2002).
156. Cao, L., Jiao, X., Zuzga, D. S., Liu, Y., Fong, D. M., Young, D. & During, M. J. VEGF links hippocampal activity with neurogenesis, learning and memory. Nat Genet 36, 827-35 (2004).

157. Aberg, M. A., Aberg, N. D., Hedbacker, H., Oscarsson, J. & Eriksson, P. S. Peripheral infusion of IGF-I selectively induces neurogenesis in the adult rat hippocampus. J Neurosci 20, 2896-903 (2000).
158. Wagner, J. P., Black, I. B. & DiCicco-Bloom, E. Stimulation of neonatal and adult brain neurogenesis by subcutaneous injection of basic fibroblast growth factor. J Neurosci 19, 6006-16 (1999).
159. Shen, Q., Goderie, S. K., Jin, L., Karanth, N., Sun, Y., Abramova, N., Vincent, P., Pumiglia, K. & Temple, S. Endothelial cells stimulate self-renewal and expand neurogenesis of neural stem cells. Science 304, 1338-40 (2004).
160. Leuner, B., Gould, E. & Shors, T. J. Is there a link between adult neurogenesis and learning? Hippocampus 16, 216-24 (2006).
161. Mirescu, C. & Gould, E. Stress and adult neurogenesis. Hippocampus 16, 233-8 (2006).
162. Olson, A. K., Eadie, B. D., Ernst, C. & Christie, B. R. Environmental enrichment and voluntary exercise massively increase neurogenesis in the adult hippocampus via dissociable pathways. Hippocampus 16, 250-60 (2006).
163. Kempermann, G., Kuhn, H. G. & Gage, F. H. More hippocampal neurons in adult mice living in an enriched environment. Nature 386, 493-5 (1997).
164. Kronenberg, G., Reuter, K., Steiner, B., Brandt, M. D., Jessberger, S., Yamaguchi, M. & Kempermann, G. Subpopulations of proliferating cells of the adult hippocampus respond differently to physiologic neurogenic stimuli. J Comp Neurol 467, 455-63 (2003).
165. Kirschenbaum, B., Doetsch, F., Lois, C. & Alvarez-Buylla, A. Adult subventricular zone neuronal precursors continue to proliferate and migrate in the absence of the olfactory bulb. J Neurosci 19, 2171-80 (1999).
166. Rochefort, C., Gheusi, G., Vincent, J. D. & Lledo, P. M. Enriched odor exposure increases the number of newborn neurons in the adult olfactory bulb and improves odor memory. J Neurosci 22, 2679-89 (2002).
167. Arvidsson, A., Collin, T., Kirik, D., Kokaia, Z. & Lindvall, O. Neuronal replacement from endogenous precursors in the adult brain after stroke. Nat Med 8, 963-970 (2002).
168. Kronenberg, G., Wang, L. P., Synowitz, M., Gertz, K., Katchanov, J., Glass, R., Harms, C., Kempermann, G., Kettenmann, H. & Endres, M. Nestin-expressing cells divide and adopt a complex electrophysiologic phenotype after transient brain ischemia. J Cereb Blood Flow Metab 25, 1613-24 (2005).
169. Kokaia, Z. & Lindvall, O. Neurogenesis after ischaemic brain insults. Curr Opin Neurobiol 13, 127-32 (2003).
170. Enwere, E., Shingo, T., Gregg, C., Fujikawa, H., Ohta, S. & Weiss, S. Aging results in reduced epidermal growth factor receptor signaling, diminished olfactory neurogenesis, and deficits in fine olfactory discrimination. J Neurosci 24, 8354-65 (2004).
171. Maslov, A. Y., Barone, T. A., Plunkett, R. J. & Pruitt, S. C. Neural stem cell detection, characterization, and age-related changes in the subventricular zone of mice. J Neurosci 24, 1726-33 (2004).
172. Kuhn, H. G., Dickinson-Anson, H. & Gage, F. H. Neurogenesis in the dentate gyrus of the adult rat: age-related decrease of neuronal progenitor proliferation. J Neurosci 16, 2027-33 (1996).
173. Cameron, H. A. & McKay, R. D. Restoring production of hippocampal neurons in old age. Nat Neurosci 2, 894-7. (1999).
174. Rakic, P. Specification of cerebral cortical areas. Science 241, 170-6. (1988).
175. Guardavaccaro, D., Corrente, G., Covone, F., Micheli, L., D'Agnano, I., Starace, G., Caruso, M. & Tirone, F. Arrest of G(1)-S progression by the p53-inducible

gene PC3 is Rb dependent and relies on the inhibition of cyclin D1 transcription. Mol Cell Biol 20, 1797-815 (2000).
176. Lin, W. J., Gary, J. D., Yang, M. C., Clarke, S. & Herschman, H. R. The mammalian immediate-early TIS21 protein and the leukemia-associated BTG1 protein interact with a protein-arginine N-methyltransferase. J. Biol. Chem. 271, 15034-15044 (1996).
177. Rouault, J. P., Prevot, D., Berthet, C., Birot, A. M., Billaud, M., Magaud, J. P. & Corbo, L. Interaction of BTG1 and p53-regulated BTG2 gene products with mCaf1, the murine homolog of a component of the yeast CCR4 transcriptional regulatory complex. J Biol Chem 273, 22563-9 (1998).
178. Prevot, D., Voeltzel, T., Birot, A. M., Morel, A. P., Rostan, M. C., Magaud, J. P. & Corbo, L. The leukemia-associated protein Btg1 and the p53-regulated protein Btg2 interact with the homeoprotein Hoxb9 and enhance its transcriptional activation. J Biol Chem 275, 147-53. (2000).
179. Lin, W. J., Chang, Y. F., Wang, W. L. & Huang, C. Y. Mitogen-stimulated TIS21 protein interacts with a protein-kinase-Calpha- binding protein rPICK1. Biochem J 354, 635-43. (2001).
180. Iacopetti, P., Barsacchi, G., Tirone, F., Maffei, L. & Cremisi, F. Developmental expression of PC3 gene is correlated with neuronal cell birthday. Mech. Dev. 47, 127-137 (1994).
181. el-Ghissassi, F., Valsesia-Wittmann, S., Falette, N., Duriez, C., Walden, P. D. & Puisieux, A. BTG2(TIS21/PC3) induces neuronal differentiation and prevents apoptosis of terminally differentiated PC12 cells. Oncogene 21, 6772-78 (2002).
182. Malatesta, P., Sgadò, P., Caneparo, L., Barsacchi, G. & Cremisi, F. In vivo PC3 overexpression by retroviral vector affects cell differentiation of rat cortical precursors. Dev. Brain Res. 128, 181-185 (2001).
183. Fanarraga, M. L., Avila, J. & Zabala, J. C. Expression of unphosphorylated class III beta-tubulin isotype in neuroepithelial cells demonstrates neuroblast commitment and differentiation. European Journal Of Neuroscience 11, 517-27 (1999).
184. Hayes, N. L. & Nowakowski, R. S. Dynamics of cell proliferation in the adult dentate gyrus of two inbred strains of mice. Brain Res Dev Brain Res 134, 77-85 (2002).
185. Yamaguchi, M., Saito, H., Suzuki, M. & Mori, K. Visualization of neurogenesis in the central nervous system using nestin promoter-GFP transgenic mice. Neuroreport 11, 1991-6. (2000).
186. Overstreet, L. S., Hentges, S. T., Bumaschny, V. F., de Souza, F. S., Smart, J. L., Santangelo, A. M., Low, M. J., Westbrook, G. L. & Rubinstein, M. A transgenic marker for newly born granule cells in dentate gyrus. J Neurosci 24, 3251-9 (2004).
187. Davis, F. M., Tsao, T. Y., Fowler, S. K. & Rao, P. N. Monoclonal antibodies to mitotic cells. Proc Natl Acad Sci U S A 80, 2926-30 (1983).
188. Campbell, R. E., Tour, O., Palmer, A. E., Steinbach, P. A., Baird, G. S., Zacharias, D. A. & Tsien, R. Y. A monomeric red fluorescent protein. Proc Natl Acad Sci U S A 99, 7877-82 (2002).
189. Macara, I. G. Parsing the polarity code. Nat Rev Mol Cell Biol 5, 220-31 (2004).
190. Cerione, R. A. Cdc42: new roads to travel. Trends Cell Biol 14, 127-32 (2004).
191. Wu, X., Quondamatteo, F., Lefever, T., Czuchra, A., Meyer, H., Chrostek, A., Paus, R., Langbein, L. & Brakebusch, C. Cdc42 controls progenitor cell differentiation and beta-catenin turnover in skin. Genes Dev 20, 571-85 (2006).
192. Iwasato, T., Datwani, A., Wolf, A. M., Nishiyama, H., Taguchi, Y., Tonegawa, S., Knopfel, T., Erzurumlu, R. S. & Itohara, S. Cortex-restricted disruption of

NMDAR1 impairs neuronal patterns in the barrel cortex. Nature 406, 726-31 (2000).
193. Eto, K. & Osumi-Yamashita, N. Whole embryo culture and the study of postimplantation mammalian development. Develop. Growth Differ. 37, 123-32 (1995).
194. Calegari, F., Marzesco, A. M., Kittler, R., Buchholz, F. & Huttner, W. B. Tissue-specific RNA interference in post-implantation mouse embryos using directional electroporation and whole embryo culture. Differentiation 72, 92-102 (2004).
195. Cappello, S., Attardo, A., Wu, X., Iwasato, T., Itohara, S., Wilsch-Brauninger, M., Eilken, H. M., Rieger, M. A., Schroeder, T. T., Huttner, W. B., Brakebusch, C. & Gotz, M. The Rho-GTPase cdc42 regulates neural progenitor fate at the apical surface. Nat Neurosci (2006).
196. Lee, M. K., Rebhun, L. I. & Frankfurter, A. Posttranslational modification of class III beta-tubulin. Proc Natl Acad Sci U S A 87, 7195-9 (1990).
197. Zhang, Y., Buchholz, F., Muyrers, J. P. & Stewart, A. F. A new logic for DNA engineering using recombination in Escherichia coli. Nat Genet 20, 123-8 (1998).
198. Muyrers, J. P., Zhang, Y., Testa, G. & Stewart, A. F. Rapid modification of bacterial artificial chromosomes by ET-recombination. Nucleic Acids Res 27, 1555-7 (1999).
199. Riederer, B. & Matus, A. Differential expression of distinct microtubule-associated proteins during brain development. Proc Natl Acad Sci U S A 82, 6006-9 (1985).
200. Sanchez, C., Diaz-Nido, J. & Avila, J. Phosphorylation of microtubule-associated protein 2 (MAP2) and its relevance for the regulation of the neuronal cytoskeleton function. Prog Neurobiol 61, 133-68 (2000).
201. Linstedt, A. D. & Hauri, H. P. Giantin, a novel conserved Golgi membrane protein containing a cytoplasmic domain of at least 350 kDa. Mol Biol Cell 4, 679-93 (1993).
202. Liu, Y., Fisher, D. A. & Storm, D. R. Intracellular sorting of neuromodulin (GAP-43) mutants modified in the membrane targeting domain. J Neurosci 14, 5807-17 (1994).
203. Mullen, R. J., Buck, C.R. & Smith, A. M. NeuN, a neuronal specific nuclear protein in vertebrates. Development 116, 201-211 (1992).
204. Bagri, A., Gurney, T., He, X., Zou, Y. R., Littman, D. R., Tessier-Lavigne, M. & Pleasure, S. J. The chemokine SDF1 regulates migration of dentate granule cells. Development 129, 4249-60 (2002).
205. Nadarajah, B., Alifragis, P., Wong, R. O. & Parnavelas, J. G. Ventricle-directed migration in the developing cerebral cortex. Nat Neurosci 5, 218-24. (2002).
206. Smart, I. H. M. & McSherry, G. M. Growth patterns in the lateral wall of the mouse telencephalon. II. Histological changes during and subsequent to the period of isocortical neuron production. J. Anat. 134, 415-442 (1982).
207. Noctor, S. C., Flint, A. C., Weissman, T. A., Wong, W. S., Clinton, B. K. & Kriegstein, A. R. Dividing precursor cells of the embryonic cortical ventricular zone have morphological and molecular characteristics of radial glia. J Neurosci 22, 3161-3173. (2002).
208. Hämmerle, B., Vera-Samper, E., Speicher, S., Arencibia, R., Martinez, S. & Tejedor, F. J. Mnb/Dyrk1A is transiently expressed and asymmetrically segregated in neural progenitor cells at the transition to neurogenic divisions. Dev Biol 246, 259-73 (2002).

209. Zhong, W. Diversifying neural cells through order of birth and asymmetry of division. Neuron 37, 11-4 (2003).
210. Cai, L., Hayes, N. L., Takahashi, T., Caviness, V. S., Jr. & Nowakowski, R. S. Size distribution of retrovirally marked lineages matches prediction from population measurements of cell cycle behavior. J Neurosci Res 69, 731-44 (2002).
211. Kornack, D. R. & Rakic, P. Radial and horizontal deployment of clonally related cells in the primate neocortex: relationship to distinct mitotic lineages. Neuron 15, 311-321 (1995).
212. Mione, M. C., Cavanagh, J. F., Harris, B. & Parnavelas, J. G. Cell fate specification and symmetrical/asymmetrical divisions in the developing cerebral cortex. J Neurosci 17, 2018-2029. (1997).
213. Reid, C. B., Tavazoie, S. F. & Walsh, C. A. Clonal dispersion and evidence for asymmetric cell division in ferret cortex. Development 124, 2441-2450 (1997).
214. Reznikov, K., Acklin, S. E. & van der Kooy, D. Clonal heterogeneity in the early embryonic rodent cortical germinal zone and the separation of subventricular from ventricular zone lineages. Dev Dyn 210, 328-43. (1997).
215. Qian, X., Goderie, S. K., Shen, Q., Stern, J. H. & Temple, S. Intrinsic programs of patterned cell lineages in isolated vertebrate CNS ventricular zone cells. Development 125, 3143-3152 (1998).
216. Qian, X., Shen, Q., Goderie, S. K., He, W., Capela, A., Davis, A. A. & Temple, S. Timing of CNS cell generation: a programmed sequence of neuron and glial cell production from isolated murine cortical stem cells. Neuron 28, 69-80. (2000).
217. Noctor, S. C., Flint, A. C., Weissman, T. A., Dammerman, R. S. & Kriegstein, A. R. Neurons derived from radial glial cells establish radial units in neocortex. Nature 409, 714-720 (2001).
218. Haydar, T. F., Ang, E., Jr. & Rakic, P. Mitotic spindle rotation and mode of cell division in the developing telencephalon. Proc Natl Acad Sci U S A 100, 2890-2895 (2003).
219. Sanada, K. & Tsai, L. H. G protein betagamma subunits and AGS3 control spindle orientation and asymmetric cell fate of cerebral cortical progenitors. Cell 122, 119-31 (2005).
220. Anthony, T. E., Klein, C., Fishell, G. & Heintz, N. Radial glia serve as neuronal progenitors in all regions of the central nervous system. Neuron 41, 881-890 (2004).
221. Gal, J. S., Morozov, Y. M., Ayoub, A. E., Chatterjee, M., Rakic, P. & Haydar, T. F. Molecular and morphological heterogeneity of neural precursors in the mouse neocortical proliferative zones. J Neurosci 26, 1045-56 (2006).
222. Feng, G., Mellor, R. H., Bernstein, M., Keller-Peck, C., Nguyen, Q. T., Wallace, M., Nerbonne, J. M., Lichtman, J. W. & Sanes, J. R. Imaging neuronal subsets in transgenic mice expressing multiple spectral variants of GFP. Neuron 28, 41-51 (2000).
223. Pratt, T., Sharp, L., Nichols, J., Price, D. J. & Mason, J. O. Embryonic stem cells and transgenic mice ubiquitously expressing a tau-tagged green fluorescent protein. Dev Biol 228, 19-28 (2000).
224. Gong, S., Zheng, C., Doughty, M. L., Losos, K., Didkovsky, N., Schambra, U. B., Nowak, N. J., Joyner, A., Leblanc, G., Hatten, M. E. & Heintz, N. A gene expression atlas of the central nervous system based on bacterial artificial chromosomes. Nature 425, 917-25 (2003).

225. Moriyoshi, K., Richards, L. J., Akazawa, C., O'Leary, D. D. M. & Nakanishi, S. Labeling neural cells using adenoviral gene transfer of membrane-targeted GFP. Neuron 16, 255-260 (1996).
226. Bellion, A., Baudoin, J. P., Alvarez, C., Bornens, M. & Metin, C. Nucleokinesis in tangentially migrating neurons comprises two alternating phases: forward migration of the Golgi/centrosome associated with centrosome splitting and myosin contraction at the rear. J Neurosci 25, 5691-9 (2005).
227. Hayashi, K., Kawai-Hirai, R., Harada, A. & Takata, K. Inhibitory neurons from fetal rat cerebral cortex exert delayed axon formation and active migration in vitro. J Cell Sci 116, 4419-28 (2003).
228. McCarthy, R. A. & Argraves, W. S. Megalin and the neurodevelopmental biology of sonic hedgehog and retinol. J Cell Sci 116, 955-60 (2003).
229. Dehay, C., Giroud, P., Berland, M., Killackey, H. & Kennedy, H. Contribution of thalamic input to the specification of cytoarchitectonic cortical fields in the primate: effects of bilateral enucleation in the fetal monkey on the boundaries, dimensions, and gyrification of striate and extrastriate cortex. J Comp Neurol 367, 70-89 (1996).
230. Dehay, C., Savatier, P., Cortay, V. & Kennedy, H. Cell-cycle kinetics of neocortical precursors are influenced by embryonic thalamic axons. J Neurosci 21, 201-14. (2001).
231. Price, D. J., Kennedy, H., Dehay, C., Zhou, L., Mercier, M., Jossin, Y., Goffinet, A. M., Tissir, F., Blakey, D. & Molnar, Z. The development of cortical connections. Eur J Neurosci 23, 910-20 (2006).
232. Takahashi, M., Sato, K., Nomura, T. & Osumi, N. Manipulating gene expressions by electroporation in the developing brain of mammalian embryos. Differentiation 70, 155-162 (2002).

VI List of abbreviations

ANOVA	Analysis Of VAriance
ANR	Anterior Neural Ridge
AP	Apical progenitor. Neurogenic progenitor dividing asymmetrically on the apical side of the neuroepithelium
BAC	Bacterial artificial Chromosome
bHLH	basic Helix-Loop-Helix
BMP	Bone Morphogenetic Protein
BP	Basal Progenitor. Neurogenic progenitor dividing symmetrically on the basal side of the neuroepithelium
BrdU	Bromo deoxy Uridine
CNS	Central Nervous System
Dcx	Doublecortin
GABAergic	Gamma Amino Butirric Acid ergic
GCL	Granule Cell Layer
DG	Dentate gyrus
DMEM	Dulbecco's Modified Eagle Medium
DNA	DeoxyriboNucleic Acid
DRG	Dorsal Root Ganglia
DV	Dorso-Ventral
E	Embryonic day
FCS	Foetal Calf Serum
GFP	Green Fluorescent Protein (the enhanced form)
INM	Interkinetic Nuclear Migration
LGE	Lateral Ganglionic Eminence
MGE	Medial Ganglionic Eminence
MIP	Maximum Intensity Projection
mRFP	monomeric Red Fluorescent Protein
MTOC	MicroTubules Organizing Centre
NE	Neuro Epithelial
NL	Neuronal Layer
OB	Olfactory Bulb
ORF	Open Reading Frame

OSVZ	Outer Sub Ventricular Zone
p	Probability
P	Postnatal
PBS	Phosphate Buffered Saline
PCR	Polymerase Chain Reaction
PNS	Peripheral Nervous System
PH3	Phosporylated Histone 3
RG	Radial Glia
RMS	Rostral Migratory Stream
RNA	Ribo-Nucleic Acid
SC	Spinal Cord
SEZ	Sub Ependymal Zone
SGCL	Sub Granule Cell Layer
Shh	Sonic HedgeHog
SVZ	Sub Ventricular Zone
TCA	Thalamo-Cortical Axons
VZ	Ventricular Zone

Haubensak W., **Attardo A**., Denk W. and Huttner W. B.
Generation of neurons from progenitors dividing at the basal side of the neuroepithelium during early development of the mammalian telencephalon
PNAS (2004) 101(9): 3196-201.

Cappello S., **Attardo A**., Wu X., Iwasato T., Itohara S., Wilsch-Brauninger S., Eilken H.M., Rieger M.A., Schroeder T., Huttner W.B., Brakebusch C. and Götz M.
The Rho-GTPase cdc42 regulates neural progenitor fate at the apical surface
Nature Neuroscience (2006) in press.

Attardo A., Haubensak W., Calegari F. and Huttner W. B.
Neurons express βIIItubulin earlier when originating from basal mitoses than apical mitoses
Manuscript in preparation

*Fabel K., ***Attardo A**., Haubensak W., Kempermann G. and Huttner W.B.
Tis21-GFP marks the neurogenic cells during postnatal and adult mouse neurogenesis
Manuscript in preparation

*These authors contributed equally.

Communications to scientific conferences

ELSO, September 2003
Haubensak W., **Attardo A**. and Huttner W. B.
Neuron generating divisions of neuroepithelial cells during early mammalian neurogenesis
- Speaker in the symposium on stem cells the 22nd of September 2003
Neuron generating divisions of neuroepithelial cells during early mammalian neurogenesis

FENS::Hertie winter school, Dec. 2003.
Attardo A., Haubensak W. and Huttner W. B.
Neuron-generating divisions of neuroepithelial cells during early mammalian neurogenesis

4th Forum of European Neuroscience, July 2004
Attardo A., Calegari F., Haubensak W. and Huttner W.B.
Characterization of novel transgenic mouse lines as tools to study mammalian neurogenesis

Cortical development: Neural stem cells to neural circuits, May 2005
Attardo A., Calegari F., Haubensak W. and Huttner W.B
Symmetric and asymmetric cell divisions during early development of the mouse telencephalon

5th Forum of European Neuroscience, July 2006
Attardo A., Fabel K., Haubensak W., Kempermann G. and Huttner W.B.
Tis21 expression to study adult mouse neurogenesis

VIII Declaration

I herewith declare that I have produced this paper without the prohibited assistance of third parties and without making use of aids other than those specified; notions taken over directly or indirectly from other sources have been identified as such. This paper has not previously been presented in identical or similar form to any other German or foreign examination board.

The thesis work was conducted from the 15th of September 2002 to the 5th of august 2006 under the supervision of Prof. Dr. Huttner W.B. at the Max Planck Institute of Molecular Cell Biology and Genetics, Dresden.

Dresden, 24 August 2006

Acknowledgments

Summary 1

I Introduction 3

The birth of the neurons 4

I -1. The specification and patterning of the mouse cortex 6

I - 1.1. From forebrain to telencephalon 7

I -2. The mechanisms regulating neurogenesis in the embryo 10
I - 2.1. The neuroepithelium changes with neurogenesis 10
I - 2.2. Cell divisions in the neuroepithelium are symmetric and asymmetric as defined by daughter cells fate 12
I - 2.2.1. Asymmetric cell division correlates with asymmetric distribution of cell fate determinants 15
I - 2.3. Segregation versus accumulation, the role of cell cycle length 17
I - 2.4. The BP is a different cell intermediate 20
I - 2.5. Neurogenesis and evolution 21

I -3. Neurogenesis during adulthood 24

I - 3.1. Neurogenesis continues from the embryo to the adult
I - 3.2. Adult neurogenesis is modulated similarly to embryonic neurogenesis but is restricted to specific "niches" 28
I - 3.3. The modulation and significance of adult neurogenesis 30

I - 4. Aims of this study 32

I - 4.1. Embryonic neurogenesis 32

I - 4.1.2. The use of Tis21 and βIIItubulin as markers for studying neurogenesis 32
I - 4.2. Adult neurogenesis 35
I - 4.2.1 The *Tis21*-GFP mouse line is a tool to study adult neurogenesis 36

II Results 38

II -1. Tis21-GFP as a tool for studying basal progenitors 39

II - 1.1. Tis21 is a pan neurogenic marker 39
II - 1.2. The abundance of basal progenitors changes during development 41

II -2. The role of the apical contact in BPs 45

II - 2.1. The dynamic approach: imaging of basal progenitors loosing their apical contact 45
II - 2.2. The static approach: the apical plasma membrane domain is lost in both neurogenic and non-neurogenic basal dividing cells 48
II - 2.3. Imaging of the apical plasma membrane domain in the Tis21-GFP mouse 52
II - 2.4. The role of cell polarity in the generation of BPs 54

II -3. The study of mitosis of neurogenic NE/RG cells by imaging 57

II - 3.1. Generation of the new BAC transgenic line "Tubb3-GFP" 57
II - 3.2 βIIItubulin-GFP is restricted to the neuronal plasma membrane and Golgi apparatus 59
II - 3.3. The double transgenic TisTubb-GFP line allows detection of neurogenic progenitors and neurons 65
II - 3.4. High-resolution study of neuronal migration at the onset of neurogenesis 66
II - 3.5. Study of neurogenic divisions and tracking of neurons immediately after their birth 69
II - 3.6. The kinetic of βIIItubulin-GFP expression differs between daughters of APs and BPs 73

II -4. Study of adult neurogenesis 76

II - 4.1. Tis21-GFP is expressed in the adult neurogenic regions 76
II - 4.2. Tis21-GFP is first expressed in a subset of the transit amplifying progenitors and it is inherited by the young neurons 80
II - 4.3. The proliferation of Tis21-GFP cells overtime 88

III Discussion 91

III -1. Tis21-GFP and the study of neurogenic cells 92

III - 1.1. Tis21 is a pan-neurogenic marker 92
III - 1.2. The early sub ventricular zone is neurogenic 93

III -2. The study of neurogenic divisions 94

III - 2.1. The strategy and the new tool 94
III - 2.2. High-resolution study of neuronal migration at the onset of neurogenesis 96
III - 2.3. Abundance of neurogenic divisions and kinetics of βIIItubulin expression 97
III - 2.4. Loss of the apical contact of BPs and evolution 99

III -3. The Tis21-GFP mouse and the study of adult neurogenesis 102

III - 3.1. Tis21-GFP in the lineage of adult progenitors 102
III - 3.2. Tis21-GFP expression marks the neurogenic subpopulation of the mitotic Dcx positive cells in the dentate gyrus 103
III – 3.3. Tis21-GFP correlates with the level of neurogenesis in the DG 106

III -4. Perspectives 107

IV Materials and Methods 109

IV -1. Materials 109

IV - 1.1. Antibodies 109
IV - 1.2. Bacterial and mouse strains 110
IV - 1.3. Buffers and culture media 111
IV - 1.4. Chemicals, enzymes, DNA standards and films 113
IV - 1.5. Devices and computer applications 113
IV - 1.6. Kits 114
IV - 1.7. Oligonucleotides 114
IV- 1.8. Plasmids 115

IV -2. Methods 116

IV - 2.1. BAC modification 116
IV - 2.2. DNA preparation 116
IV - 2.2.1. Miniprep (QUIAprep spin Miniprep Kit) 116
IV - 2.2.2. Maxiprep (Endofree Plasmid Maxi Kit) 116
IV - 2.2.3. Genomic DNA preparation from a tail biopsy 117
IV - 2.3. Embryo electroporation 117
IV - 2.3.1. *In* utero electroporation 117
IV - 2.3.2. *Ex* utero electroporation and whole embryo culture 118
IV - 2.4. Genotyping 118
IV - 2.4.1. Genotyping via Polymerase Chain Reaction 118
IV - 2.4.2 Genotyping *via* Southern blot hybridization 119
IV - 2.5. Immunofluorescence 119
IV - 2.6. Mice handling, embryos, organ collection and cryosectioning 120
IV - 2.7. Microscopy 120
IV - 2.7.1. Confocal microscopy 120
IV - 2.7.2. Stereomicroscopy 120
IV - 2.7.3. Two-photon microscopy 120
IV - 2.7.4. Two-photon time-lapse microscopy 121
IV - 2.8. Pronuclear injection and transgenesis 122
IV - 2.9. Restriction analysis 122
IV - 2.10. Statistical analysis of the data 122

V	**References**	124
VI	**List of abbreviations**	139
VII	**List of publications**	141
VIII	**Declaration**	143
IX	**Table of contents**	144